Univerzita Tomáše Bati ve Zlíně
Fakulta aplikované informatiky

Anastasia Sluštíková Lebedik, MSc.

Evolutionary Modeling of Cell Processes

Doctoral thesis

Course:	Engineering informatics
Selected field:	Engineering informatics
Supervisor:	prof. Ing. Ivan Zelinka, Ph.D.

Zlín, 2013

ACKNOWLEDGEMENTS

This project would not have been possible without the support of many people. Foremost, I would like to express my sincere gratitude to my supervisor Prof. Ivan Zelinka for his support, motivation and valuables ideas helped me to complete this work.

I would like to thank Anton Salykin from the stem cell laboratory at Department of Biology, Faculty of Medicine, Masaryk University (Brno) for providing experimental data and researcher Dominique Chu from School of Computing, University of Kent (Canterbury, Kent, Great Britain) for help with mathematical modeling questions.

My sincere thanks also go to Assoc. prof. Zuzana Kominkova Oplatkova for help with calculations and some mathematical questions.

I need to express my gratitude to Eric Afful Dadzie, who revised my English in the dissertation.

Many thanks go to supportive friends and extended family, who always encourage me to finish my study.

Thanks to my parents for giving me everything I need for my life (birth, love, education and all kinds of support throughout my life).

Finally, most of all, I would like to thank my husband Radek, who encouraged me to start my study, to continue it and to finish it. Thank you for your patience and support during many stressful periods, for your love and understanding.

ABSTRACT

In order to extend knowledge of biological regulation mechanisms modeling, it is necessary to investigate metabolic networks that control cellular processes. Complexity of interactions between components of these networks makes prediction of system behavior extremely challenging.

The study of a metabolic system dynamics includes parameter estimation of the system. Due to a large number of reactions, non-linear interactions between different metabolites, enzymes and other components of the system, parameters estimation of metabolic systems can be formulated as non-linear programming (NLP) problem.

The dissertation investigated parameter estimation of well-studied metabolic systems using modern evolutionary techniques. It also included comparison of algorithms performance in identifying model parameters. Furthermore, selected evolutionary algorithms were applied to modeling of metabolic system with unknown properties. The doctoral thesis provides a theoretical basis for the study of metabolic networks. It also describes the application of evolutionary algorithms to metabolic networks modeling problems.

Experimental part consisted of four case studies. In first three case studies three evolutionary techniques namely Genetic Algorithm, Differential Evolution and Self-Organizing Migrating Algorithm were applied to define parameters of three well-studied metabolic systems: the urea cycle, a three-step pathway and the model of glycogenolysis in skeletal muscle. The last case study included parameter estimation of model of energy metabolism in human stem cell based on experimentally measured data. This investigation is one of the main parts in whole study of human stem cell metabolism, which is carried out in stem cell laboratory in Masaryk University (Brno).

One of remarkable contributions of this study is the application of SOMA, a novel evolutionary technique in bioscience, to optimization of kinetic parameters in metabolic systems. Kinetic parameters of the urea cycle model and model of glycogenolysis in skeletal muscle were firstly defined using evolutionary techniques.

Overall, the results of modeling show that evolutionary algorithms provide an effective approach in parameter estimation of metabolic models and could be used even in large-scale problems.

Keywords: metabolic networks, evolutionary algorithms, parameter estimation.

ABSTRAKT

Za účelem rozšíření znalostí biologických omezení mechanismů modelování je nezbytně nutné prozkoumat metabolické sítě, které řídí buněčné procesy. Složitost vazeb mezi jednotlivými komponenty těchto sítí dělá předpověď chování systému extrémně komplikovanou.

Studium dynamiky metabolického systému zahrnuje identifikaci parametrů systému. Na základě vysokého počtu reakcí, nelineárních interakcí mezi různými metabolity, enzymy a jinými komponenty systému můžeme posouzení parametrů metabolických systémů formulovat jako problém nelineárního programování (NLP).

V disertační práci zkoumáme výkon moderních evolučních metod v identifikaci parametrů známých metabolických systémů. Navíc jsou ještě vybrané evoluční algoritmy použity k modelování metabolického systému s neznámými vlastnostmi.

Disertační práce poskytuje teoretické základy pro studium metabolických sítí. Evoluční algoritmy použité na problém modelování metabolických sítí jsou popsány v teoretické části.

Experimentální část se skládá ze čtyř studií. Tři evoluční techniky: Genetický Algoritmus, Diferenciální Evoluce a SamoOrganizující se Migrační Algolritmus, jsou použity k definování parametrů tří známých metabolických systémů: močovinový cyklus, three-step pathway a glykogenolýza v kosterní svalovině. Jednou z unikátních předností této disertační práce je novátorské použití algoritmu SOMA, dosud nepoužitého v oblasti bioscience, k definici parametrů systému na základě experimentálně získaných dat. Zároveň je naše studie jednou z hlavních částí výzkumu metabolismu lidských kmenových buněk.

Celkově výsledky modelování ukázali, že evoluční algoritmy poskytují efektivní přístup v nalezení parametrů metabolických modelů a mohou být aplikovány při hledání řešení rozsáhlých problémů modelování metabolických sítí.

Klíčová slova: metabolické sítě, evoluční algoritmy, identifikace parametrů

CONTENTS

LIST OF FIGURES

LIST OF TABLES

LIST OF SYMBOLS AND ABBREVIATIONS

mRNA - messenger Ribonucleic acid

NCBI - National Center for Biotechnology Information

KEGG) - Kyoto Encyclopedia of Genes and Genomes

ExPASy - Expert Protein Analysis System

BRENDA - BRaunschweig ENzyme DAtabase

DB - database

IUBMB - Union of Biochemistry and Molecular Biology

GENRE - genome-scale network reconstruction

E. coli - Escherichia coli

M. tuberculosis - Mycobacterium tuberculosis

ODEs - ordinary differential equations

GRNs - genetic regulatory networks

DNA - Deoxyribonucleic acid

RNA - Ribonucleic acid

SA - Simulated Annealing algorithm

EAs - Evolutionary Algorithms

CPU - central processing unit

GA - Genetic Algorithm

EP - Evolutionary Programming

ES - Evolution Strategies

DE - Differential Evolution

SOMA - Self-Organizing Migrating Algorithm

SOMAATO - AllToOne version of SOMA

SOMAATR - AllToOne Rand version of SOMA

ATP - adenosine triphosphate

PPi - pyrophosphate

Pi - orthophosphate

CP - carbamoyl phosphate

AMP - adenosine monophosphate

Std. Dev. - standard deviation

QSSA - quasi-steady-state assumption

SRES - Evolution Strategy using Stochastic Ranking

GLY - glucose

LAC - lactate

G1P - glucose 1-phosphate

G6P - glucose 6-phosphate

F6P - fructose 6-phosphate

FBP - fructose1,6-biphosphate

13BPG - glycerate 1,3-biphosphate

GAP - glyceraldehyde 3-phosphate

3PG - glycerate 3-phosphate

2PG - glycerate 2-phosphate

PEP - phosphoenolpyruvate

PYR - pyruvate

DHAP - dihydroxyacetone_br_phosphate

SBML - Systems Biology Markup Language

1 INTRODUCTION AND STATE OF ART

Cell is the main form of existence of life inherent in all living organisms, except viruses. Cell is the only organism, which has capability to construct a new cell out of raw materials from the environment based on the hereditary information [1]. To understand cellular systems, dynamic modeling of cellular processes has become an important task in systems biology. Cellular processes are features that define cell as a unit of living being. There are a vast number of different processes including cell division, cell death, cell cycle, differentiation, proliferation, etc. More specifically, cellular processes include from gene to cell level upwards: gene expression, transcription, translation, metabolism, physiological, and immunological response and control processes [2].

In order to extend knowledge of the biological regulation mechanisms, it is necessary to investigate large-scale biochemical, metabolic, signaling, protein, mRNA and gene regulatory networks that control cellular processes [3]. The complexity of interactions between components of the networks makes the prediction of the system behavior extremely challenging.

The dissertation is mainly focused on metabolic networks. These complex systems were chosen because of the fact that metabolic networks play a central role in the control of cellular processes [4]. Understanding complex biological networks requires the integration of experimental, theoretical research and computational tools. Therefore, mathematical modeling and computational simulation are now an indispensable part of modern biological investigation.

The use of computational modeling and simulation allow collection and systematization of biological knowledge, the discovery of new relationships that were not previously known and the revelation of new pathways. Good models may lead to new conceptual developments in Biology. Overall, modeling and simulation give us better understanding of biological interactions from both qualitative and quantitative points of view [5].

There are three major difficulties to model such complex systems. These are nonlinearity, a large scale, and stochasticity [6], [7]. To overcome these problems, evolutionary algorithms (EAs) were applied on different metabolic networks to define model parameters. In present study also investigated performance of modern evolutionary techniques in parameter estimation of well-studied metabolic systems. Moreover, selected evolutionary algorithms were applied to metabolic system with unknown properties.

Recent studies have successfully applied metaheuristic approaches to parameter optimization problem [8]-[10]. Researchers have used different types of evolutionary techniques such as genetic algorithms (GA), evolutionary programming (EP), differential evolution (DE), evolution strategies (ES), hybrid strategies and others. These algorithms were applied to various types of

biological networks: gene regulatory networks [4], [11]-[13], metabolic networks [9], [10], [14], [15] and different biological models [16], [17].

GA is probably the most popular approach for parameter estimation among systems biologists [18]. For instance, in [19] GA was used to estimate 18 unknown parameters of a signal transduction network described by the system of ordinary differential equations (ODEs). In [20], GA was successfully applied to define two parameters of glucose metabolism model consisted of insulin and C-peptide experimental data. To define four kinetic parameters in dynamical model of the human ^{M}MSAC mechanism, the authors used an evolutionary optimization procedure [21]. The above-mentioned studies are examples of GA application on parameter estimation of metabolic systems described by ODEs. GA was also used for parameter estimation of genetic regulatory networks [11], [22]. Overall, in many studies GA performance was improved by incorporating biologist's expert knowledge [18]. DE was applied in few comparison studies [10], [23]. It should be noted that these studies, where traditional evolutionary algorithms are compared, use the same benchmark problem. Evolutionary techniques could perform differently on other metabolic systems. The choice of objective function could also influence the result. Moreover, parameter estimation process depends on a scale and nonlinearity of a problem. There are few above-mentioned studies that apply EAs to real-world optimization problems in metabolic modeling. Obviously, the question of effectiveness of EAs application on parameter estimation of metabolic networks is still open.

In recent review [18], the authors provided comparison of different optimization techniques and gave recommendations according to existing results. In most studies new methods were suggested for model identification and then compared with already existed techniques. Comparison of existing metaheuristic methods could give more objective understanding of current state of the problem. The authors also noted that a question of application different types of EAs in a given problem type remains a matter of open research. New optimization techniques and new examples are needed to improve current state of the problem.

The dissertation investigates parameter estimation of three well-studied large-scale metabolic systems using modern evolutionary techniques. It also includes comparison of algorithms performance in identifying model parameters. Furthermore, selected evolutionary algorithms are applied to modeling of metabolic system with unknown properties.

This dissertation is divided into four main parts: introduction, theoretical part, experimental part and conclusions.

First chapter provides an importance of studying metabolic networks, especially the use of computational methods in this question. The chapter also gives current state in application of evolutionary techniques for biological

systems modeling. In the following second chapter, the dissertation goals are outlined.

The theoretical part includes two chapters. Chapter 3 suggests an introduction to metabolic modeling. In particular, it describes a place of metabolic modeling in current bioscience, provides steps in metabolic reconstruction process, gives basis of kinetic modeling and, finally, presents a common approach for analysis of regulatory systems. Chapter 4 gives overview of evolutionary techniques, applied in this dissertation.

The experimental part is divided into four case studies according to four investigated metabolic systems. In chapter 5, we provide the case study 1, where various evolutionary techniques are applied to parameter identification of the urea cycle. The next chapter, chapter 6, describes case study 2: metabolic modeling of a three-step pathway. Case study 3 in chapter 7 contains metabolic modeling of glycogenolysis in skeletal muscle. The last chapter in experimental part shows application of evolutionary techniques to metabolic modeling of glycolysis in human stem cells with real experimental data.

Finally, chapter 9 provides conclusions, achieved goals of the dissertation and future research related to the dissertation.

2 DISSERTATION GOALS

The global aim of the research is to expand knowledge about modeling of cellular processes. In particular, the main interests of the research are application and evaluation of evolutionary algorithms performance used for parameter estimation of various metabolic networks.

Subjects of the research:

1. Metabolic systems.
2. Methods for metabolic systems modeling.
3. Evolutionary algorithms and their application to biological systems modeling problem.

Objectives of the research:

1. To apply various evolutionary techniques to modeling of well-studied metabolic systems.
2. To evaluate and compare the performance of each algorithm.
3. To apply selected evolutionary techniques to estimate parameters of the model of glycolysis in human stem cell based on real experimental data.

▪ THEORETICAL PART

3 METABOLIC MODELING

3.1 Metabolic modeling – a key topic in Systems Biology

Systems biology is an integrative research area that focuses on the systematic study of complex interactions in biological systems by combining experimental and computational biology methods. The main objectives of systems biology are to identify the molecular mechanisms of a complex biological system and to obtain a quantitative description. In this rapidly developing area, predictive mathematical models of metabolic systems are used for analysis of observed experimental data, for extending biological knowledge or for providing predictive simulations [24].

In recent years, the main directions in systems biology are synthesis of specialty chemicals such as pharmaceuticals and biofuels, the development of computational tools for metabolic engineering, the discovery of new enzyme activities [6], [7]. The development of new computational methods for metabolic engineering is widely appreciated.

Due to the continuous progress of high-throughput experimental and computational technologies, the systems medicine approach became one of the most developing research areas in modern bioscience [24]. This approach offers the prospects of modeling complex diseases, providing new diagnostic and therapeutic techniques, identifying new drug targets. Systems medicine allows for better understanding associations between biological functions and different diseases (e.g. immunological, inflammatory, infectious, neurological) [25]. Since metabolism plays an essential role in cell growth and proliferation, genes regulating metabolism have been used as drug targets in the treatment of cancer and other diseases involving metabolic disorders, including diabetes, atherosclerosis and fatty liver disease [26]. Thus, understanding the human metabolic system is important for the study and treatment of complex human diseases. In order to extend our knowledge in study of complex human metabolism-related diseases, it is necessary to reconstruct and analyze metabolic networks.

Metabolic systems are highly non-linear with complex structure and dynamics. The complexity of interactions between components of metabolic system makes the prediction of the system behavior extremely challenging [18]. To overcome this challenge, many researchers use computational and mathematical modeling methods.

For better understanding of metabolic systems investigation, we provide a brief overview of metabolic network reconstruction.

3.2 Metabolic network reconstruction

The main steps of metabolic reconstruction process were described by Feist [27]. For the implementation of metabolic reconstruction process, the following information is required:

1) substrates and products which an enzyme act on,
2) the stoichiometric coefficients for each metabolite participating in the reaction(s) catalyzed by an enzyme,
3) type of the outlined reactions (reversible or irreversible),
4) cellular localization (e.g., cytoplasm, periplasm, etc.).

This data can be found in different types of sources. There are databases of chemical equations. The additional information about each reaction such as cellular localization, thermodynamics, and genetic/genomic information, is also required. The metabolic network reconstruction process consists of four fundamental steps (see Figure 3.1 [27]).

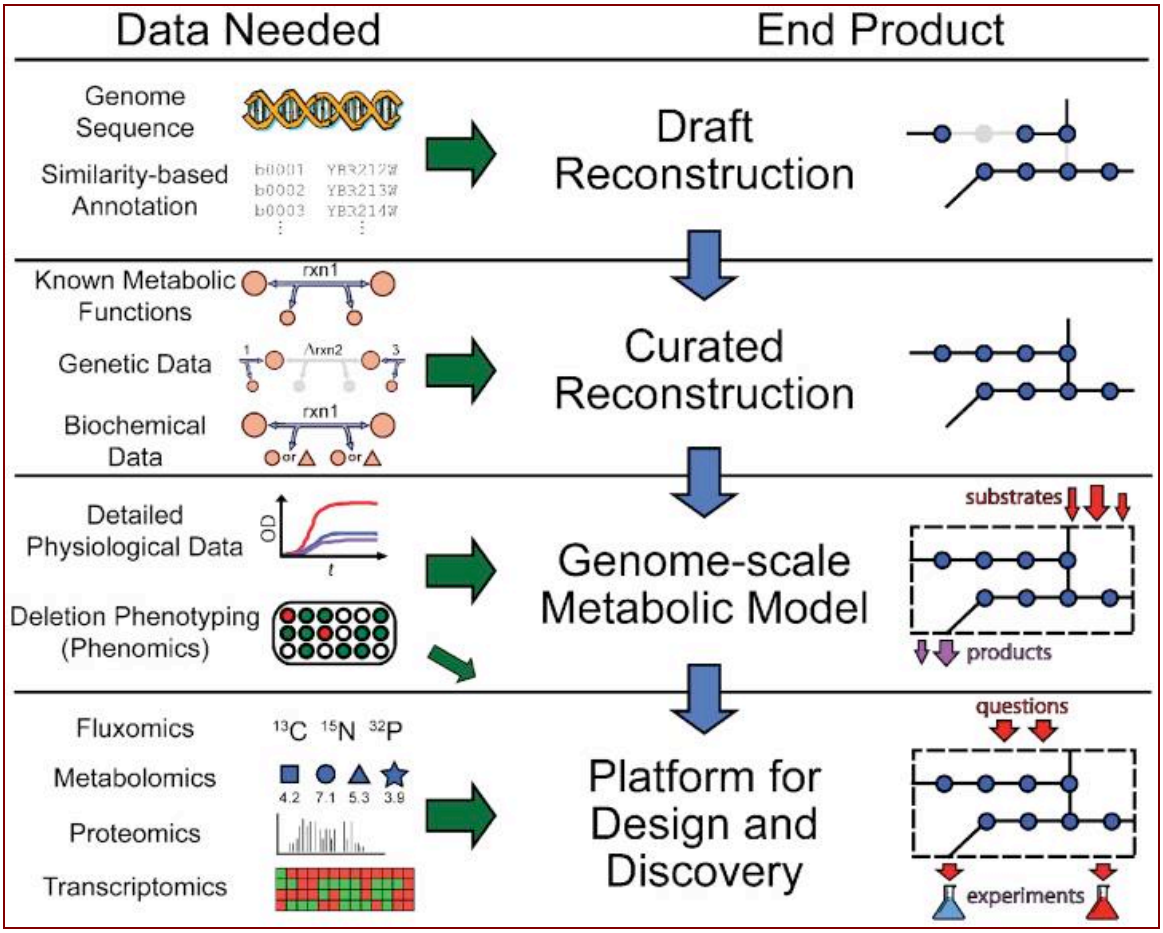

Fig. 3.1: The phases of metabolic network reconstruction process

Step 1: Automated genome-based reconstruction

The reconstruction of the metabolic network uses a bottom-up approach. Researchers begin by compiling reactions of cellular metabolism to build a

network through the collection of gene annotations, enzymes and pathway information from genome (e.g., NCBI, Ensembl) and pathway (e.g., KEGG, ExPASy) databases. The genome annotation provides unique identifiers for the reconstruction content and a list of the metabolic enzymes and can indicate how the gene products interact. Metabolic databases such as Kyoto Encyclopedia of Genes and Genomes (KEGG) [28], BRENDA [29], MetaCyc [30] and Transport DB [31] contain collections of metabolic and transport reactions. In particular, BRENDA, ENZYME [32] and the databases of Union of Biochemistry and Molecular Biology (IUBMB) provide stoichiometries of reactions, enzyme properties information, substrate specificities and cofactor usage. Transport DB is usually used to retrieve the transport functions encoded by sequenced genomes.

The process of automated reconstruction of metabolic network provides only the first stage of real network reconstruction. The output on this stage is a draft metabolic network, which is represented as an initial set of candidate biochemical reactions.

Step 2: Curating the draft reconstruction

After the first step, the draft network is not complete and fully appropriate for further investigation. It does not provide certain organism-specific features such as substrate or cofactor specificity and sub-cellular localization. In addition, the draft network may have gaps and mistakenly included reactions. Manual curation is therefore required to add and correct information, which was missed or was not accurate after the automated reconstruction. The manual curation in contrast with the automated reconstruction is a time-consuming process.

Researchers refine the network using literature evidences, including journal articles, reviews and textbooks on metabolic functions, biomass composition, growth conditions and gene-reaction associations. Expert's opinions are also one of the important sources of the manual curation. These sources provide information about different properties of the network such as reaction directionality and location. The availability of additional information for manual curation is highly variable and depends on the type of network or an organism. The main objective of manual curation is to fill in gaps in the draft networks by using different sources.

A combination of automated reconstruction with literature-based manual curation provides a high-quality network reconstruction. The result of this process is a biochemically, genomically and genetically structured knowledge base.

There are two global human metabolic networks: the Edinburgh Human Metabolic Network [33] and the human Recon 1 [34]. They consist of a list of human reactions, metabolites and gene-protein-reaction relationships.

Step 3: Converting a network reconstruction to a computational model

The conversion of a reconstructed metabolic network to a mathematical representation is a crucial step before the network can be used for further investigation. The mathematical model of the network provides different opportunities for researchers to analyze network properties.

There are two approaches are used for modeling of metabolic networks. The constraint-based approach describes mathematically the network by a stoichiometric matrix. The stoichiometric matrix captures the stoichiometry of the reactions. Analysis is performed under the assumption of steady state. The constraint-based models of metabolic networks lack the ability to directly predict the dynamics of the system [35].

Kinetic models describe the complete dynamics of the network. Creation of reliable kinetic models involves estimation of parameters. Complexity of this task is increasing with size of the network. Systems of ordinary differential equations (ODEs) are applied to model this kind of dynamical systems. ODEs are the most refined mathematical method to describe metabolic processes. Such detailed descriptions of the dynamics are essential to an accurate understanding of regulatory networks but they require substantial prior knowledge about the system [26], [36]. Introduction to kinetic modeling can be found in section 3.3 of this chapter.

The formulation of model equation system is challenging task. For many large networks, which are available in databases like KEGG or MetaCyc, the mechanism of reaction remains unknown. Generally, reliable rate equations for the reactions are not known because of the fact that the each equation has to be derived for each enzyme individually [37]. Therefore, it is common approach to apply approximate rate laws, which characterize the most important features of the reaction rate. Many rate laws exist which can be related to probabilistic [38], [39], phenomenological [40], [41], or semi-mechanistic approaches [42], [43].

The creation of reliable kinetic models involves the estimation of parameters. The models contain rate law equations for the reactions, their kinetic parameters and initial metabolite concentrations. For selecting appropriate rate laws, the deep understanding of enzyme mechanism is required. The dynamic ODE formulation requires significant information, including rate constants, total enzyme concentrations, reaction mechanisms. However, this approach provides unique and detailed solution.

The dynamic models of metabolic networks contain certain number of model parameters, including the reaction rates, Michaelis-Menten constants or constants describing the influence of certain inhibitors. The parameter values of model can often be measured. However, this process time-consuming, expensive, and usually impractical [8].

The main source of the kinetic parameters is published literature. Nevertheless, most of them are not available. Online databases are also one of the possible sources providing measured parameter values. The main drawback

of such data is differences between measured parameters, which are caused by variations in the experimental settings. It means that most parameters defined in experiments in vitro are different from parameters measured in vivo. Therefore, one of the principal questions in modeling of metabolic networks is the model parameter estimation [8].

The complexity of interactions between components of metabolic system makes the parameter estimation of model extremely challenging. Due to a large number of reactions, non-linear interactions between different metabolites, enzymes and other components of the system, the parameters estimation of metabolic systems can be formulated as non-linear programming (NLP) problem [9].

Step 4: Reconstruction uses and integration of high-throughput data

High-throughput data sets, which evaluate a large number of interactions across different growth or genetic conditions, can be utilized to refine and expand the metabolic network. These types of comparisons and analyses have the potential to truly evaluate genome-scale omics data sets in an integrated manner by placing them in a functional and structured context. The main aim of this step is to uncover new metabolic knowledge using systematic data from metabolic reconstruction. There are three main directions of investigations after the metabolic network reconstruction:

1) studies that have utilized a reconstruction to examine topological network properties,
2) studies that have utilized a reconstruction in constraint-based modeling for quantitative or qualitative analyses,
3) studies that are purely data driven.

3.3 Kinetic modeling

Biochemical kinetics is based on principle of mass action. It provides instruments for description of the rate of a chemical reaction in mathematical equations form. This principle sounds the following way: “the rate of a chemical reaction is proportional to the product of the concentrations of the reactants involved in the elementary chemical process” [44].

The fundamental events in chemical reaction networks are elementary reactions [45]. There are two types of elementary reactions:

$$\begin{array}{ll} \text{linear} & x \xrightarrow{v} \\ \text{bilinear} & x_1 + x_2 \xrightarrow{v} \end{array} \qquad (1)$$

Elementary reactions are irreducible events of chemical transformations. It is important to know that rates v and concentrations x are nonnegative variables.

$$x \geq 0,\ v \geq 0 \tag{2}$$

Reaction rates are proportional to the collision frequency of molecules taking part in a reaction. The probability of a collision between two different molecules depends on the concentration of a chemical species in a three-dimensional unconstrained domain. This dependence can be formulated as:

linear	$v = k\,x$	where the units on k are time^{-1}	(3)
bilinear	$v = k\,x_1\,x_2$	where the units on k are time^{-1} conc^{-1}	

Enzymes increase the probability of required collision. It means there are collisions that more likely produce a reaction at certain angles than others. Molecules bind to the surface of an enzyme at certain angles, which increases the probability of a reaction, see Figure 3.2 [45]. This binding process is characterized by certain numerical values of the rate constants. The rate constants are genetically determined as the structure of a protein for every individual in population. Thus, there are no common values of rate constants for whole population.

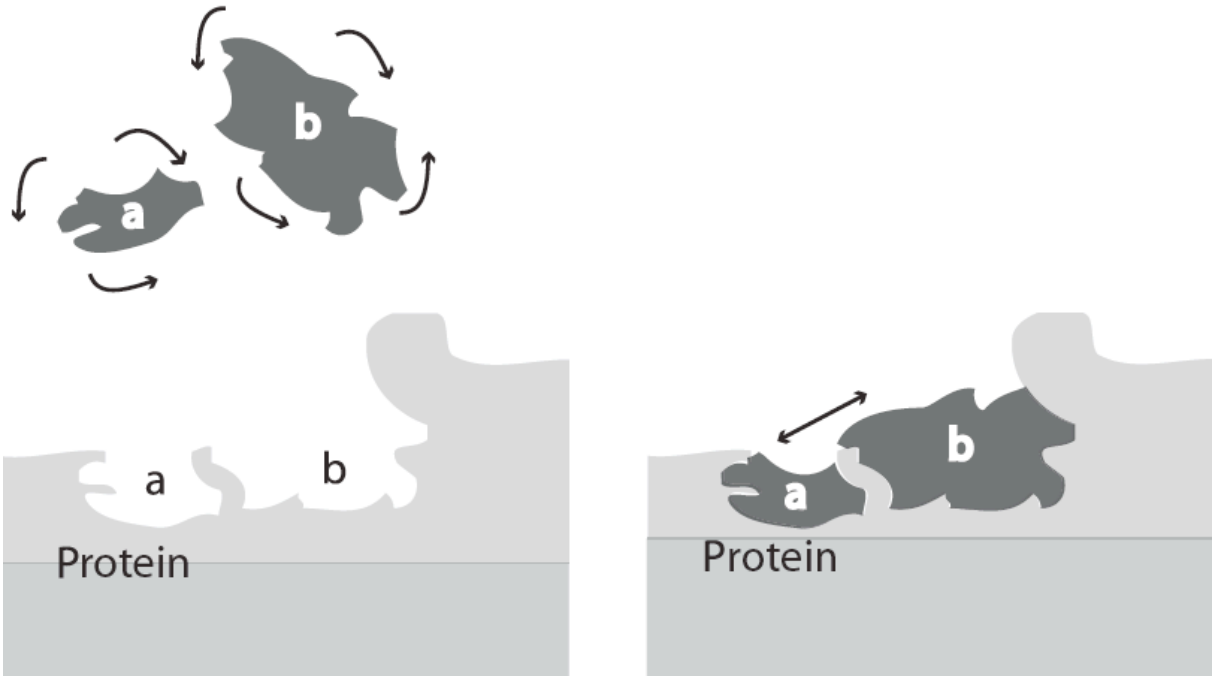

Fig. 3.2:Binding of two molecules on an enzyme

Elementary reaction mechanisms can be mathematically described by so called rate laws.

Reversible reactions

Thermodynamically reversible reaction is presented the following way:

$$x_1 \underset{v^-}{\overset{v^+}{\rightleftharpoons}} x_2 \tag{4}$$

The overall rate (the net rate) of the reaction is described by the difference between the forward and reverse reactions:

$$v_{\text{net}} = v^+ - v^- = k^+ x_1 - k^- x_2, \qquad \text{K}_{\text{eq}} = x_2/x_1 = k^+/k^- \tag{5}$$

where K_{eq} is the equilibrium constant for the reaction.

Bilinear reaction can be presented as:

$$x_1 + x_2 \underset{v^-}{\overset{v^+}{\rightleftharpoons}} x_3 \tag{6}$$

The net rate of the reaction can be written following way:

$$v_{\text{net}} = v^+ - v^- = k^+ x_1 x_2 - k^- x_3, \qquad \text{K}_{\text{eq}} = x_3/x_1 x_2 = k^+/k^- \tag{7}$$

Enzymatic reactions

There are different ways to describe enzymatic reactions. In this chapter, we consider the most common – classical irreversible Michaelis-Menten mechanism, which consists of three elementary reactions:

$$\text{S+E} \underset{v_{-1}=k_{-1}[\text{X}]}{\overset{v_1=k_1[\text{S}][\text{E}]}{\rightleftharpoons}} \text{X} \xrightarrow{v_2=k_2[\text{X}]} \text{P+E} \tag{8}$$

where S is a substrate, E and P are an enzyme and product, respectively. A complex X is a result of binding S to E, the intermediate.

Under a quasi-steady-state assumption (QSSA) – d[X]/dt=0, the classical rate law of Michaelis-Menten mechanism can be written as:

$$v = \frac{d[S]}{dt} = \frac{-V_m[S]}{K_m + [S]} \tag{9}$$

where parameter V_{m} is the maximal reaction rate and $K_{\text{m}}=(k_{-1}+k_2)/k_1$ is the Michaelis-Menten constant [45].

The general expression for reversible Michaelis-Menten reaction can be presented as:

$$v = \frac{V_f[S]/K_s - V_r[P]/K_p}{1+[S]/K_s+[P]/K_p} \tag{10}$$

where V_f and V_r are the rates of forward and reverse reaction, respectively [46].

In special cases, researchers use other rate laws. For example:

Inhibition rate laws

For instance, Irreversible Competitive Inhibition:

$$v = \frac{V_f \dfrac{[S]}{K_s}}{1+\dfrac{[S]}{K_s}+\dfrac{[P]/[S]}{K_{eq}}} \tag{11}$$

where [*S*] is substrate concentration, [*P*] is product concentration, V_f is the rate of forward reaction, K_{eq} is equilibrium constant, K_s is rate constant for substrate, K_p is rate constant for product.

Two Substrate Rate Laws

For instance, Random Order Bi-Bi Rate Law:

$$v = \frac{V_f \dfrac{[S_1]}{K_{s_1}}\dfrac{[S_2]}{K_{s_2}}\left(1-\dfrac{[P]/[S]}{K_{eq}}\right)}{\left(1+\dfrac{[S_1]}{K_{s_1}}+\dfrac{[P_2]}{K_{P_2}}\right)\left(1+\dfrac{[S_2]}{K_{s_2}}+\dfrac{[P_1]}{K_{P_1}}\right)} \tag{12}$$

where $[S_i]$ is substrate concentration, $[P_i]$ is product concentration, V_f is the rate of forward reaction, K_{eq} is equilibrium constant, K_{si} is rate constant for substrate, K_{pi} is rate constant for product [46].

In theoretical part, we provide only examples of common rate laws. In fact, there are many of them that can be used in kinetic modeling. However, the classical one is the Michaelis-Menten mechanism.

Overall, kinetic modeling of metabolic processes is based on rate laws. Therefore, system of ODEs, which describes the system dynamics, consists of nonlinear differential equations with high number of unknown parameters such as reaction rates and rate constants.

4 EVOLUTIONARY ALGORITHMS

Evolutionary algorithms were inspired by Darwin's theory of evolution and Mendel's genetic laws. The main principles and ideas of evolutionary computation were based on works A.M. Turing [47] and N.A. Barricelli [48].

Simulating process of natural evolution on a computer results in stochastic optimization techniques that can often outperform classical methods of optimization when applied to difficult real-world problems [49], [50].

All the evolutionary techniques are based on the same idea: given a population of individuals, the environmental pressure causes natural selection, which causes a rise in the fitness of the population. At the beginning, a set of candidate solutions is randomly created. The aim is to maximize a quality function. In other words, the quality function is applied as an abstract fitness measure – the higher the better. The choice of the better candidates is based on this fitness. Then, the chosen candidates (the parents) seed the next generation (the offspring) by applying recombination and/ or mutation to them. Recombination can be applied to two or more candidates whereas mutation can be applied to one. The new generation competes with the "old" candidates based on their fitness [51], [52].

The general scheme of an evolutionary algorithm is given in Figure 4.1.

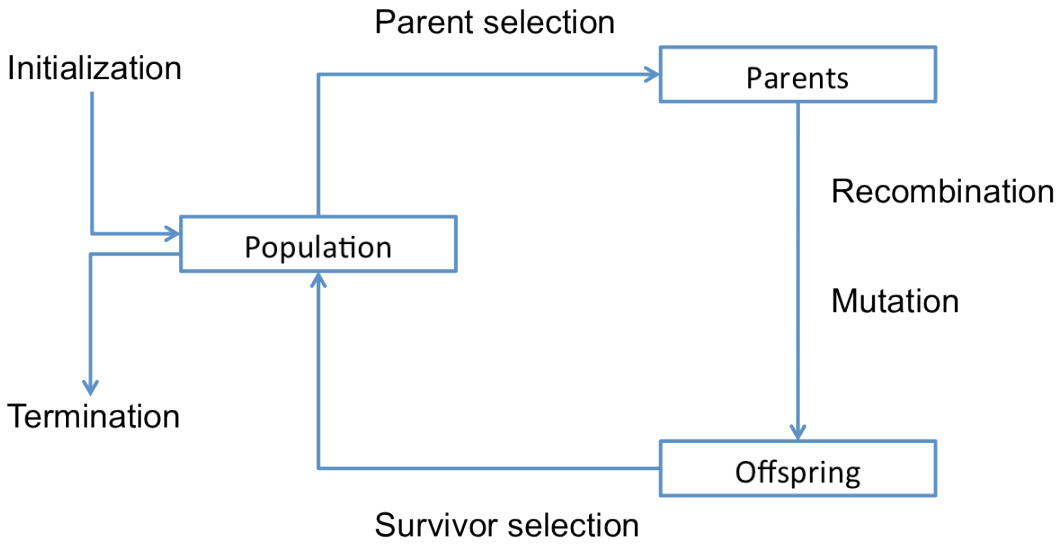

Fig. 4.1: A general scheme of an evolutionary algorithm as a flow-chart

EAs have a number of components and procedures that must be specified. The main components are following:

- Representation is definition of individuals, which means the formulation of the problem into terms used in evolutionary computation.

- Evaluation function (fitness function) forms the basis for selection, and thereby it facilitates improvements. The fitness function represents the requirements to adapt to.
- Population forms the unit of evolution. Defining a population means specifying how many individuals are in it. In some algorithms, it also means specifying a distance measure or a neighborhood relation.
- Parent selection mechanism role is to distinguish among individuals based on their quality to allow the better individuals to become parents of the next generation.
- Variation operators, which include mutation and recombination (crossover), create new individuals from old ones.
- Survivor selection mechanism (replacement) distinguishes among individuals based on their quality. It is similar to parent selection but in a different stage of the evolutionary cycle [51].

The main procedures are the initialization and the termination, which must be also defined. Initialization is kept simple in most EA applications: the first population is seeded by randomly generated individuals. Termination procedure is represented by termination conditions. Commonly used termination conditions are the following [51]:

1) The maximally allowed CPU time elapses.
2) The total number of fitness evaluations reaches a given limit.
3) For a given period of time or a number of generations or fitness evaluations, the fitness improvement remains under a threshold value.
4) The population diversity drops under a given threshold.

A number of evolutionary algorithms were developed in recent decades: genetic algorithm (GA) [53] and its different versions, evolutionary programming (EP) [52], evolution strategies (ES) [54], differential evolution (DE) [55]. Other evolutionary algorithms include memetic algorithms [56], [57], scatter search [54], self-organizing migrating algorithm (SOMA) [58], and tabu search [59], [60]. For our investigation, we have chosen differential evolution and self-organizing migrating algorithm. Thus, the following sections are devoted to only these algorithms.

4.1 Genetic Algorithms

Genetic algorithms were introduced by John Holland in the 1970s, inspired by Darwin's theory of evolution [61].

Firstly, "initialization" procedure generates an initial population. Then the initial population evolves into offspring until the termination conditions are fulfilled. For evolving, three evolutionary operations – selection, crossover, and mutation – are executed in sequence.

The selection operator distinguishes among individuals based on their quality (fitness values) and produces a temporary population. There are three the most

common schemes of selection: roulette-wheel, ranking and tournament selection.

The crossover operator mates individuals in the mating pool by pairs and generates children by crossing over the mated pairs with certain probability, one of the control parameters of genetic algorithms. Among many existing crossover schemes, there are four the most common: one-point crossover, multi-point crossover, binomial crossover and exponential crossover.

The mutation operator uses only one parent and creates one child by applying some kind of randomized change. The following mutation schemes are the most common: creep mutation, swap mutation, insert mutation, scramble and inversion mutation.

There are some features of GA that differ it from other techniques:

- GA searches many peaks in parallel, and hence reducing the possibility of local minimum trapping.
- GA works with a coding of parameters instead of the parameters themselves.
- GA evaluates the fitness of each string to guide its search instead of the optimization function.
- GA explores the search space where the probability of finding improved performance is high.

4.2 Differential Evolution

DE is a floating-point encoded evolutionary algorithm for global optimization introduced by Storn and Price [62].

Similarly to other evolutionary algorithms, the initial population is randomly selected. New population members are generated using recombination and mutation. One of the remarkable features of DE is the reversed order of mutation and recombination. Another feature is that for mutation DE uses four parents instead of two. For each individual, three other individuals from population are selected. A mutant vector νi is generated using three randomly selected individuals r1, r2, r3 from generation G:

$$\nu i = x_{r3,i}^{G} + F\left(x_{r1,i}^{G} + x_{r2,i}^{G}\right) \tag{13}$$

where F is a real and constant factor $\in$ [0, 2] which controls the amplification of the differential variation $\left(x_{r1,i}^{G} + x_{r2,i}^{G}\right)$.

In order to increase the diversity of the perturbed parameter vectors, crossover is performed on the next stage. The crossover operator uses the trial vector ui. The trial vector is generated by using the crossover constant CR$\in$ [0,1] which has to be determined by user. There two schemes of crossover: binomial and exponential [62].

The performance of DE depends on the choice of the mutation and crossover strategies and control parameters.

There are ten different strategies of DE with DE/x/y/z notation. According to this notation, x specifies the vector to be mutated which can be "rand" (a randomly chosen population vector) or "best" (the vector of lowest cost from the current population), y is the number of difference vectors used, and z is the crossover scheme. The strategies differ form each other by the vector ν [63].

Table 4.1 DE strategies

Strategy	Formulation
DE/best/1/exp	$\nu = x_{best,j}^{G} + F \cdot \left(x_{r2,j}^{G} - x_{r3,j}^{G} \right)$
DE/rand/1/exp	$\nu = x_{r1,j}^{G} + F \cdot \left(x_{r2,j}^{G} - x_{r3,j}^{G} \right)$
DE/rand-to-best/1/exp	$\nu = x_{i,j}^{G} + \lambda \cdot \left(x_{best,j}^{G} - x_{i,j}^{G} \right) + F \cdot \left(x_{r1,j}^{G} - x_{r2,j}^{G} \right)$
DE/best/2/exp	$\nu = x_{best,j}^{G} + F \cdot \left(x_{r1,j}^{G} + x_{r2,j}^{G} - x_{r3,j}^{G} - x_{r4,j}^{G} \right)$
DE/rand/2/exp	$\nu = x_{5,j}^{G} + F \cdot \left(x_{r1,j}^{G} + x_{r2,j}^{G} - x_{r3,j}^{G} - x_{r4,j}^{G} \right)$
DE/best/1/bin	$\nu = x_{best,j}^{G} + F \cdot \left(x_{r2,j}^{G} - x_{r3,j}^{G} \right)$
DE/rand/1/bin	$\nu = x_{r1,j}^{G} + F \cdot \left(x_{r2,j}^{G} - x_{r3,j}^{G} \right)$
DE/rand-to-best/1/bin	$\nu = x_{i,j}^{G} + \lambda \cdot \left(x_{best,j}^{G} - x_{i,j}^{G} \right) + F \cdot \left(x_{r1,j}^{G} - x_{r2,j}^{G} \right)$
DE/best/2/bin	$\nu = x_{best,j}^{G} + F \cdot \left(x_{r1,j}^{G} + x_{r2,j}^{G} - x_{r3,j}^{G} - x_{r4,j}^{G} \right)$
DE/rand/2/bin	$\nu = x_{5,j}^{G} + F \cdot \left(x_{r1,j}^{G} + x_{r2,j}^{G} - x_{r3,j}^{G} - x_{r4,j}^{G} \right)$

The main advantages of DE are finding true global minimum regardless of the initial parameter values, fast convergence and using few control parameters [62].

4.3 Self Organizing Migrating Algorithm

SOMA is a new optimization technique [58]. This algorithm differs from other evolutionary algorithms. The evolutionary computation techniques are generally based on the principle of natural evolution and genetics whereas the main idea of SOMA is the cooperative-competitive behavior of individuals. The notable feature of SOMA is that there is no producing offspring by parents. In this case, the social group of individuals searches for the best solution of problem. To achieve their aim, the intelligent individuals migrate in the search space.

Similarly to other evolutionary techniques, the population is generated randomly. Instead of evolution cycle (generation), the term "migration loop" is used. In each migration loop, the population is evaluated. The best individual, called leader L, is chosen based on the value of cost function. Other individuals

choose their direction based on the position of leader. The individuals move according to

$$\vec{r} = \vec{r}_0 + \vec{m}tPRTvector \tag{14}$$

where is a new candidate solution, is original individual, *m* is the difference between leader and start position of individual, t ∈[0, PathLength], PRTvector is control vector for perturbation. PathLength is control parameter defining how far an individual stops behind the leader.

The mutation operator is presented in SOMA as the PRT vector. The crossover operator can be thought as the movement of an individual, which is described by Equation 2.

There are several strategies of SOMA (AllToOne, AllToAll, AllToOne Rand, AllToAllAdaptive, Clusters), which differ by the way how individuals interact with each other [58].

▪ EXPERIMENTAL PART

5 CASE STUDY 1. METABOLIC MODELING OF THE UREA CYCLE

In this research, the urea cycle model was chosen for parameter optimization using evolutionary algorithms. Three modern efficient evolutionary techniques were applied to an optimization task, which is described below.

5.1 The urea cycle model

It is known that inborn errors of the enzymes of the urea cycle can change the concentrations of the metabolic intermediates. Moreover, slowing of metabolic reactions of the urea cycle can lead to serious effects on the patients condition due to increase of free ammonia. Nausea, vomiting, loss of consciousness, convulsions, and even more ultimately death are possible consequences of the high ammonia concentrations in the body.

The model of urea cycle was developed by [44] to investigate dependence of metabolite concentrations on various kinetic parameters of the enzymes. The model includes four enzyme reaction schemes: arginase, ornithine carbomoyl transferase, argininosuccinate lyase, and argininosuccinate synthetase (see Figure 5.1 [44]).

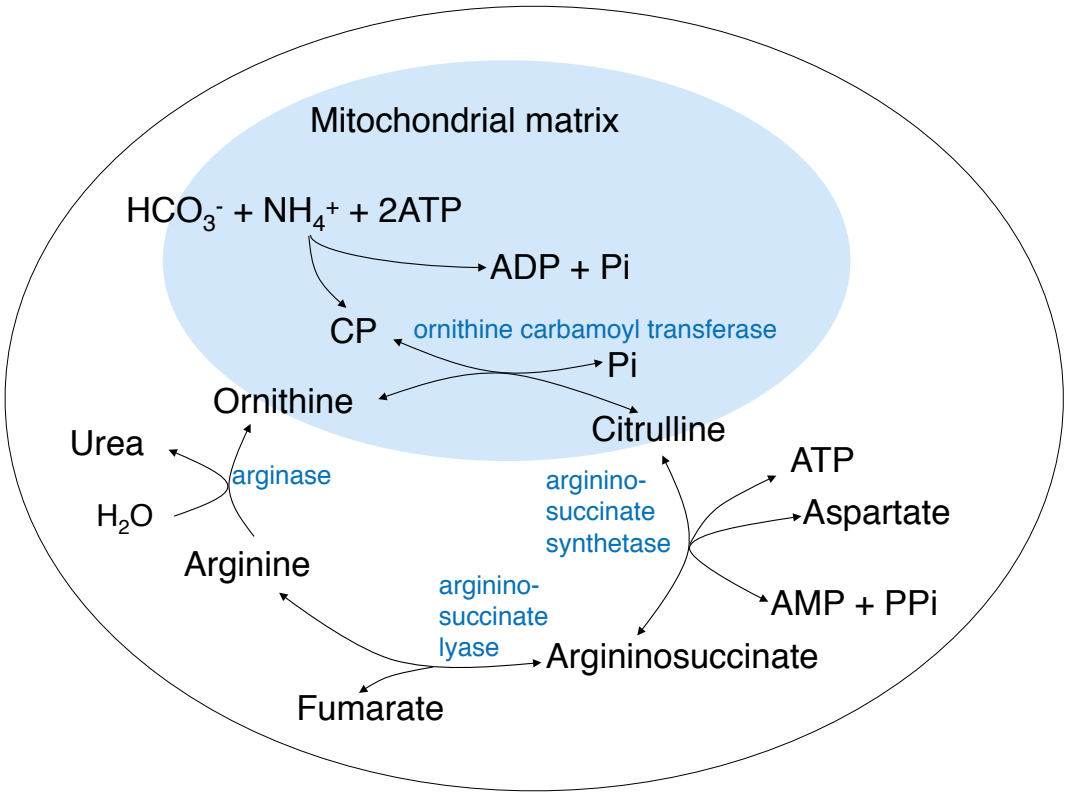

Fig. 5.1: The urea cycle in the mammalian hepatocyte

There were defined the rate equations for the four main enzymes, co-substrates and products. The original model consists of 12 differential equations and set of known values of the unitary rate constants and the steady-state parameters. For detailed description of the urea cycle model, see Appendix A.

The rate equations for the four main enzymes are represented in the system as v_{oct} (ornithine carbomoyl transferase), v_{ass} (argininosuccinate synthetase), v_{as} (argininosuccinate lyase), v_{arg} (arginase). In the model, v_{atp} (ATP), v_{pp} (PPi), v_f (Fumarate), v_{cp} (CP), v_{amp} (AMP), v_{asp} (Aspartate), v_p (Pi) stand for the rate equations for the co-substrates and products of peripheral reactions (see Figure 5.1). The unitary rate constants and the steady-state parameters V_m and K_m (parameters of a Michaelis-Menten reaction) were used for defining of the rate equations.

Overall, the number of kinetic parameters was 45. Due to the large number of unknown parameters, the parameter estimation of this problem is related to NLP problem.

5.2 Cost function

Generally, parameter estimation of nonlinear systems is formulated as a task of minimization of cost function. The cost function in our research was stated as the sum of differences between experimentally measured and simulated data.

$$\delta = \sum_{i=0}^{T} \left| y_{pred}(i) - y_{\exp}(i) \right| \tag{15}$$

In our case, the experimentally measured data were replaced by simulated data using the nominal values of the model parameters obtained from [44], see Appendix A. Initial concentration of the studied metabolites: ornithine, citrulline, arginine and urea, were taken from the same source as the nominal values of the parameters.

5.3. Used algorithms and their settings

Three variants of optimization algorithms, called Genetic Algorithm, Differential Evolution, Self Organizing Migrating Algorithm have been used in the experiments.

To find the model parameters that give the best fit to experimental data using GA, we varied population size and mutation factor.

For the DE approach, the impact of population size on the algorithm performance was firstly studied. Then, we investigated the influence of factor F, which controls the amplification of the differential variation. The above-mentioned settings with the minimum cost function value were used for identification the best value of CR, the crossover constant. The details of the experiments are described in the section Results.

In SOMA experiments, we varied only population size (PopSize) due to time-consuming calculations.

The minimum of cost function value was used as a quality measure of every set of algorithm settings.

The experiments were conducted using *Mathematica 7*. Each experiment was repeated 40 times. We have used the DERand1Bin version of DE and the AllToOne version of SOMA. All calculations were done using grid computer that includes 16 XServers, each 2x2 GHz Intel Xeon, 1 GB RAM, 80 GB HD i.e. 64 CPUs.

5.4. Results

Two of applied optimization techniques yielded meaningful results. DE and SOMA algorithms were capable of precise parameter estimation of the urea cycle model. In contrast, GA predicted correctly behavior of only three from four metabolites.

As a result of search of parameters that give the best fit to experimental data, the comparison of algorithms performance was carried out. Performance of GA, DE and SOMA is presented in Figure 5.2.

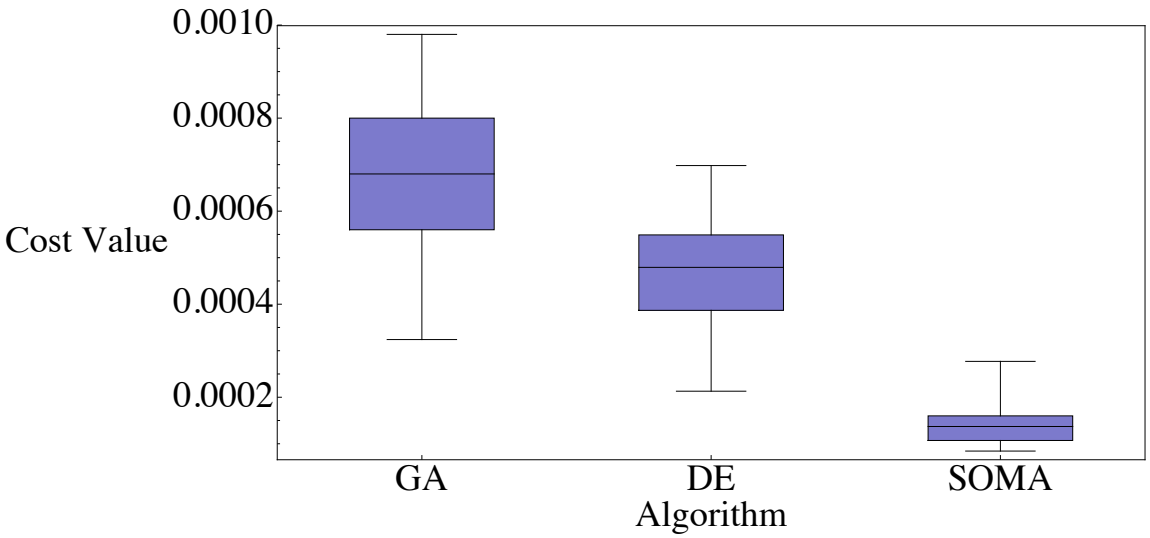

Fig. 5.2: Comparison of the optimization algorithms applied to the urea cycle model

The minimal cost function value 3.24×10^{-4} GA reaches for population size 900. DE gives the best result with F=0.8, CR=0.6 and population size 900. The minimum of cost function value with these settings is 2.13×10^{-4}. In contrast to DE, SOMA reaches the best cost function of 5.61×10^{-5} with PopSize=135. However, in order to compare the performance of these three algorithms, we also take into account number of cost function evaluations. Hence, there have been chosen the results of SOMA simulations with PopSize=90. In this case, the cost function value is 8.43×10^{-5}, which is slightly higher than for PopSize=135 but still lower in comparison with the best DE and GA results. The implemented

experimental setting in the above mentioned simulations are presented in Table 5.1.

Table 5.1 Settings for the algorithms applied to the urea cycle model

GA settings		**DE settings**		**SOMA settings**	
PopSize	900	NP	900	PathLength	3
MutationConstant	0.2	F	0.8	Step	0.11
Generations	150	CR	0.6	PRT	0.1
		Generations	150	PopSize	90
				Migrations	50
				MinDiv	-0.1

5.4.1 GA experiments

To find the model parameters that give the best fit to experimental data using GA, firstly, mutation constant was varied. Then, the most successful value was applied to experiments with varying population size. The minimum of cost function value is used as a quality measure of every set of algorithm settings.

Figure 5.3 shows the impact of mutation constant on cost function value. The mutation constant was varied at value of 0.2, 0.5 and 0.8. We limited our experiments to these values because of the fact that calculations of such complex systems are time consuming. GA yielded the best result with cost function value 3.96×10^{-4} with mutation constant 0.2. For comparison, for mutation constant 0.5 cost function value was 6.45×10^{-4} and for 0.8 cost function value reached only 1.26×10^{-3}.

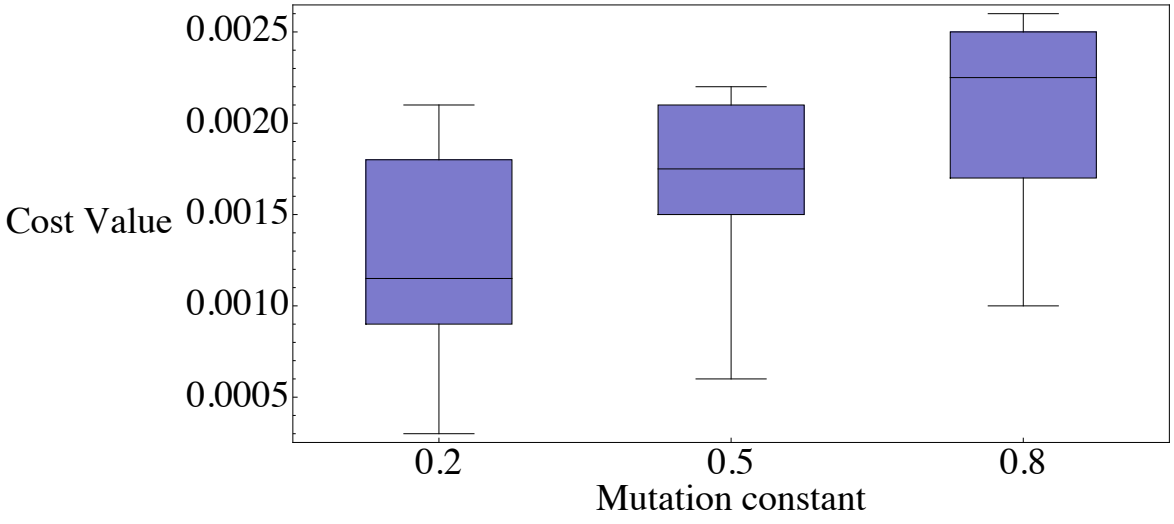

Fig. 5.3: The influence of mutation constant on the cost function value for GA

Despite the fact that the result of calculations was already acceptable, we continued to study GA performance by varying population size. We chose 3 sets of population size 90, 450 and 900, which is equal to 2D, 10D and 20D, where

D is a number of cost function arguments. In the urea cycle model, it is 45. The result can be found in Figure 5.4.

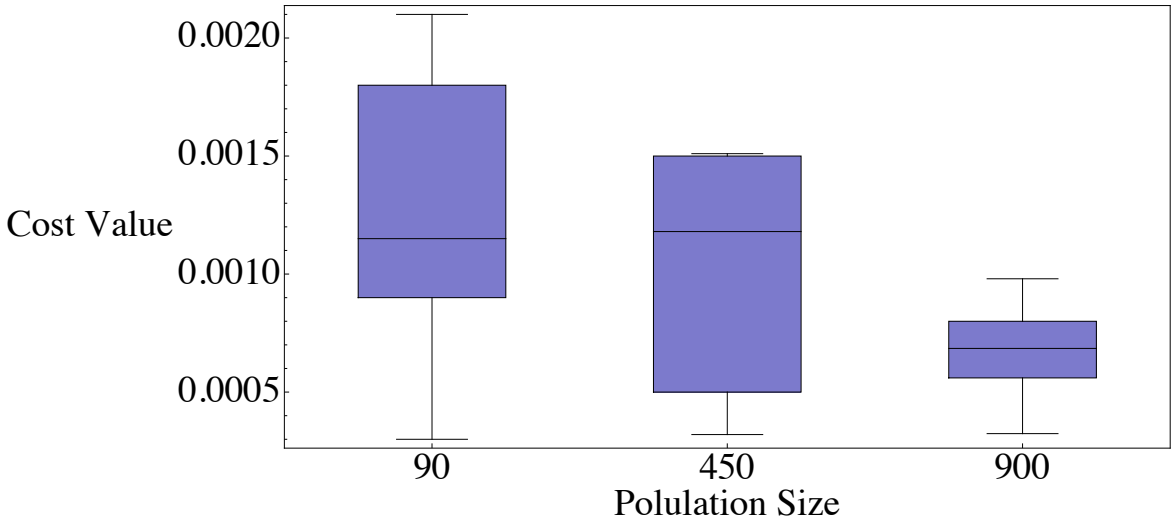

Fig. 5.4: The impact of population size on the cost function value for GA

The best result with minimal cost function value 3.24×10^{-4} reached GA with population size of 900. As can be seen from Figure 5.4, increasing population size 10 times has not given significant improvement in minimizing cost function value.

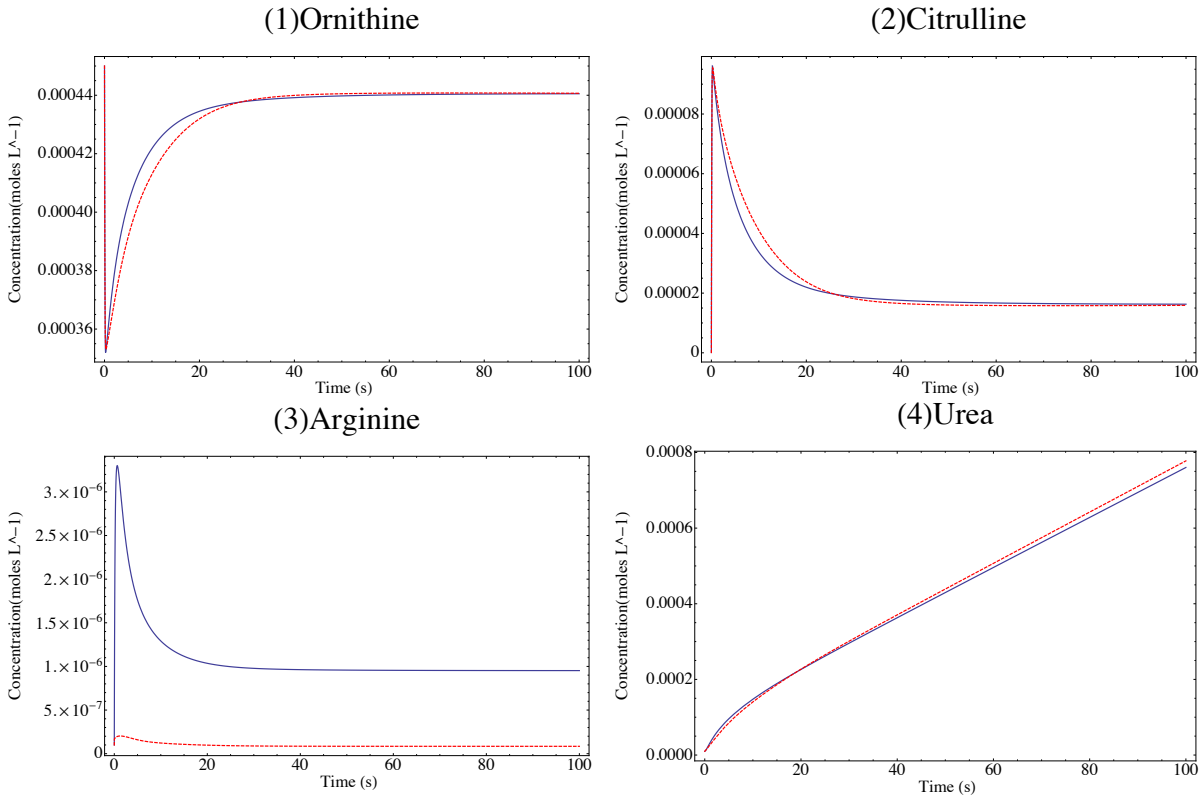

Fig. 5.5: The time courses of (1) ornithine, (2) citrulline, (3) arginine and (4) urea where predicted behavior by GA is dashed and original is solid

In Figure 5.5, the time courses of four main metabolites are presented with original behavior and predicted by GA. We can see that the behavior of three metabolites: ornithine, citrulline and urea, are predicted relatively well. However, the dynamics of arginine was not correctly estimated.

This is exactly case study where we can find not accurate the system dynamics prediction with relatively low cost function value.

5.4.2 DE experiments

To find the model parameters using DE algorithm, we vary population size, the F value and CR. The minimum of cost function value is used as a quality measure of every set of algorithm settings.

Figure 4.1 depicts dependence of cost function value on various population sizes. To investigate the impact of population size, we apply a population size of 90, 450 and 900. These settings are equal to 2D, 10D and 20D, where D is a number of cost function arguments. In our case, it is 45.

We limit the investigation to only 3 sets of population size because of the execution time, which depends on the dimension of the problem.

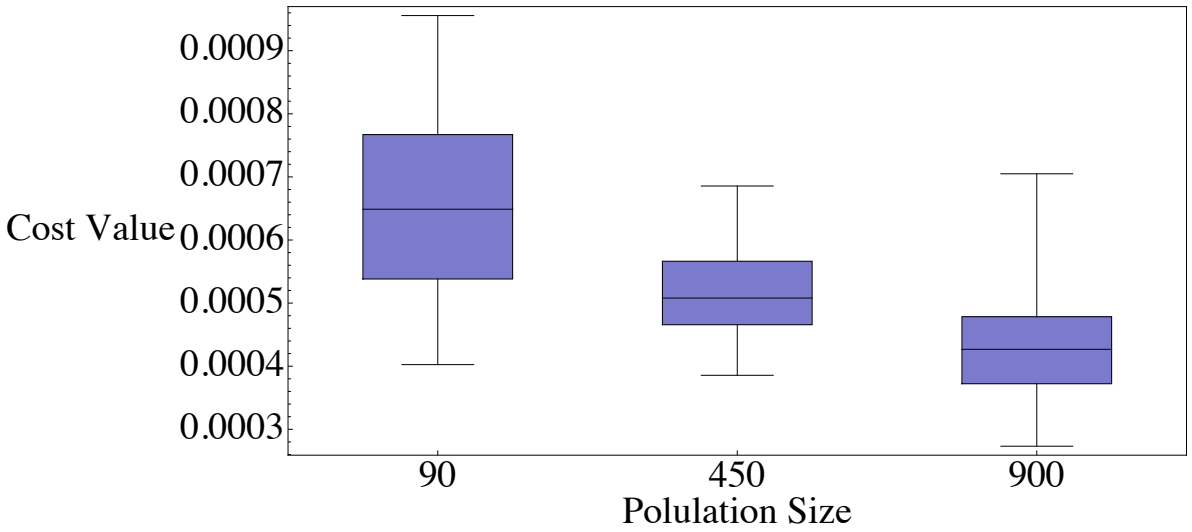

Fig. 5.6: The impact of population size on the cost function value for DE

The boxplots show that a population size of 900 reaches the best minimum result. The average cost function value decreases with increasing population size. However, all results give very low cost function value.

We continue to study the DE performance by varying the values for F (see Figure 5.7) and CR (see Figure 5.8). The influence of the F is tested using three F values: 0.1, 0.5 and 0.8. The CR value is set on 0.5. The DE algorithms yields the best results for F=0.8. Therefore, the best settings F=0.8 and population size of 900 are used for the next investigation.

To find the most successful combination of the algorithm settings, we vary CR from 0.1 to 0.9. Similarly to the above-mentioned experiments, each

calculation is repeated 40 times. Figure 5.8 depicts that CR=0.6 yields the best minimum result. It should be noticed that DE with all values of CR reaches meaningful results with the cost function value from 2.13×10^{-4} to 9.48×10^{-4}.

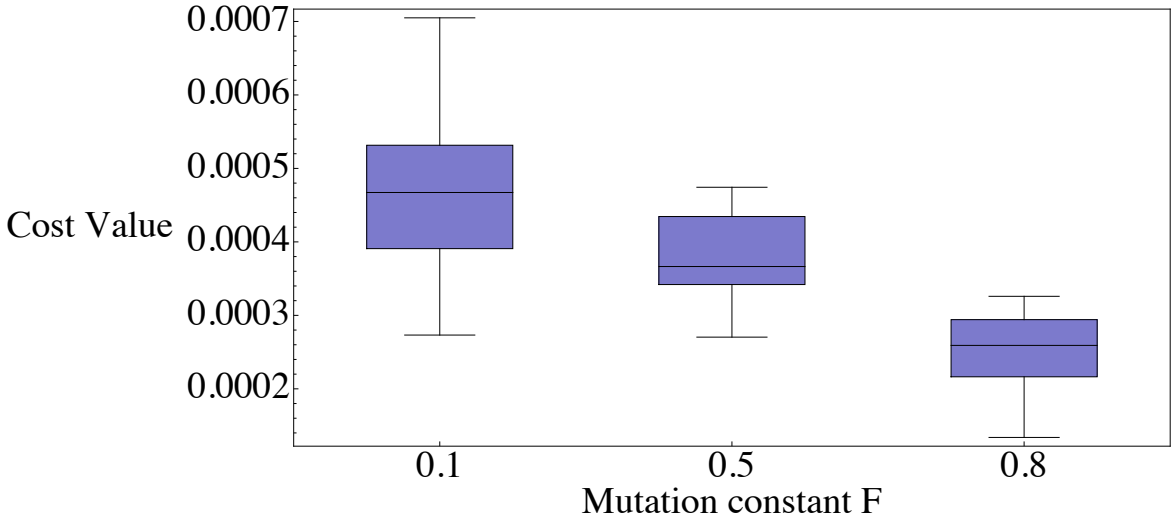

Fig. 5.7: The influence of mutation constant F on the cost function value for DE

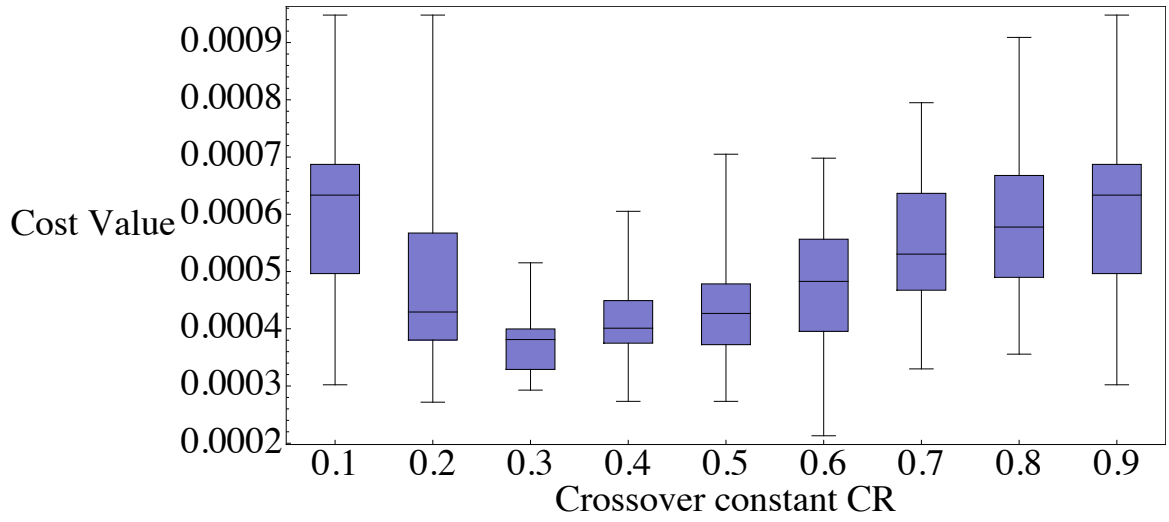

Fig. 5.8: The influence of crossover constant CR on the cost function value for DE

Figure 5.9 shows simulation of the system dynamics using predicted parameters (dashed) together with original parameters (solid). There are time courses of 4 main metabolites concentrations in the urea cycle simulation: ornithine, citrulline, arginine and urea. The figure depicts the best result of DE algorithm with F=0.8, CR=0.6 and population size 900.

The DE algorithm performs very well. It is obvious that parameters of the model are predicted precisely, see Figure 5.9.

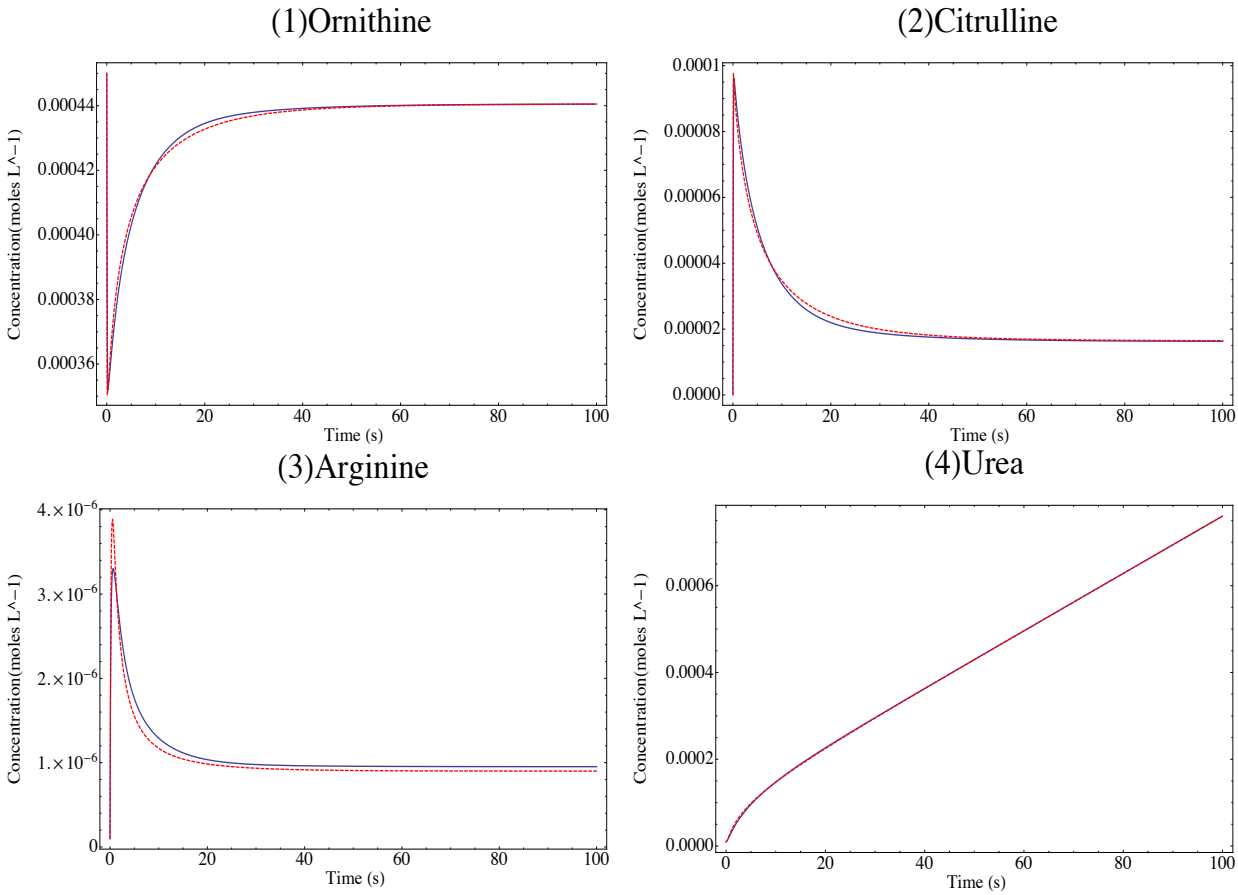

Fig. 5.9: The time courses of (1) ornithine, (2) citrulline, (3) arginine and (4) urea where predicted behavior by DE is dashed and original is solid

5.4.3 SOMA experiments

To define the best model parameters using SOMA algorithm, the population size (PopSize) was varied. The minimum of cost function value was used as a quality measure of every set of algorithm settings.

Similarly to DE, the study was limited to 3 sets of settings with population size of 45, 90 and 135, which equal 1D, 2D and 3D. The choice of population sizes for SOMA algorithm was based on recommendations in [63]. The number of repetitions is again 40. The results of the experiments are shown in Figure 5.10.

The boxplots show that varying PopSize has similar impact on estimation process as in case of DE - the higher population size, the lower cost function value. SOMA yields the minimum of cost function value 5.61×10^{-5} with PopSize=135. The worst result of SOMA algorithm is 2.77×10^{-4}, which is slightly higher than the best result of DE algorithm 2.13×10^{-4}.

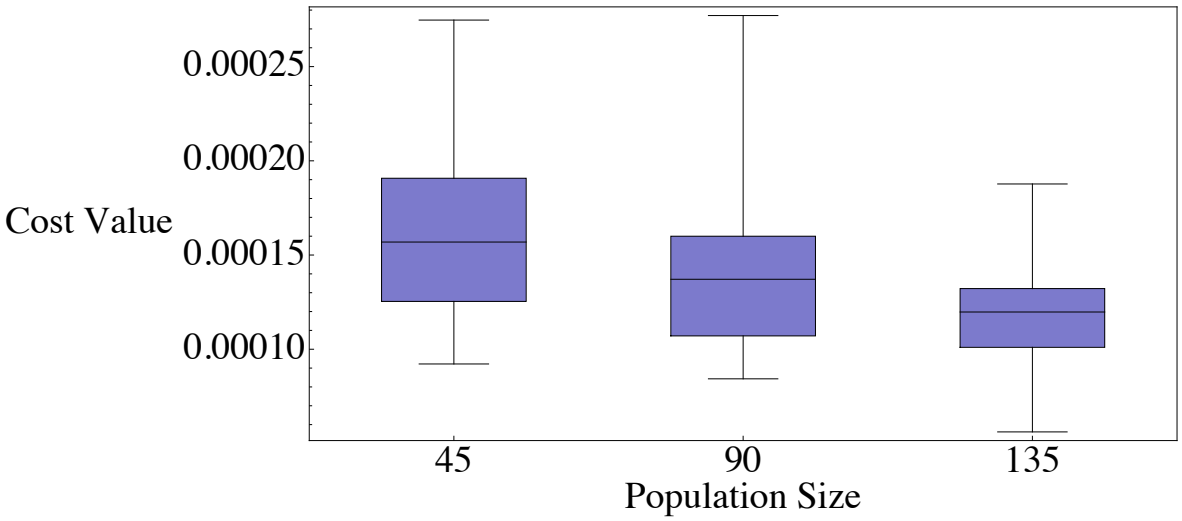

Fig. 5.10: The impact of population size (PopSize) on the cost function value for SOMA

Figure 5.11 depicts the time courses of 4 urea cycle metabolites with predicted and original parameters. The behavior of the system is predicted precisely. The estimated parameters values can be found in Appendix A.

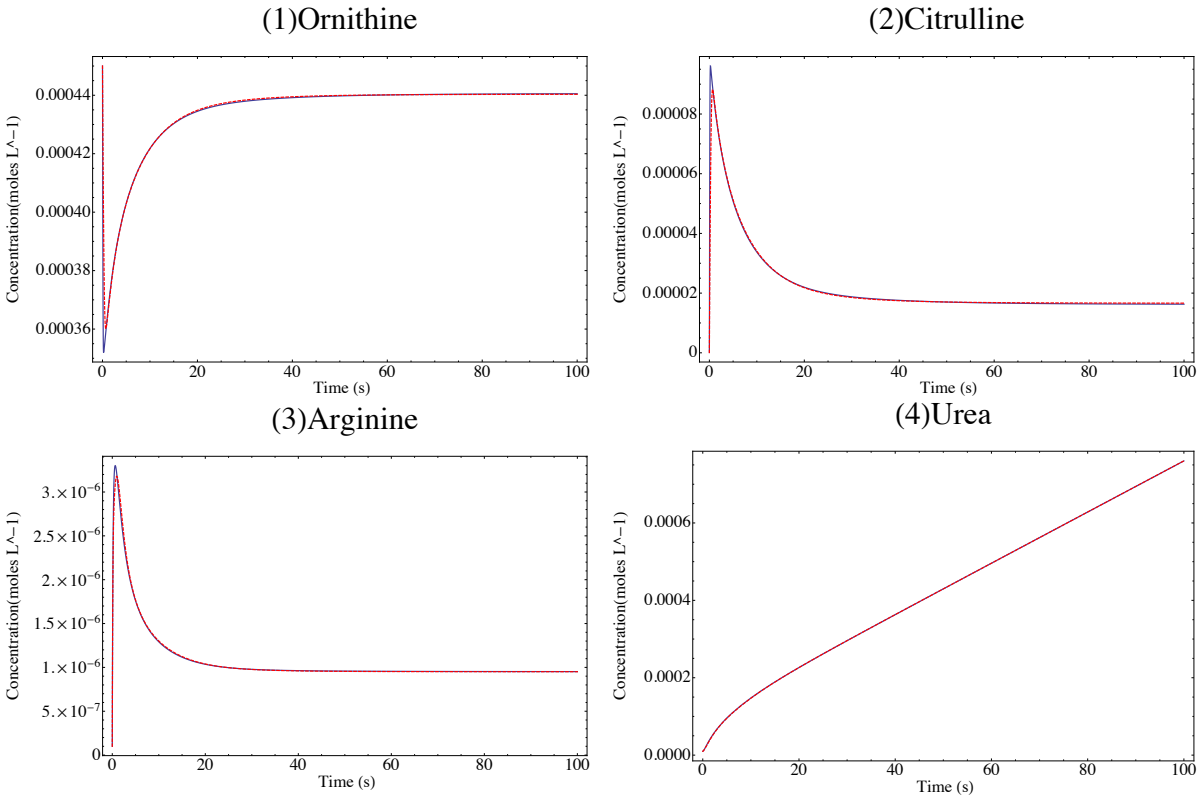

Fig. 5.11: The time courses of (1) ornithine, (2) citrulline, (3) arginine and (4) urea where predicted behavior by SOMA is dashed and original is solid

5.5 Conclusions for the urea cycle experiments

Two of applied optimization techniques yielded meaningful results. DE and SOMA algorithms were capable of precise parameter estimation of the urea cycle model. In contrast, GA predicted correctly behavior of only three from four metabolites.

Interestingly, increasing population size in GA case has not given significant improvement in minimizing cost function value. Varying algorithms settings could improve the DE and SOMA algorithms performance. In both cases DE and SOMA, increasing population size gave significantly better results. On the other hand, it required large computational effort. Considering computational time, the most time-consuming calculations were observed in SOMA simulations. However, it should be noted that SOMA provided the best performance in estimating parameters.

Taking into account that DE and SOMA algorithms performed better in comparison with GA, and the fastest was DE, it is reasonable to apply DE in experiments with limited computational time.

The urea cycle experiment shows that in case where GA relatively failed, other evolutionary techniques such as DE and SOMA definitely succeeded.

6 CASE STUDY 2. METABOLIC MODELING OF A THREE-STEP PATHWAY

In present case study, a well-studied biochemical system, called a three-step pathway is considered. Three evolutionary techniques were applied to estimate parameters of the model.

6.1 A three-step pathway model

A three-step pathway is a common biological model with known parameter values (see Figure 6.1 [23]) being considered as a benchmark for *in silico* experiments.

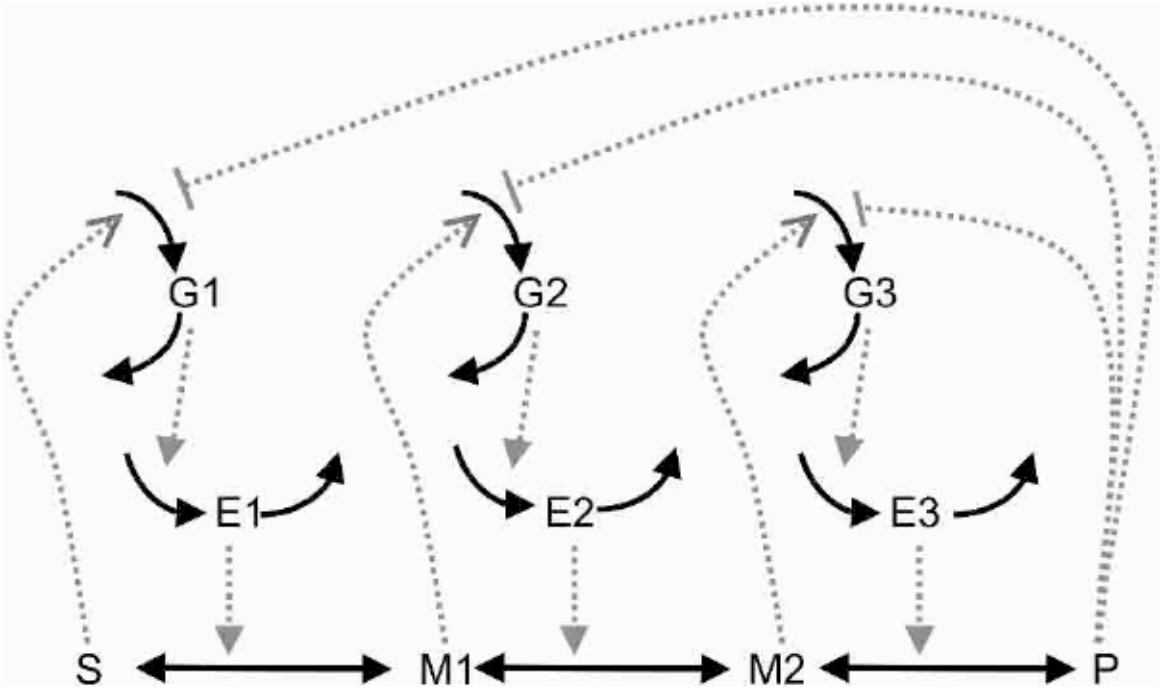

Fig. 6.1: The three-step pathway model where solid arrows are mass flows, dashed-kinetic regulation, S is the pathway substrate, P is the pathway product. M1, M2 and M3 are intermediate metabolites; E1, E2 and E3 are the enzymes; G1, G2 and G3 are the mRNA species for the enzymes

This model was originally investigated using stochastic methods by Mendes [64]. Moles [23] extended this study to 16 experiments with different initial data of S (substrate) and P (product). The author additionally used initial vector for 36 estimated parameters. The best performing algorithm was Evolution Strategy using Stochastic Ranking (SRES). In that study, author reported that DE failed in solving this problem. The cost function value for DE was 151.779 whereas

for the best performing algorithm SRES cost function value was 0.0013. For additional information, see [23].

In our study, we have considered the same system of differential equations, which can be found in Appendix B. Upper, and lower bounds for kinetic parameters are 10^{-12} and 10^{6}, respectively. The exception is the Hill coefficients (*ni*, *na*) where the range is (0.1, 10). Values of P and S are 0.05 and 0.1, respectively.

6.2 Cost function

Parameter estimation of nonlinear systems, in our case it is 36-dimention system, commonly can be formulated as task of minimization of cost function. In present study, the cost function was formulated as the sum of absolute differences between data with predicted by algorithms parameters and data with nominal parameters. Predictions for time courses were conducted every second with final time of 120 seconds.

6.3 Used algorithms and their settings

The DERand1Bin version of DE, two versions of SOMA (AllToOne and AllToOne Rand) and GA were applied in the present case study. Each experiment was run 35 times. All calculations were performed using grid computer that includes 16 XServers, each 2x2 GHz Intel Xeon, 1 GB RAM, 80 GB HD i.e. 64 CPUs.

DE was applied to define the model parameters. The result was compared with the existed study. We used the same control parameters for DE as in Moles's study. It is mean that population size was 450, and number of generation was 5000. We also extended study by varying population size, mutation constant F, crossover constant CR and upper bound.

For SOMA experiments, we varied number of migrations, population size (PopSize) and upper bound.

In GA case, we studied only influence of population size. For comparison with other algorithms, we used the same number of cost function evaluations.

The minimum of cost function value has been used as a quality measure of every set of algorithm settings.

6.4 Results

We have considered three evolutionary techniques: DE, two versions of SOMA and GA. The predicted dynamics for each algorithm are presented in the following sections. Comparison of the algorithms performance is presented in Figure 6.2. The efficiency of particular method was judged based on cost function value. As have been mentioned above, the problem consisted of 36 kinetic parameters.

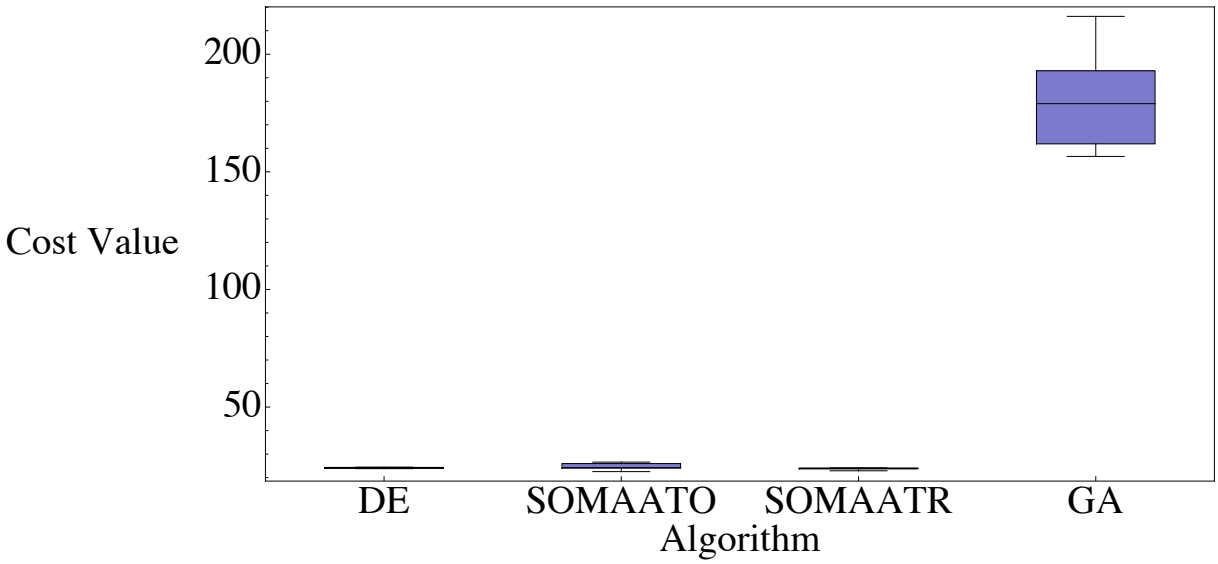

Fig. 6.2: Comparison of the algorithms performance applied to a three-step pathway

DE predicted the behavior of the studied system with cost function value 23.816 for population size of 450. Varying population size has not improved DE performance. The most successful combination of mutation and crossover constants were F=0.2, CR=0.2. However, it also did not give significant decrease of cost function value. Only varying of upper bounds gave valuable impact on cost function value.

In case of SOMA experiments, our results show that AllToOne version was able to define dynamics of the system with cost function value 22.557, which is better in comparison with AllToOne Rand version (22.903). The further investigation regarding upper bounds gave the minimal cost function value for 10^1-upper bound was 6.291. And time courses of the systems species were predicted correctly.

GA defined the system parameters with minimal cost function 161.894 for population size of 450. Taking into account time-consuming calculations, population size as control parameter was varied only. Increasing population size to 1000 improved minimal cost function value to 113.685.

Table 6.1 Settings for the algorithms applied a three-step pathway model

GA settings		**DE settings**		**SOMA settings**	
PopSize	450	NP	450	PathLength	3
MutationConstant	0.5	F	0.2	Step	0.11
Generations	5000	CR	0.2	PRT	0.1
		Generations	5000	PopSize	150
				Migrations	200
				MinDiv	-0.1

6.4.1 DE experiments

To define the model parameters using DE, both mutation constant F and crossover constant CR were varied to minimize the cost function. These settings were applied for experiments with population size of 450 and 1000. The obtained results are presented in Figure 6.3 for mutation constant F and in Figure 6.4 for crossover constant CR.

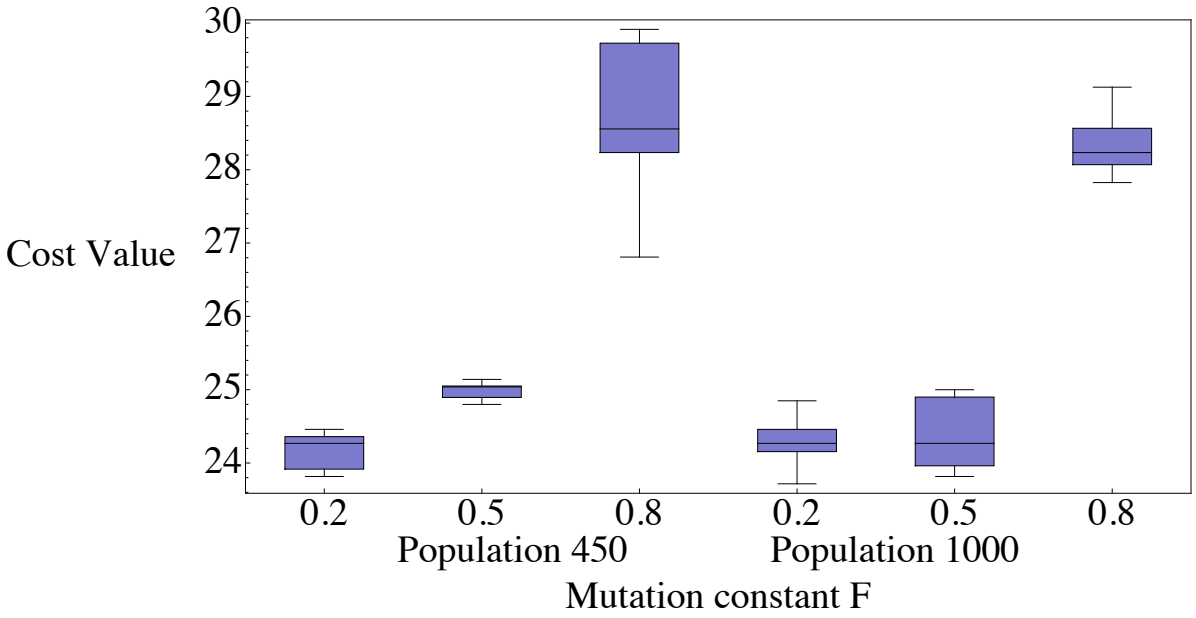

Fig. 6.3: The impact of constant F on cost function value for DE

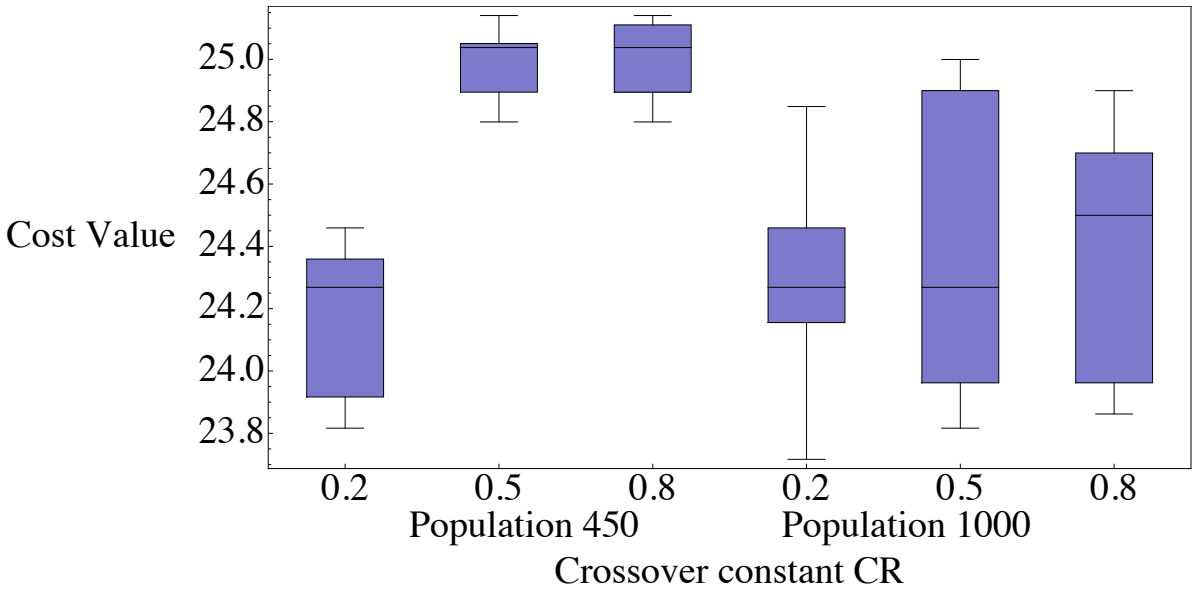

Fig. 6.4: The impact of constant CR on cost function value for DE

The boxplots show that combination F=0.2 and CR=0.2 are the most successful settings with minimal, in given experiments, cost function value. Speaking about population size, increasing it from 450 to 1000 did not give significant improvement in minimizing of cost function value. The best minimal cost function value of DE for population size of 450 was 23.816 and for population size of 1000 was 23.716. Taking into account that in paper [23] cost function was calculated every 6 seconds and in our case every second, cost function value in our DE experiments is much lower with the same number of cost function evaluations. For further experiments we used the above-mentioned constants F and CR with population size of 450.

Figure 6.5 shows simulation of the system dynamics using predicted parameters (dashed) and nominal parameters (solid). We provide an example of successfully predicted metabolite behavior (M2) and not accurately predicted behavior (G2).

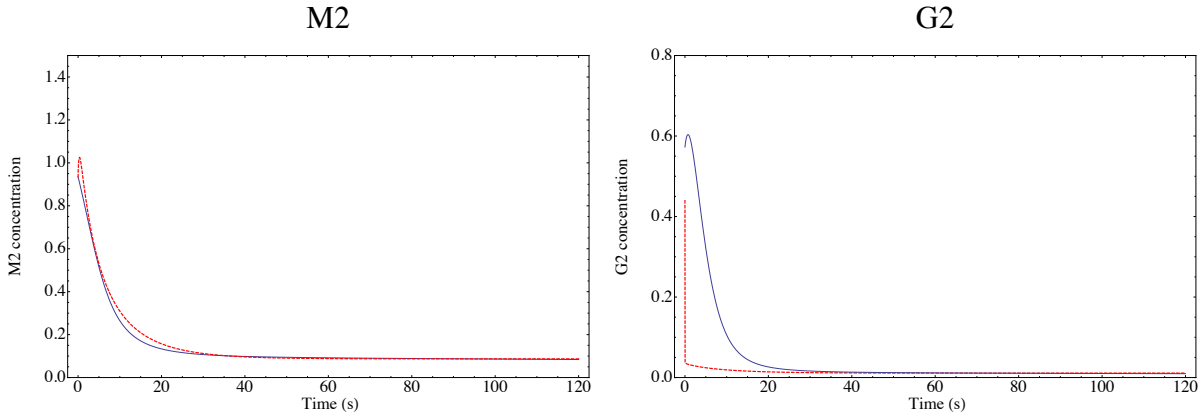

Fig. 6.5: The time courses of M2 and G2 species of the system where predicted behavior by DE is dashed and original is solid (10^6-upper bound)

DE with relatively high number of cost function evaluations was able to only partially predict behavior of systems elements, which agrees with the results from [23]. Presumably, the main reason is extremely wide range of lower and upper bounds for systems parameters.

During calculations with different algorithms settings, we noticed that range of cost function values in case of initial (randomly generated) population was very narrow. Then, we varied upper bound to see how the range of initial and final population changed, see Figure 6.6 and Figure 6.7.

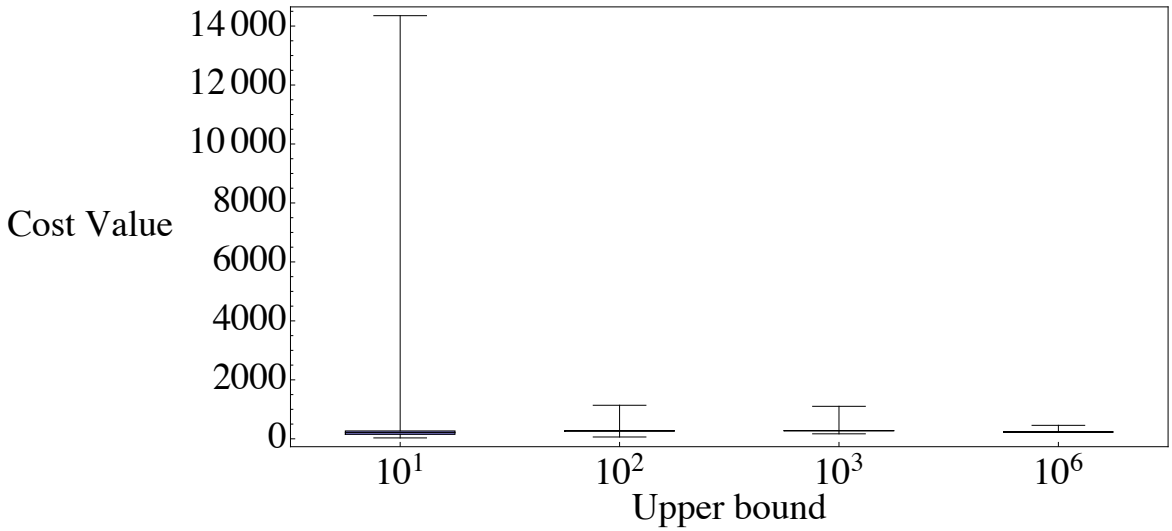

Fig. 6.6: Range of cost function values for initial population of DE

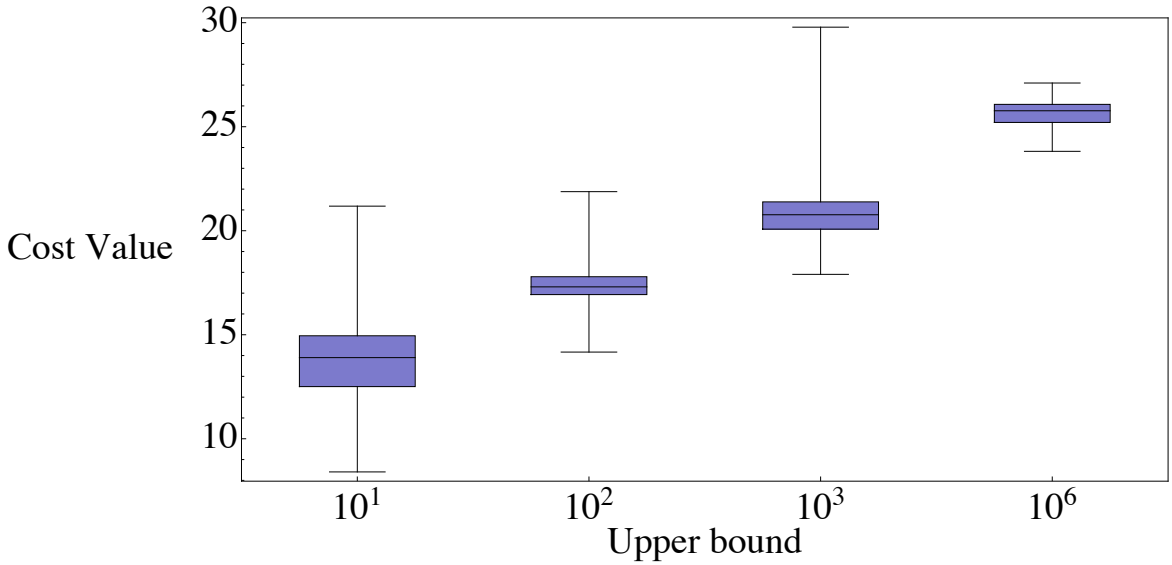

Fig. 6.7: Range of cost function values for final population of DE

The minimal and maximal cost function values for initial population, in case of 10^6-upper bound, are unusually near to each other. The cases 10^3 and 10^2-upper bounds are similar. On the other hand, for 10^1-upper bound, we can see wide range of cost function values, which is typical for random generating of initial population. Figure 6.7 depicts that cost function value of final population presumably decreases with decreasing of upper bound.

The minimal cost function value for 10^1-upper bound was 8.406. For this case, the behavior of the system with predicted and nominal parameters are presented in Figure 6.8.

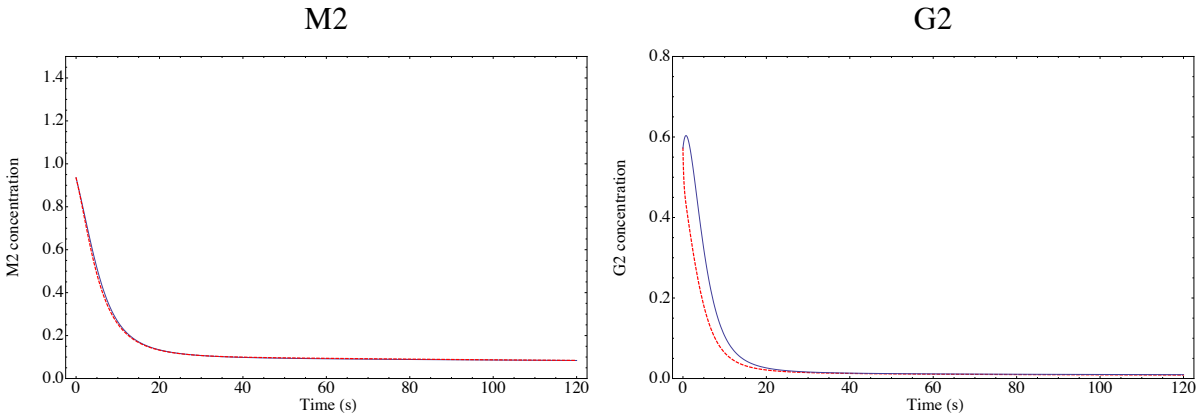

Fig. 6.8: The time courses of M2 and G2 species of the system where predicted behavior by DE is dashed and original is solid (10^1-upper bound)

In the Figure 6.8 we can see the improvement in prediction of time courses for M2 and G2 species. Other species were also predicted correctly.

6.4.2 SOMA experiments

Two versions of SOMA, called AllToOne (SOMAATO) and AllToOne Rand (SOMAATR), were applied to a three-step pathway with different algorithm settings for upper bound 10^6. Population size (PopSize) and number of migrations were varied for both versions. Obtained results are presented in Figure 6.9 and Figure 6.10.

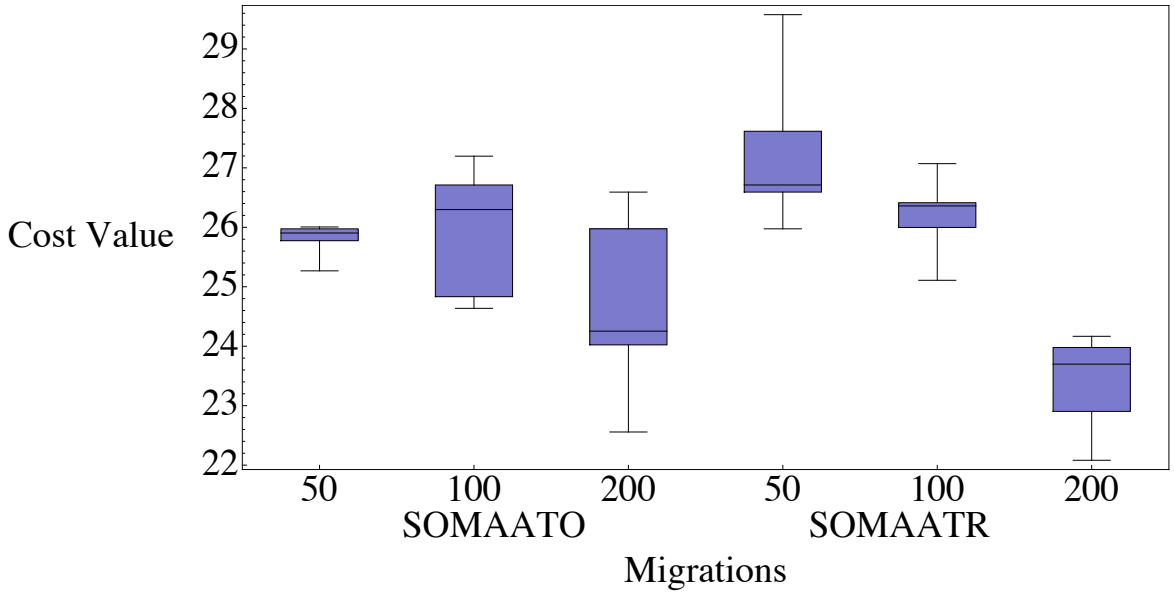

Fig. 6.9: The impact of number of migrations on the cost function value for SOMA

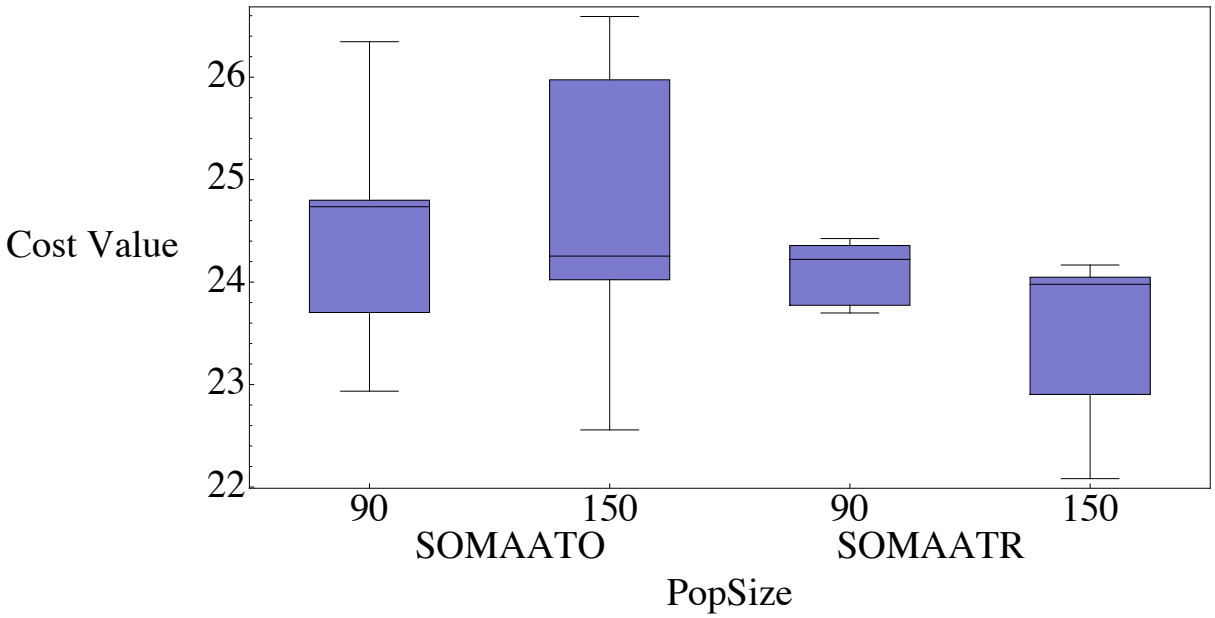

Fig. 6.10: The impact of population size (PopSize) on the cost function value for SOMA

The best minimal cost function value 22.557 was obtained in case of SOMAATO for migrations number of 200, which is slightly better in comparison with SOMAATR and DE experiments. Then, using migrations number of 200, we investigated the impact of population size, again for both versions. Figure 6.10 shows that in case of SOMAATO population size did not have significant impact on the cost function value. For SOMAATR, it slightly improved the result with cost function value 22.903. Therefore, SOMAATO reached better results in comparison with SOMAATR. For upper bound 10^6, SOMAATO was able to predict dynamics of only 4 from 8 studied elements of the system. Two of them are presented in the Figure 6.11.

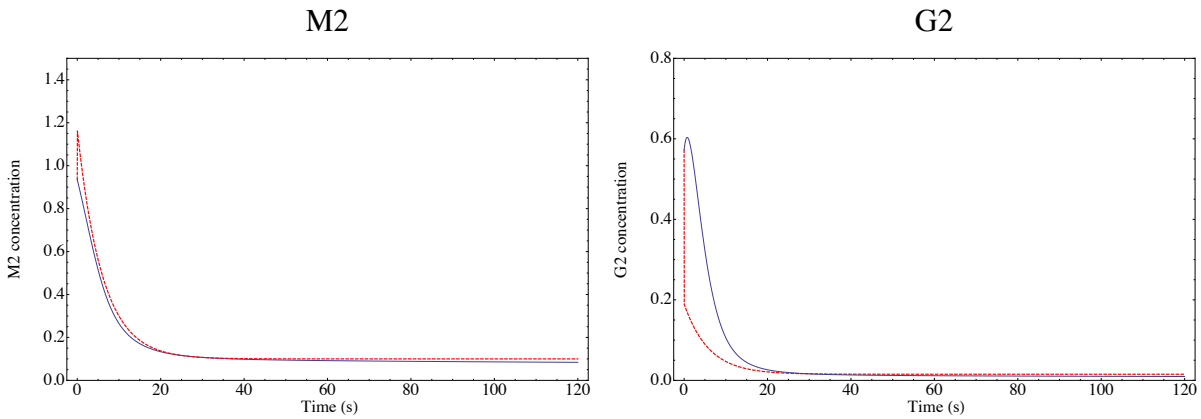

Fig. 6.11: The time courses of M2 and G2 species of the system where predicted behavior by SOMA is dashed and original is solid (10^6-upper bound)

Similarly to DE experiments, we varied upper bound for SOMAATO, see Figure 6.12 and Figure 6.13. In case of 10^6-upper bound, the range of cost function values for initial population was also narrow. For 10^1-upper bound, there is a wide range of cost function values for initial population. In case of final population, again, we can see decreasing of cost function value for 10^1, 10^2 and 10^3-upper bounds.

The minimal cost function value for 10^1-upper bound was 6.291, which is lower in comparison with the DE results. For this case, the behavior of the system with predicted and nominal parameters are presented in Figure 6.14.

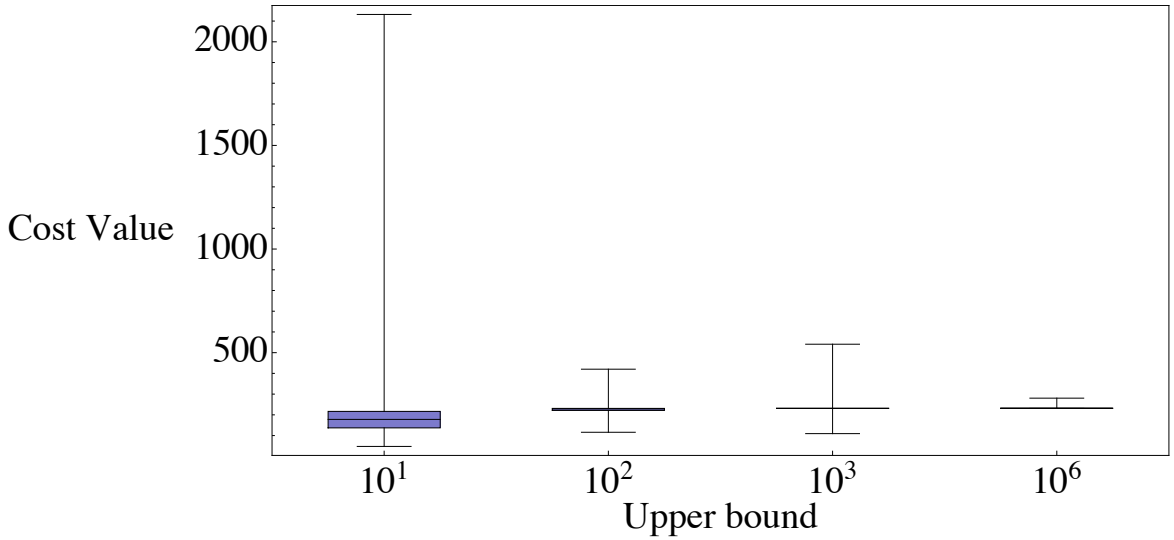

Fig. 6.12: Range of cost function values for initial population of SOMA

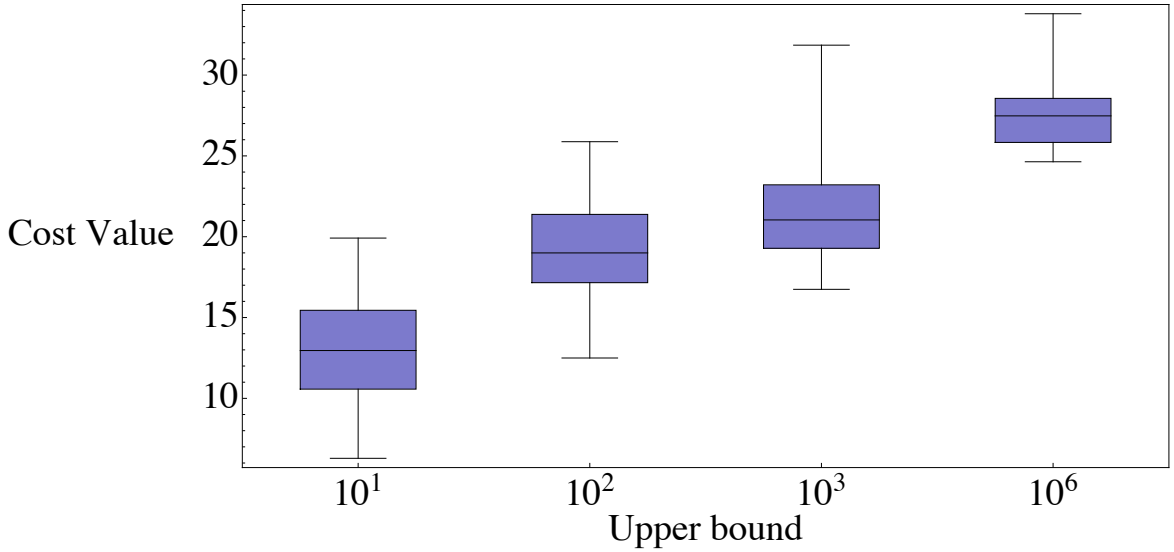

Fig. 6.13: Range of cost function values for final population of SOMA

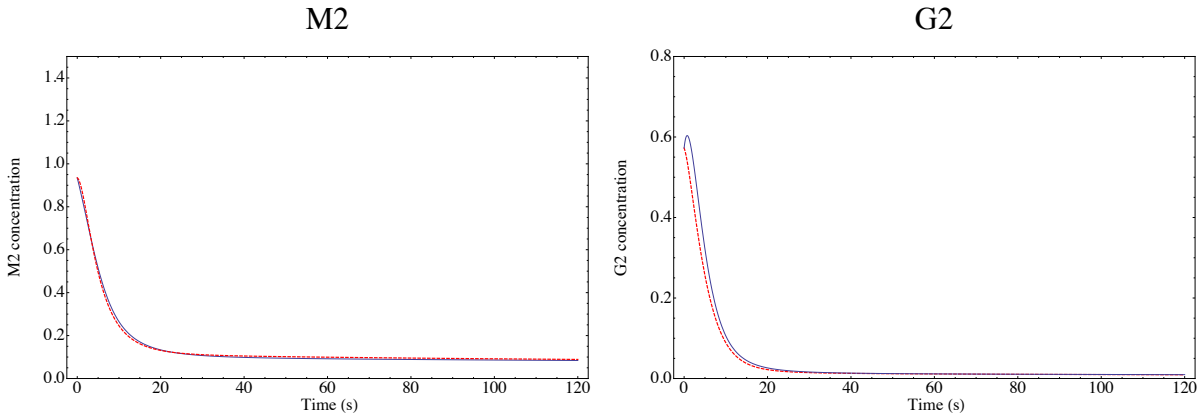

Fig. 6.14: The time courses of M2 and G2 species of the system where predicted behavior by SOMA is dashed and original is solid (10^1-upper bound)

6.4.3 GA experiments

In case GA algorithm, only one control parameter was varied, population size. Mutation constant was set to 0.5. Initial results gave us clear understanding that GA was much less accurate in defining model parameters compared to DE and two versions of SOMA. The minimal cost function value for population size of 450 was 161.894. With the same number of cost function evaluations, DE best result was 23.816. Increasing population size for GA, the result was improved to 113.685 (see Figure 6.15).

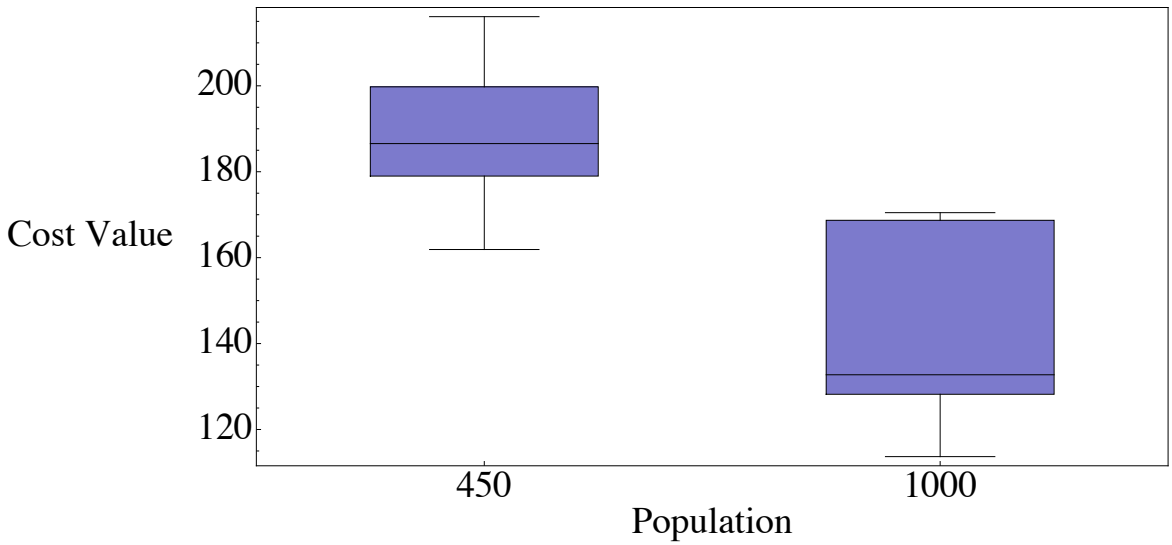

Fig. 6.15: The impact of population size on the cost function value for GA

Taking into account the fact that GA performance was significantly worse in comparison with other algorithms, we decided not to continue investigation with GA algorithm in this case study.

6.5 Conclusions for Case study 2

For parameter estimation of a three-step pathway, we have considered three evolutionary techniques: DE, SOMA and GA.

DE with relatively high number of cost function evaluations was able to only partially predict behavior of the systems species. Decreasing of upper bound to 10^1 gave significant improvement in parameter estimation. DE predicted the behavior of the studied system with cost function value 23.816 for population size of 450, which is better result in comparison with DE result in paper [23].

In case of SOMA experiments with two versions AllToOne and AllToOne Rand, our results showed that the AllToOne version was able to define dynamics of the system with minimal cost function value 22.557, which is better than AllToOne Rand and DE results but still are not enough good as SRES from [23]. The minimal cost function value for 10^1-upper bound was 6.291. And time courses of the systems species were predicted correctly.

From our point of view, the main reason that our results and the results from paper [23] are different is the fact that the authors used artificially an initial vector for initial population whereas our experiments included only randomly generated initial population.

In addition to our experiments, not accurate prediction of the system dynamics in case upper bound 10^6 could be because of extremely wide range of lower and upper bounds for systems parameters. The algorithms were not able to define parameters in such enormous search space in reasonable time. The second possible reason could be high non-linearity of the system.

7 CASE STUDY 3. METABOLIC MODELING OF GLYCOGENOLYSIS IN SKELETAL MUSCLE

To define parameters of large-scale metabolic model using evolutionary techniques, we have chosen a dynamic model of the glycogenolytic pathway to lactate in skeletal muscle.

7.1 A model for glycogenolysis in skeletal muscle

This model was developed by Melissa J. Lambeth and Martin J. Kushmerick [64] to understand the role of glycogenolysis and glycolytic fluxes in muscle energy metabolism. This model fully describes energy metabolism of skeletal muscle.

The model consists of the rate equations for 12 biochemical reactions from glycogen to lactate. The system is represented by the system of differential equations based on Michaelis-Menten kinetics. The system of ODEs is presented in Appendix C. Metabolite concentrations (initial conditions) and kinetic parameters for each enzyme were taken from the original paper [65].

Overall number of kinetic parameters was 90. It means that this problem can be related to NLP problem.

7.2 Cost function

Similarly to previous two case studies, the cost function was formulated as the sum of absolute differences between data with predicted by algorithms parameters and data with nominal parameters. Predictions for time courses were conducted every second with final time of 100 seconds.

7.3 Used algorithms and their settings

For this case study, we applied three evolutionary techniques: the DERand1Bin version of DE, SOMA AllToOne version and GA. Each experiment was run 35 times. All calculations were performed using the same grid computer.

For DE experiments, mutation constant F, crossover constant Cr and population size were varied. In SOMA case, only population size was varied because of time-consuming calculations. For GA experiments, mutation constant and population size were changed.

The minimum of cost function value was used as a quality measure of every set of algorithm settings.

7.4 Results

Three evolutionary techniques: DE, SOMA and GA have been considered in this case study. DE and SOMA yielded meaningful results in parameter

estimation. GA was not capable of accurate prediction of the system dynamics. The predicted dynamics can be found in the following sections devoted to particular algorithm.

As a result of search of parameters that give the best fit to experimental data, the comparison of algorithms performance was carried out. The minimum of cost function value is used as a quality measure of every set of algorithm settings. Taking into account number of cost function evaluations, the population size 270 is comparable with DE population size 1800.

Comparison of the algorithms performance is presented in Figure 7.1.

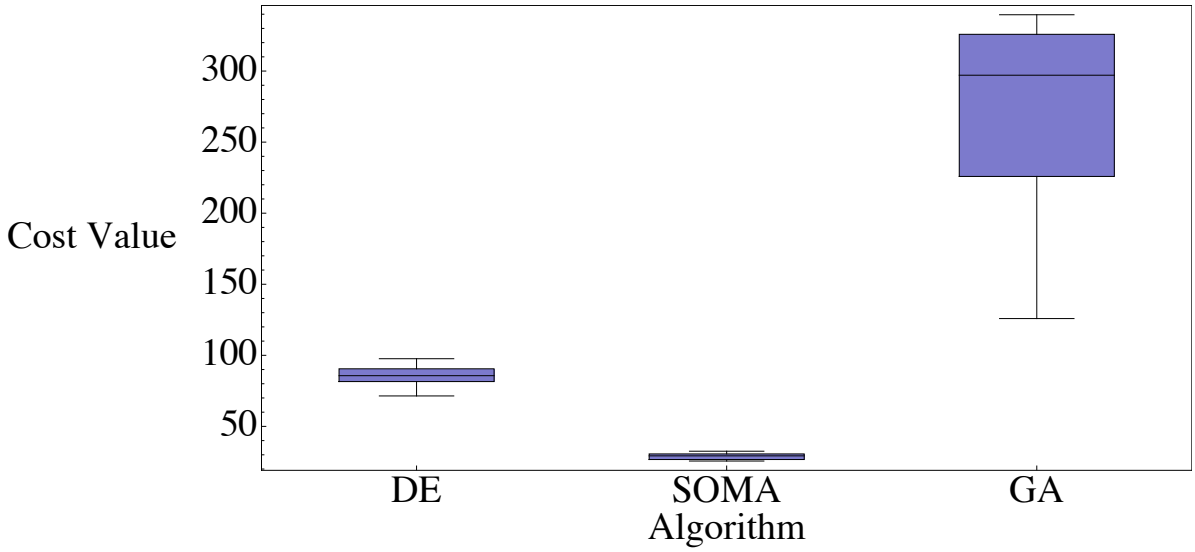

Fig. 7.1: Comparison of the optimization algorithms applied to the glycogenolysis model

SOMA reaches the best result with minimal cost function value 25.624. DE gives the minimal cost function value 71.426 with population size of 1800. In comparison with DE and SOMA, GA performed worse with the best minimal cost function value 125.861 for population size of 1800.

The best implemented algorithms settings are presented in Table 7.1.

Table 7.1 Settings for the algorithms applied to the glycogenolysis model in skeletal muscle

GA settings		**DE settings**		**SOMA settings**	
PopSize	1800	NP	1800	PathLength	3
MutationConstant	0.5	F	0.2	Step	0.11
Generations	200	CR	0.2	PRT	0.1
		Generations	200	PopSize	270
				Migrations	50
				MinDiv	-0.1

7.4.1 DE experiments

To define the model parameters that give the best fit to experimental data using DE, we varied different control parameters of the algorithm. Firstly, we set CR (crossover constant) to value of 0.2 and varied F (mutation constant) at points 0.2, 0.5 and 0.8. The initial choice of CR value was made due to the fact that in previous experiments the most successful value for crossover constant was 0.2. The population size was 180, which is equal to 2D where D=90 (number of the system parameters). The result can be seen in Figure 7.2.

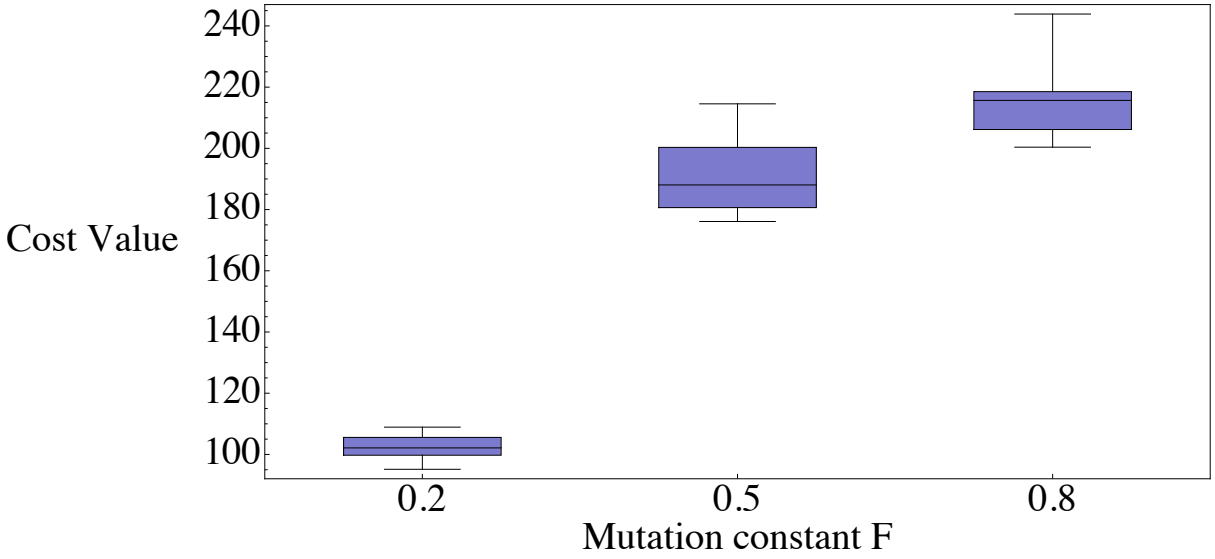

Fig. 7.2: The influence of mutation constant F on DE performance

Figure 7.3 depicts that the most successful value of F is 0.2 with cost function value 95.146. Then, to check if varying constant CR could improve the result, we apply DE with the following values of CR: 0.2, 0.5 and 0.8.

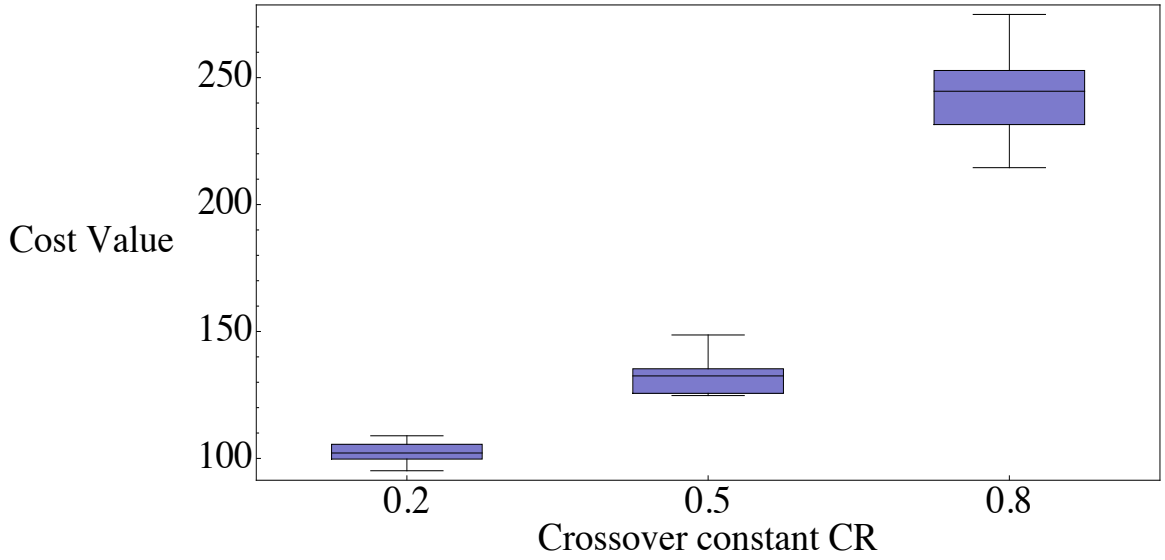

Fig. 7.3: The influence of crossover constant CR on DE performance

The boxplots show that the most successful combination of control parameters for DE in this case F=0.2, CR=0.2.

We continue to search for the best DE settings by applying population size of 180, 900 and 1800. These settings are equal to 2D, 10D and 20D, where D is a number of cost function arguments. In our case, it is 90.

Similar to the previous experiments, we limit the investigation to only 3 sets of population size because of the execution time, which depends on the dimension of the problem. In this case, the system includes 90 parameters that characterize the system as large-scale.

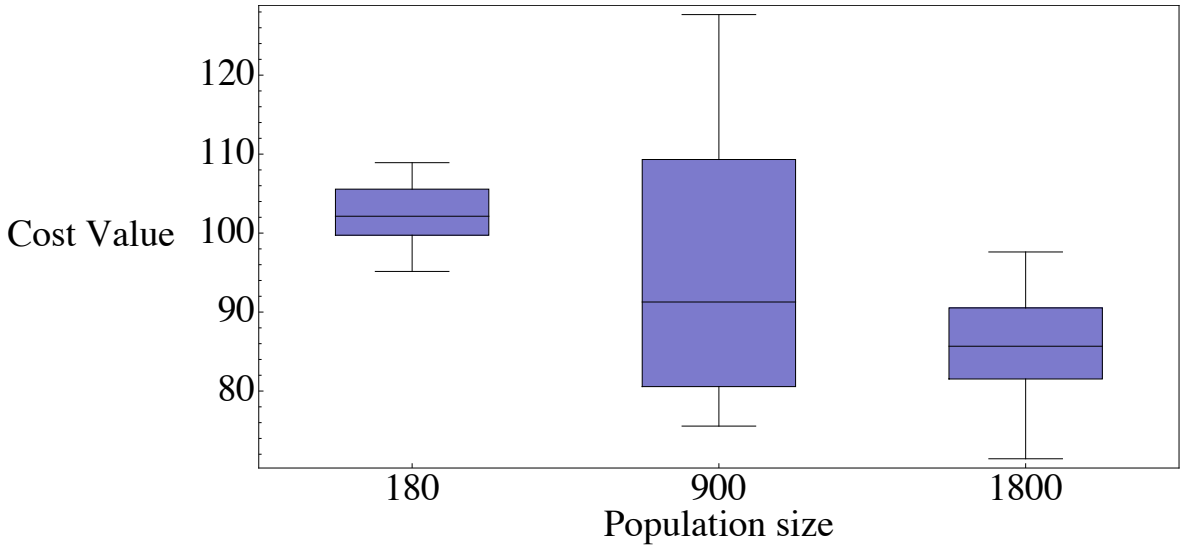

Fig. 7.4: The impact of population size on the cost function value for DE

The boxplots show that cost function value significantly decreases with increasing population size. DE reached the best minimal cost function value 71.426 with population size of 1800. As have been mentioned above, the experiment was limited to 3 sets of population size. Presumably, this result could be improved by increasing cost function evaluations. However, on this stage of our investigation, this result is acceptable taking into account that the problem is extremely complex with high number of the system parameters.

Time courses of main metabolites in glycogenolysis of skeletal muscle can be seen in the following figures. It should be noted that DE was able to predict the time courses relatively precisely.

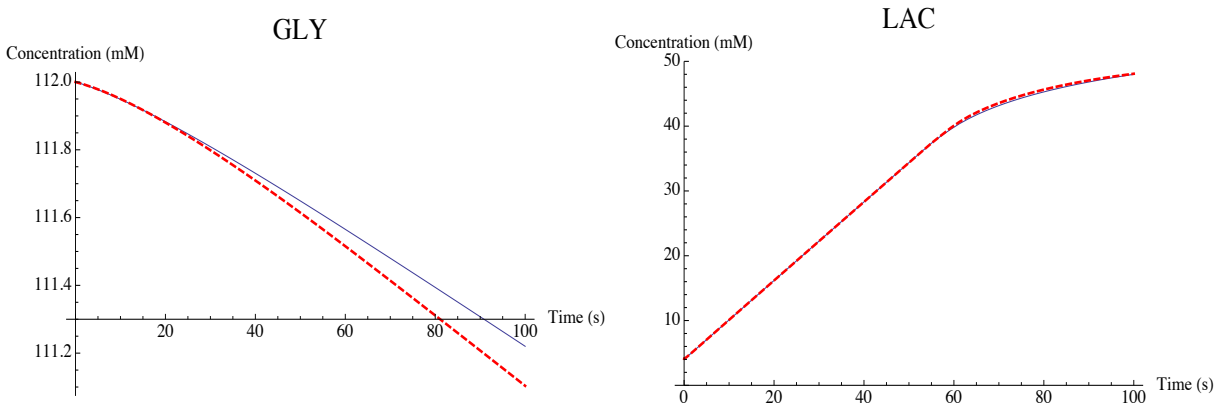

Fig. 7.5: The time courses of glucose (GLY) and lactate (LAC) where predicted behavior by DE is dashed and original is solid

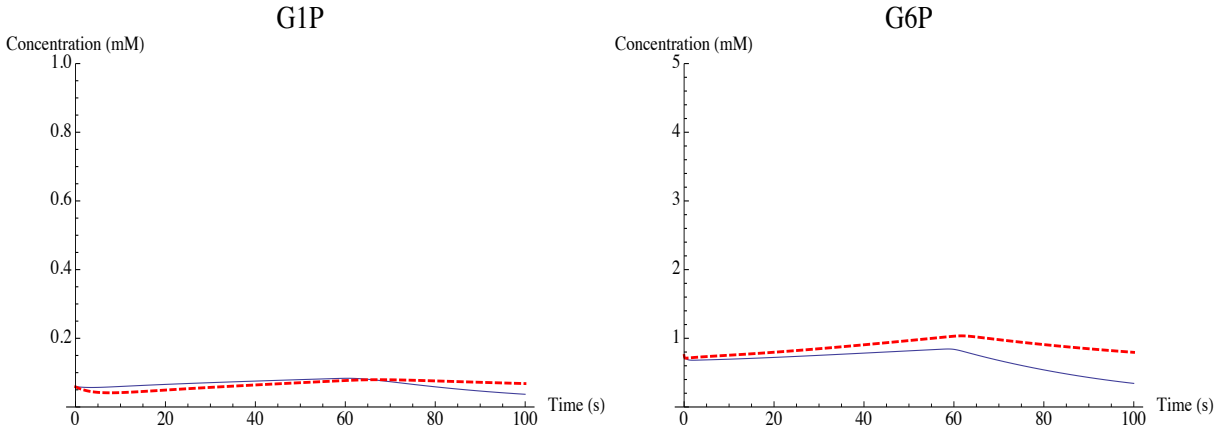

Fig. 7.6: The time courses of glucose 1-phosphate (G1P) and glucose 6-phosphate (G6P) where predicted behavior by DE is dashed and original is solid

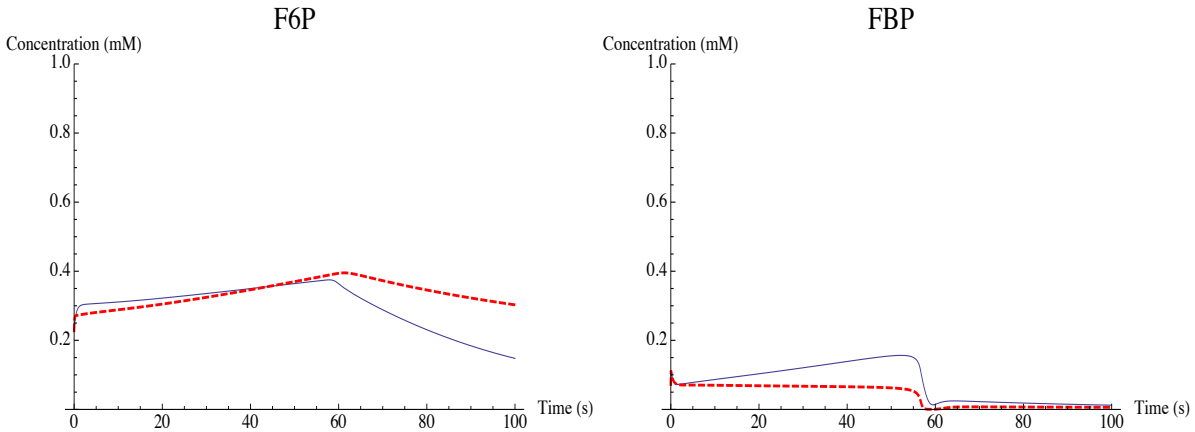

Fig. 7.7: The time courses of fructose 6-phosphate (F6P) and fructose 1,6-biphosphate (FBP) where predicted behavior by DE is dashed and original is solid

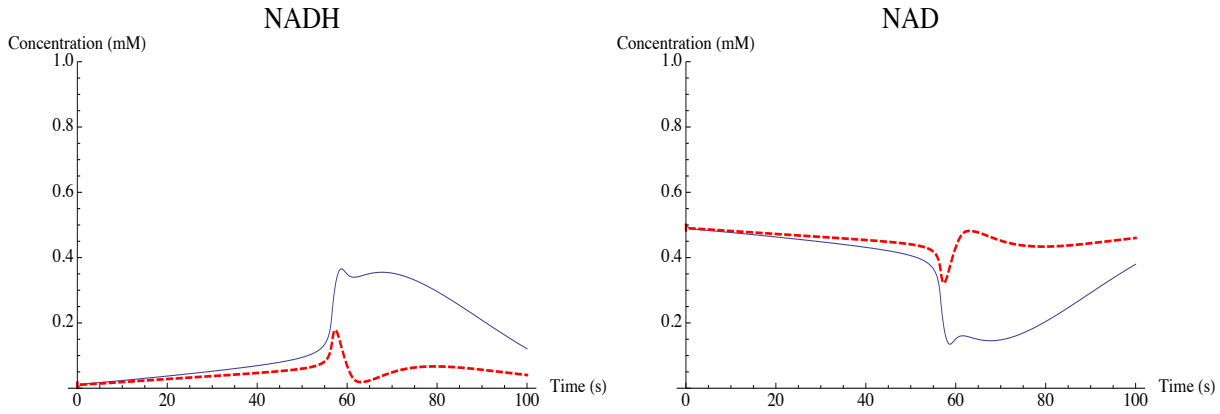

Fig. 7.8: The time courses of NADH and NAD where predicted behavior by DE is dashed and original is solid

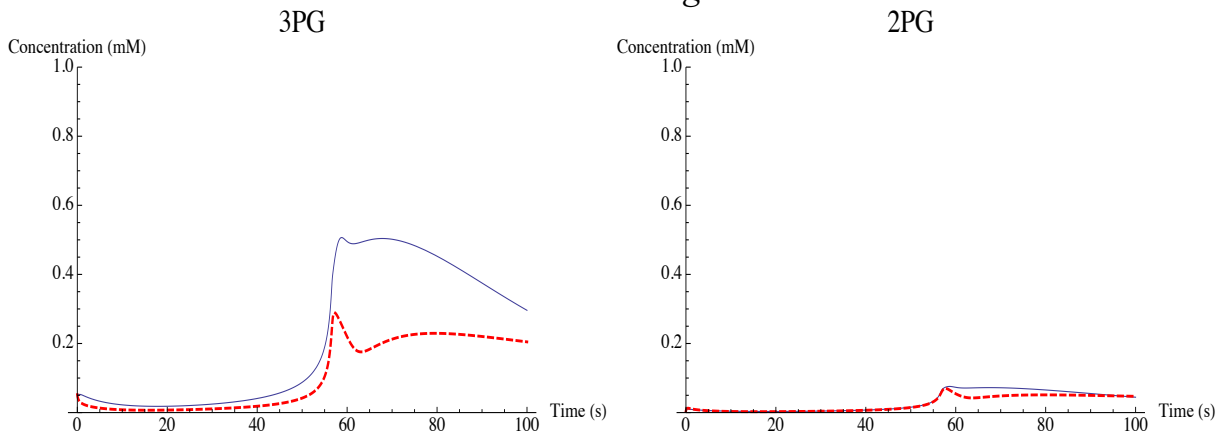

Fig. 7.9: The time courses of glycerate 3-phosphate (3PG) and glycerate 2-phosphate (2PG) where predicted behavior by DE is dashed and original is solid

Overall, the time courses of metabolites were predicted accurately. There are certain differences between original and predicted time courses in case of NADH, NAD, GAP and 3PG. However, these differences were minimal. Moreover, the dynamics was predicted correctly.

7.4.2 SOMA experiments

To define the model parameters that give the best fit to experimental data using SOMA, population size (PopSize) was varied. To compare SOMA results with DE results, we applied 3 sets of PopSize 90, 180 and 270. Each experiment was repeated 40 times. The results are presented in Figure 7.11.

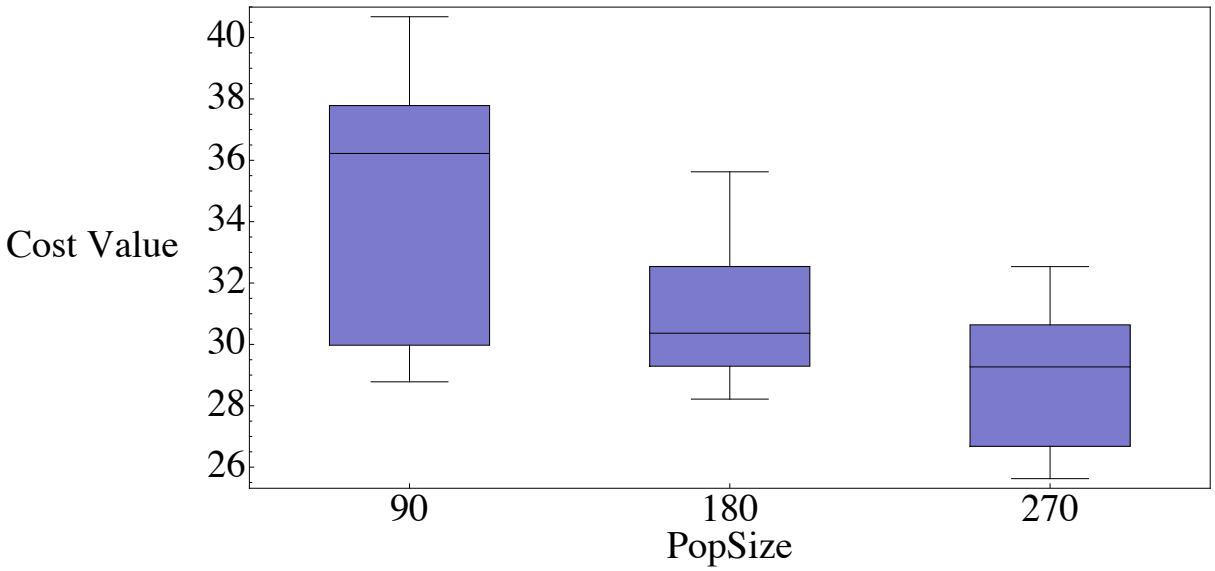

Fig. 7.10: The impact of population size (PopSize) on the cost function value for SOMA

SOMA yields the minimum of cost function value 25.624 with PopSize=270. However, it should be noted that the minimal cost function values for PopSizes 90 and 180 are 28.780 and 28.216, respectively. It means that SOMA reached relatively low cost function value with less number of cost function evaluations in comparison with DE.

The time courses of metabolites are presented in the following figures.

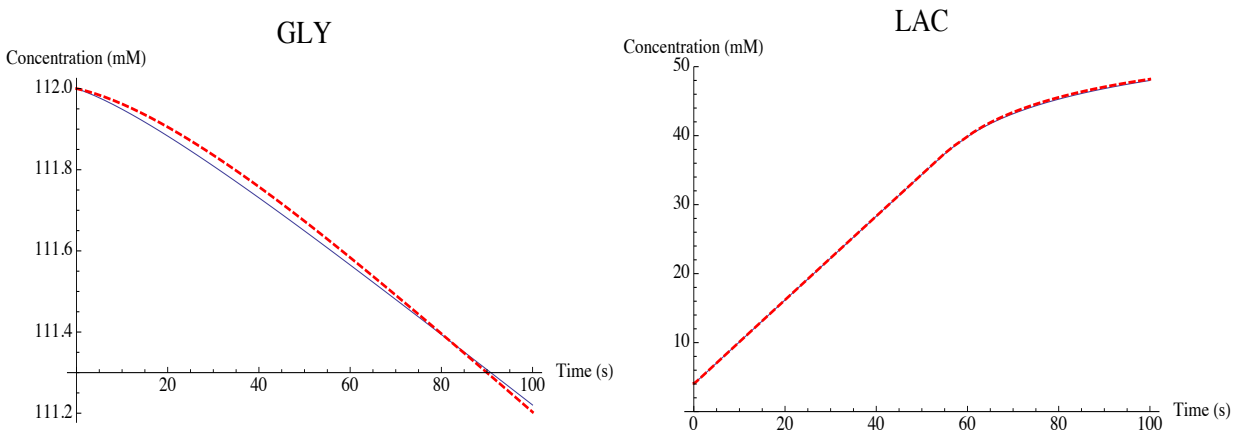

Fig. 7.11: The time courses of glucose (GLY) and lactate (LAC) where predicted behavior by SOMA is dashed and original is solid

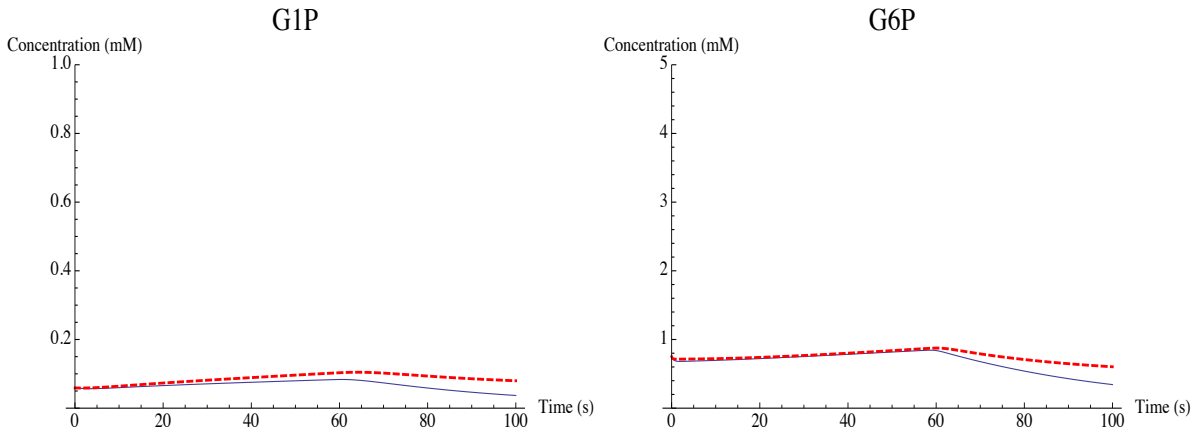

Fig. 7.12: The time courses of glucose 1-phosphate (G1P) and glucose 6-phosphate (G6P) where predicted behavior by SOMA is dashed and original is solid

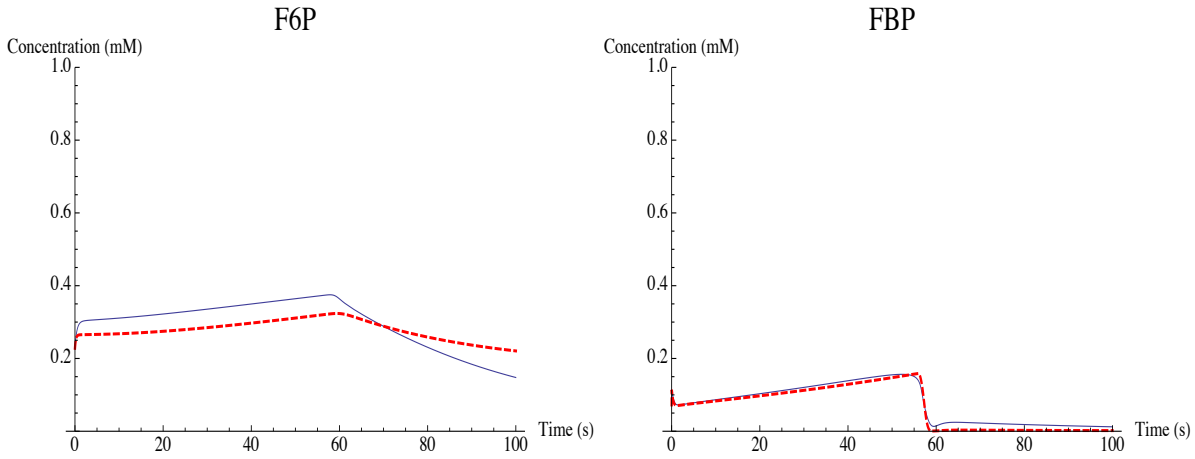

Fig. 7.13: The time courses of fructose 6-phosphate (F6P) and fructose 1,6-biphosphate (FBP) where predicted behavior by SOMA is dashed and original is solid

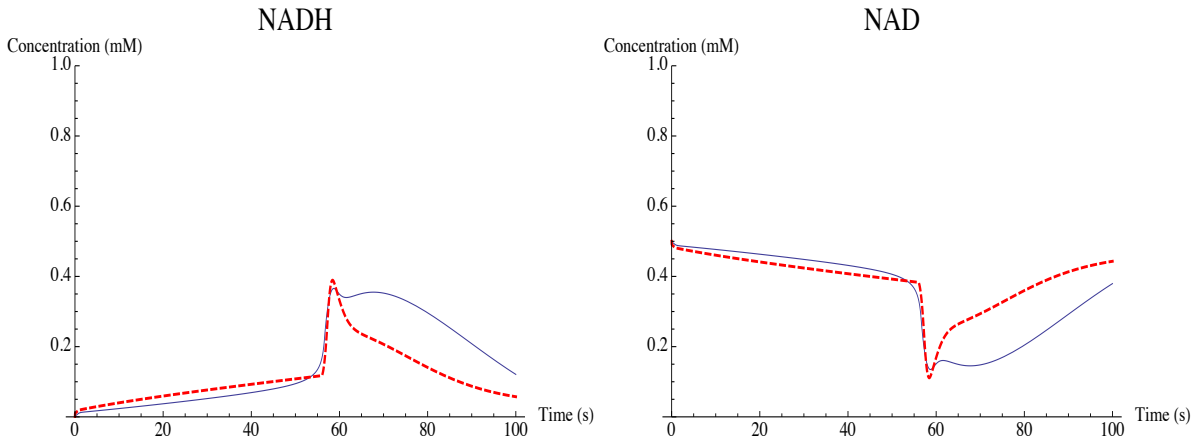

Fig. 7.14: The time courses of NADH and NAD where predicted behavior by SOMA is dashed and original is solid

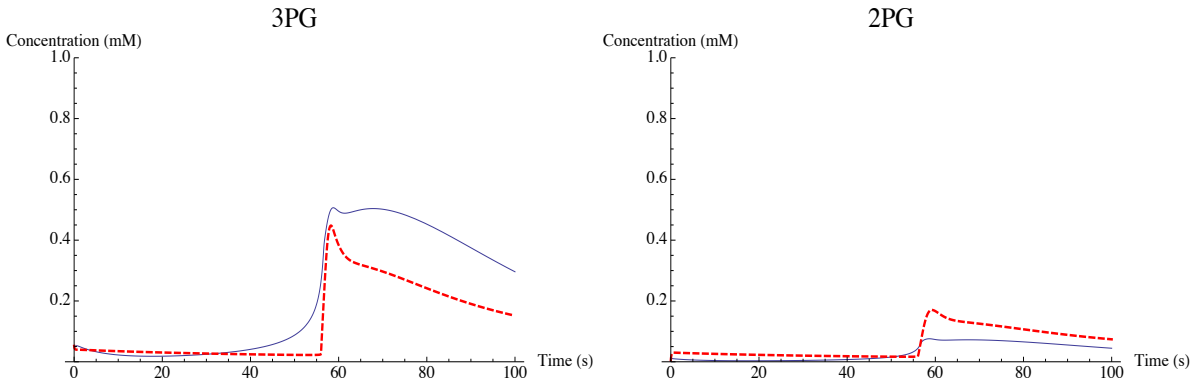

Fig. 7.15: The time courses of glycerate 3-phosphate (3PG) and glycerate 2-phosphate (2PG) where predicted behavior by SOMA is dashed and original is solid

The dynamics of the system was predicted correctly. Similarly to DE, there are certain differences in original and predicted time courses. However, these differences could not be taken into account because the dynamics of metabolites concentration was predicted accurately.

7.4.3 GA experiments

Similarly to the urea cycle case study, we firstly varied mutation constant and, then, applied the most successful value to experiments with varying population size. The minimum of cost function value is used as a quality measure of every set of algorithm settings.

Mutation constant value was set to 0.2, 0.5 and 0.8. Figure 7.18 shows the result of the experiment.

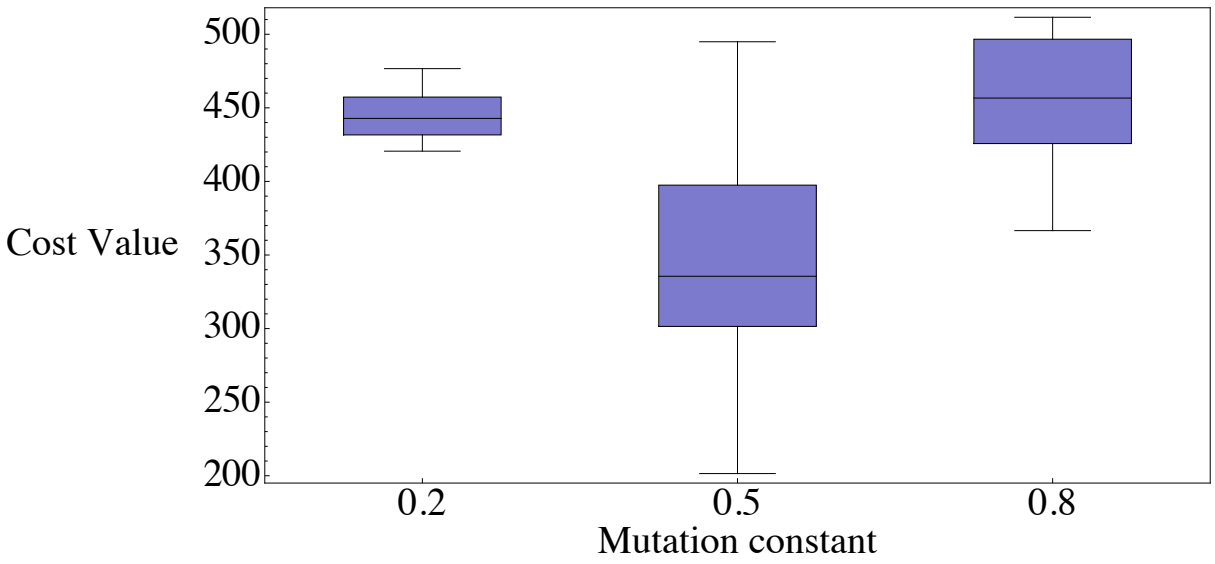

Fig. 7.16: The influence of mutation constant on the cost function value for GA

GA showed the best result with cost function value 201.481 for mutation constant 0.5. The cost function values for mutation constant 0.2 and 0.8 are 420.566 and 366.570, respectively.

To improve the result, we apply different population sizes with the best mutation constant 0.5. Three sets of population sizes were chosen, similarly to DE experiments, 90, 900 and 1800.

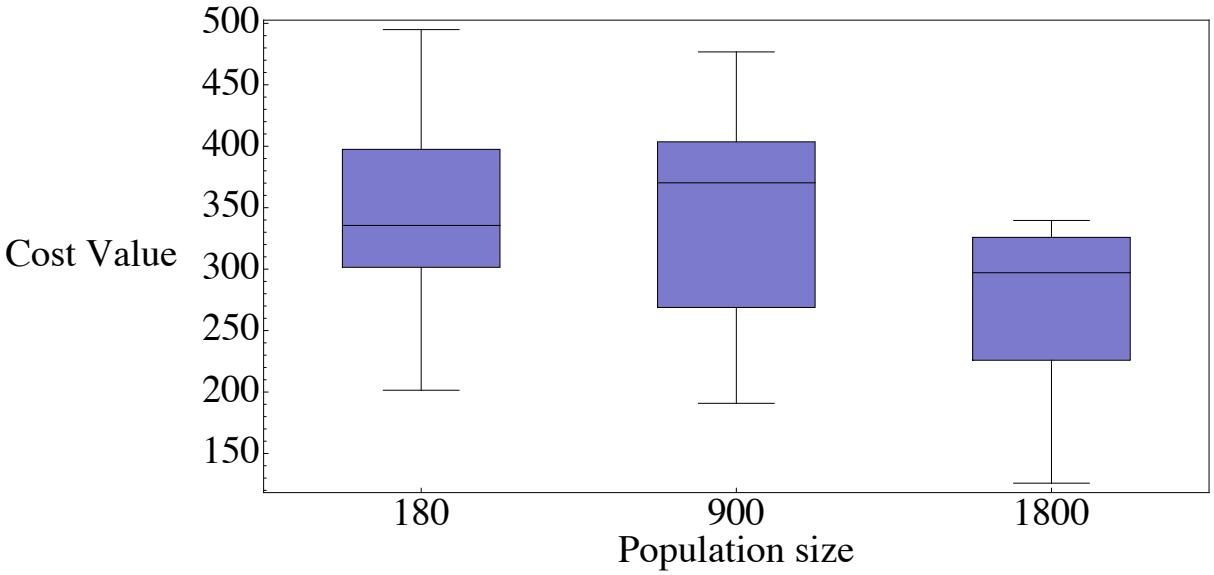

Fig. 7.17: The impact of population size on the cost function value for GA

GA yielded the best minimal cost function value 125.861 with population size of 1800. The result for population size of 900 was 190.834.

The time courses of metabolites are depicted in the following figures.

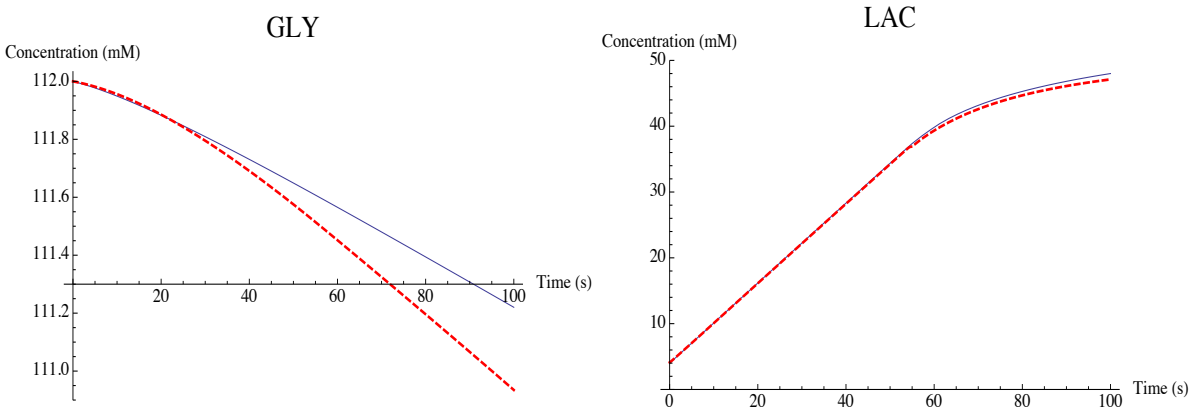

Fig. 7.18: The time courses of glucose (GLY) and lactate (LAC) where predicted behavior by GA is dashed and original is solid

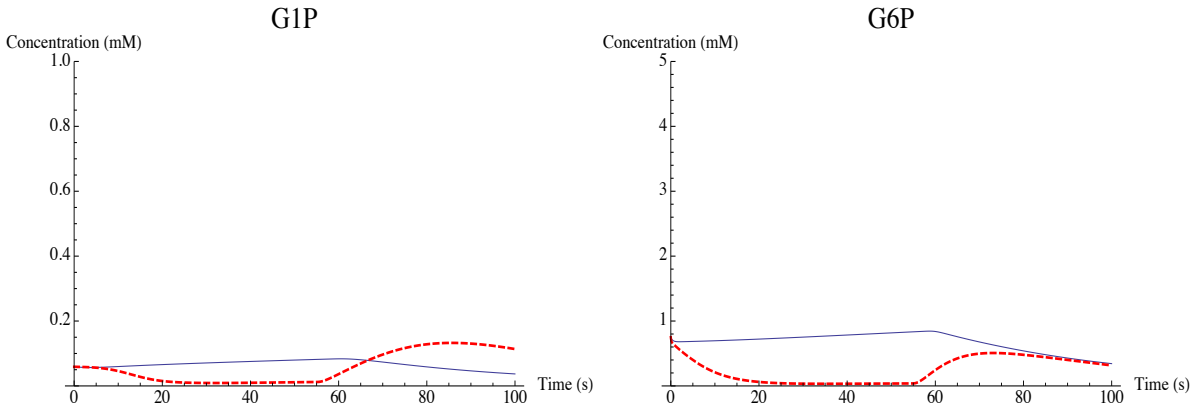

Fig. 7.19: The time courses of glucose 1-phosphate (G1P) and glucose 6-phosphate (G6P) where predicted behavior by GA is dashed and original is solid

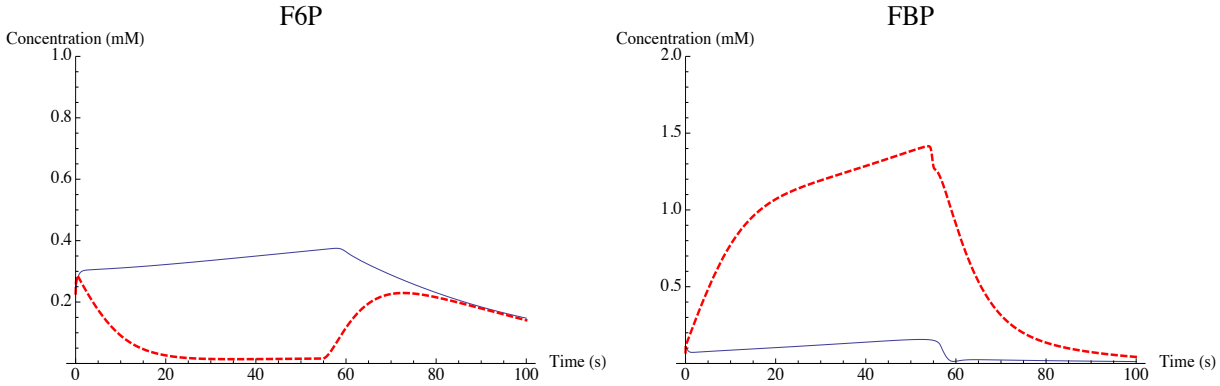

Fig. 7.20: The time courses of fructose 6-phosphate (F6P) and fructose 1,6-biphosphate (FBP) where predicted behavior by GA is dashed and original is solid

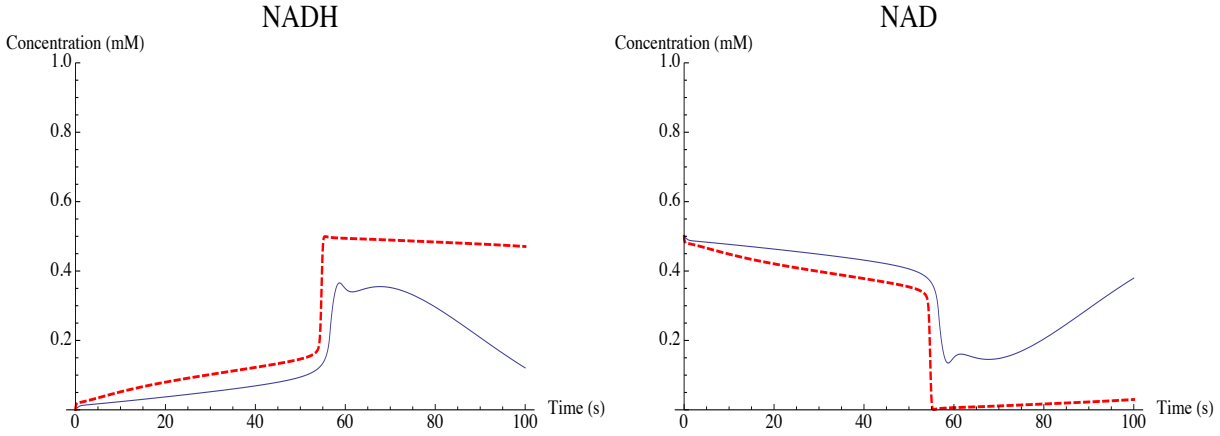

Fig. 7.21: The time courses of NADH and NAD where predicted behavior by GA is dashed and original is solid

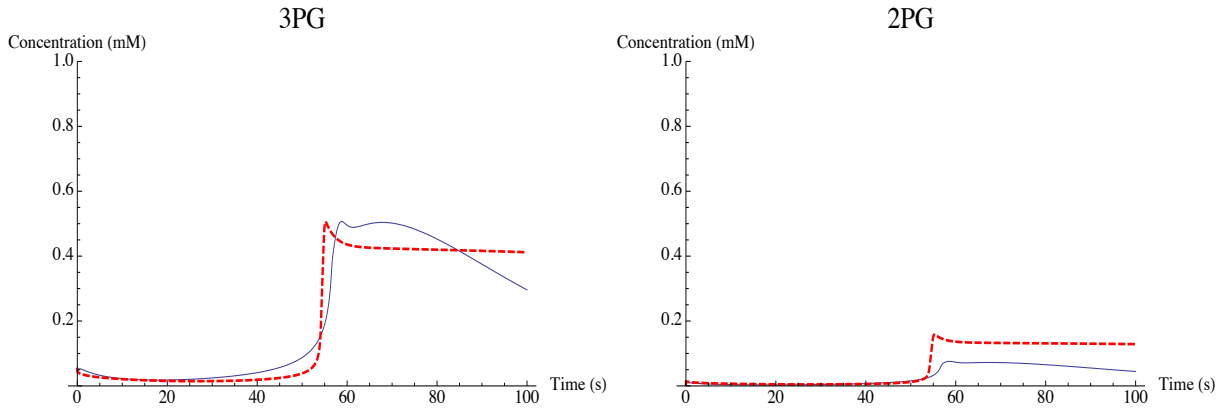

Fig. 7.22: The time courses of glycerate 3-phosphate (3PG) and glycerate 2-phosphate (2PG) where predicted behavior by GA is dashed and original is solid

In GA case, the prediction of the system behavior was not accurate. The algorithm was able to correctly simulate the dynamics LAC, 13BPG and 2PG. In other cases, the difference between original and predicted behavior was significant.

7.5 Conclusions for Case study 3

In case study 3, three evolutionary techniques, DE, SOMA and GA, were applied to parameter estimation of the glycolgenolysis model.

DE and SOMA yielded meaningful results with cost function value of 71.426 and 25.624, respectively. The dynamics of the system was predicted correctly by these two algorithms.

In contrast, GA was not capable of accurate predicting the system behavior. In estimating of most of metabolites concentration dynamics, GA failed. To find appropriate model parameters, GA settings were set to the same number of cost function evaluations as in case of SOMA and DE. The minimal cost function value for GA was 125.861.

Varying algorithms settings in all cases gave significant improvement in minimizing cost function value.

Overall, the time courses of metabolites were predicted accurately. There are certain differences between original and predicted time courses. However, these differences are minimal with correctly predicted dynamics.

Moreover, from our point of view, the result of DE and SOMA performance could be still improved by increasing cost function evaluations. However, on this stage of our investigation, this result is acceptable taking into account that the problem is extremely complex with high number of the system parameters.

8 CASE STUDY 4. METABOLIC MODELING OF GLYCOLYSIS IN HUMAN STEM CELLS

In this case study, we apply evolutionary algorithms to modeling of energy metabolism of human stem cells. In particular, this part of dissertation is primarily focused on the parameter identification of the glycolysis model in stem cells.

Specific metabolic features of stem cells are not yet well known. In this context, clearer understanding of this process is essential for regulating of stem cell differentiation. It may allow researchers to define key metabolites or required concentrations of metabolites to regulate the process of differentiation stem cell to different types of cells (e.g. neurons, cardiomyocites, etc.).

Nowadays, stem cells are used for medical therapy of leukemia, bone marrow transplantation. It is believed that stem cell therapy may completely change the treatment of human diseases such as cancer, Parkinson's disease, spinal cord injuries, Amyotrophic lateral sclerosis, multiple sclerosis, and muscle damage, etc.

This research has been carried out together with researcher Anton Salykin from the stem cell laboratory at Department of Biology, Faculty of Medicine, Masaryk University (Brno) and researcher Dominique Chu from School of Computing, University of Kent (Canterbury, Kent, Great Britain).

In general, the study can be divided into following 4 parts:

1) Formulation of the system of differential equations describing kinetic reactions of the glycolysis pathway in human stem cell.
2) Estimation of the model parameters using evolutionary techniques.
3) Simulation of the system behavior under different environmental conditions.
4) Validation of the simulation results with experimental data.

Whole research consists of two main parts: experimental and computational modeling. In present dissertation, we consider only the second part of the human stem cell metabolism research, estimation of the model parameters using evolutionary techniques.

8.1 The model of glycolysis in stem cell

The scheme of energy metabolism in human stem cell is presented in Figure 8.1, taken from [66]. The pathways can be divided into two types: catabolic and anabolic. These pathways provide stem cell energy for homeostasis. Moreover, energy is needed for cell replication. One of the main features in stem cell is that mitochondrial infrastructure is not functioning source of energy, and energy is produced mainly from glycolysis and the pentose phosphate pathway [66].

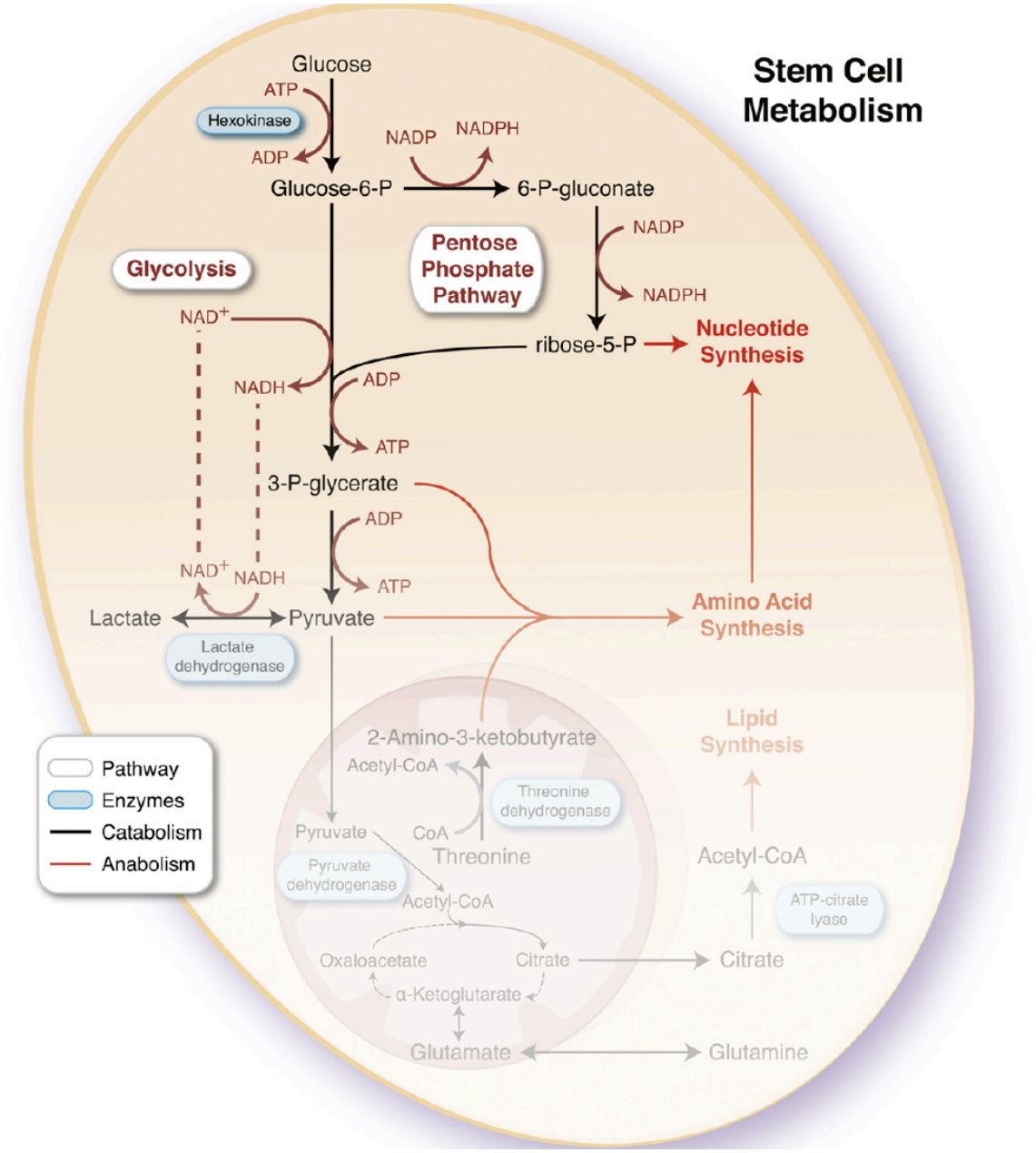

Fig. 8.1:Metabolic pathways in stem cell

Based on literature, metabolic databases KEGG and BRENDA, expert's opinion, the model of glycolysis in human stem cell has been created using special software CellDesigner, a modeling tool of biochemical reactions. This tool is diagram editor for drawing required network where the network is drawn based on the process diagram, with graphical notation system (see more in [67]). The output is a biochemical model in Systems Biology Markup Language (SBML) [68] format, a current standard for computer models of biological processes.

The SBML model consists of the following components:

- Function definition (a mathematical function that may be used in the model).

- Unit definition (a named definition of a new unit of measurement).
- Compartment type (a type of location for chemical substances).
- Species type (a type of chemical substances such as ions, molecules etc.).
- Compartment (a well-stirred container of a particular type and size where SBML species may be located).
- Species (list of chemical species).
- Parameter (a quantity with a symbolic name, for example, constants in a model).
- Initial assignment (the initial conditions of a model).
- Rule (additional mathematical expression for defining dynamics of the model).
- Constraint (a means of detecting out-of-bounds conditions).
- Reaction (a statement describing chemical transformation).
- Event (a statement describing an instantaneous, discontinuous change in a set of variables).

In fact, the SBML format enable include all known information about the system: species, compartments, initial conditions, variables, parameters, rate laws, additional constraints etc.

The model of glycolysis in stem cell is presented in Appendix D. For better understanding and also for visual reason, we provide only the system of ODEs.

Overall, the model of glycolysis describes 17 biochemical reactions. The system includes 21 differential equations. The number of kinetic parameters is 56.

The differential equations have been constructed automatically using CellDesigner based on classical reversible Michaelis-Menten mechanism.

Initial conditions and measured concentration of metabolites have been provided by the stem cell laboratory at Department of Biology, Faculty of Medicine, Masaryk University (Brno). Biological data includes concentrations of 12 metabolites in two hours intervals during 22 hours.

8.2 Cost function

Parameter estimation of the glycolysis model is formulated as a task of cost function minimization. The cost function in this research is stated as the sum of differences between experimentally measured and simulated data.

In this case, experimentally measured are the concentrations of 12 metabolites in two hours intervals during 22 hours. Therefore, simulated data are compared with measured every 2 hours (7200 seconds). Dynamics of the system has been predicted with final time of 79200 seconds.

8.3 Used algorithms and their settings

Based on the results of the previous three case studies, we have decided to apply two the most sufficient in our research evolutionary techniques – DE and SOMA. We also took into account the complexity of the system and related with it time-consuming calculations.

The DERand1Bin version of DE and versions AllToOne of SOMA have been applied in the present case study. Each experiment was run 35 times. All calculations have been performed using grid computer that includes 16 XServers, each 2x2 GHz Intel Xeon, 1 GB RAM, 80 GB HD i.e. 64 CPUs.

The following settings have been applied:

Table 8.1 Settings for the algorithms applied to the glycolysis model in human stem cell

DE settings		**SOMA settings**	
NP	560	PathLength	3 (5)
F	0.2	Step	0.11
CR	0.2	PRT	0.1
Generations	300	PopSize	150 (300)
		Migrations	200
		MinDiv	-0.1

8.4 Results

In DE experiments, the above-mentioned settings were applied. The experiment was run three times. In all cases, the calculations failed. Application of DE in this case requires more powerful computational hardware.

To find the system parameters, we applied SOMA with different population sizes (PopSize): 150 and 300.

The preliminary result with PopSize 150 showed not accurate prediction of the system behavior with minimal cost function value 4.04×10^4. Doubled PopSize gave significant improvement with cost function value 1.03×10^4.

The time courses of 12 metabolites can be found in the following figures.

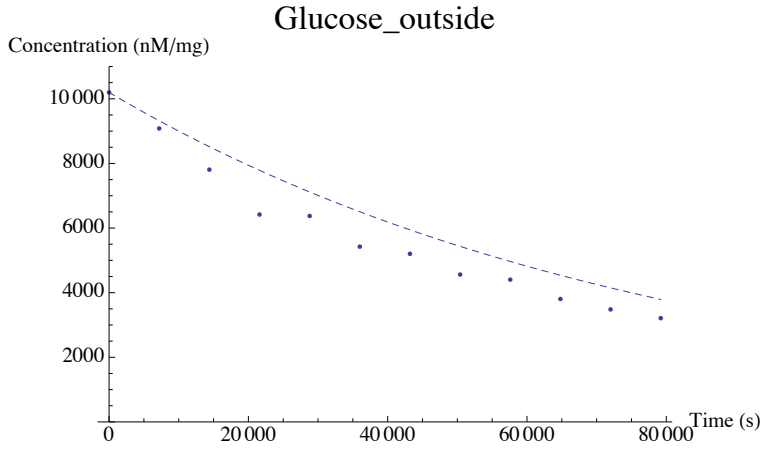

Fig. 8.2: The time course of glucose_outside metabolite (eqn 15) where the predicted behavior by SOMA is dashed and experimentally measured is dotted

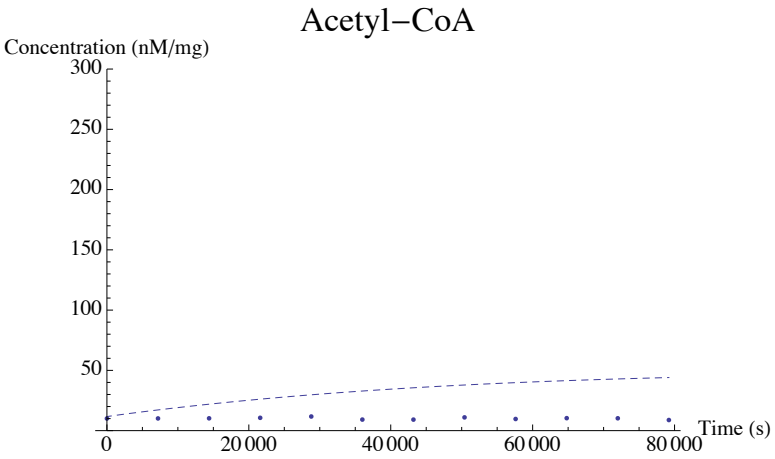

Fig. 8.3: The time course of Acetyl-CoA metabolite (eqn 17) where the predicted behavior by SOMA is dashed and experimentally measured is dotted

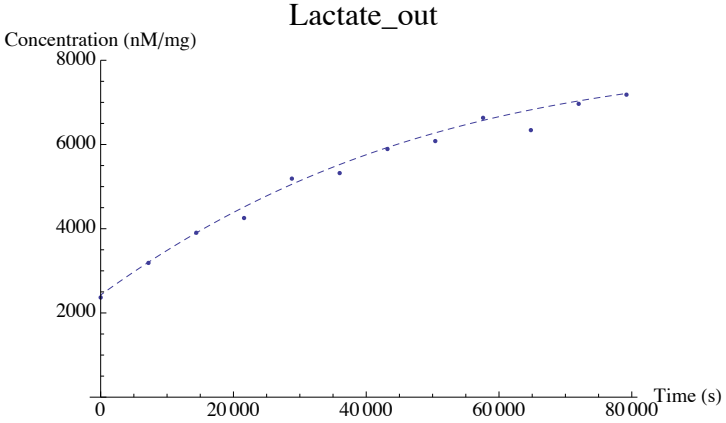

Fig. 8.4: The time course of Lactate_out metabolite (eqn 18) where the predicted behavior by SOMA is dashed and experimentally measured is dotted

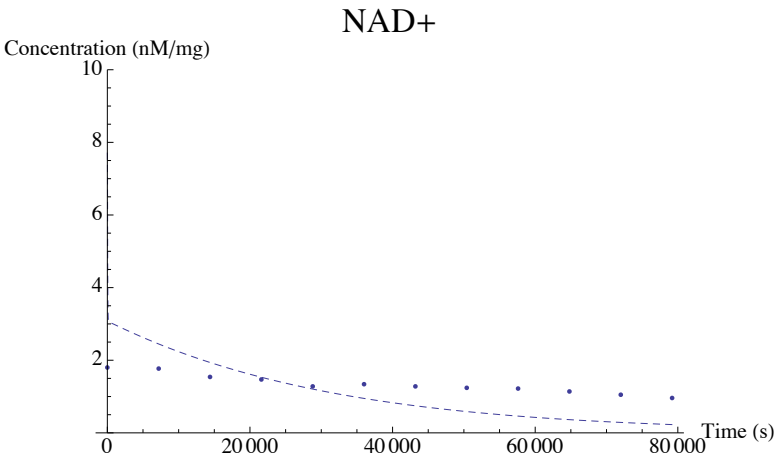

Fig. 8.5: The time course of NAD+ metabolite (eqn 12) where the predicted behavior by SOMA is dashed and experimentally measured is dotted

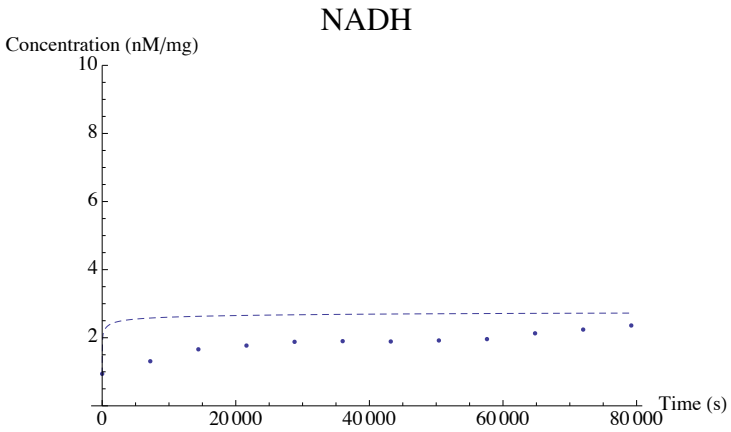

Fig. 8.6: The time course of NADH metabolite (eqn 11) where the predicted behavior by SOMA is dashed and experimentally measured is dotted

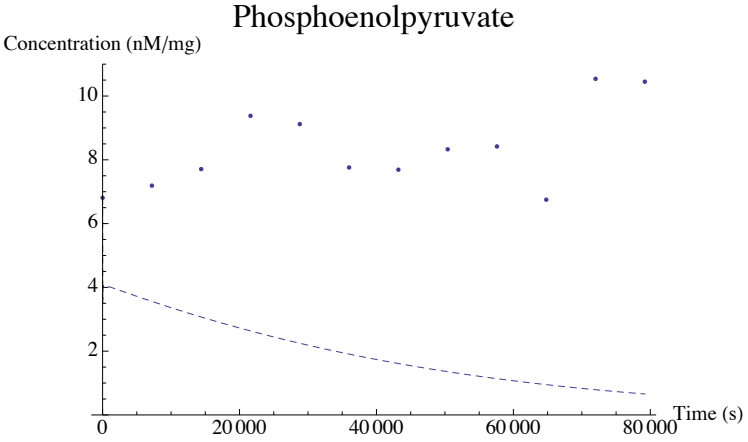

Fig. 8.7: The time course of Phosphoenolpyruvate metabolite (eqn 9) where the predicted behavior by SOMA is dashed and experimentally measured is dotted

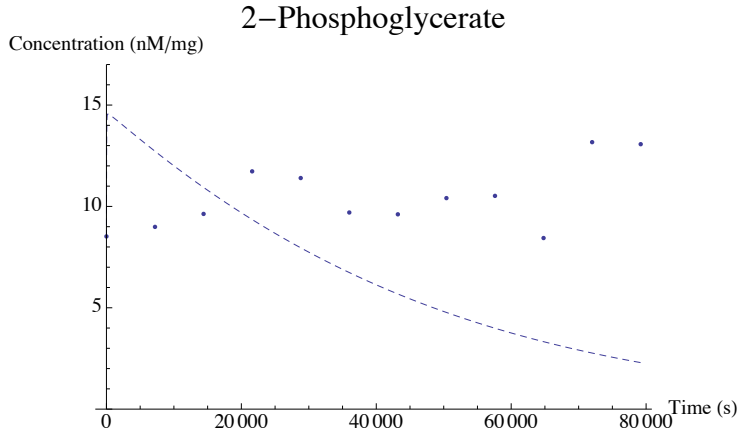

Fig. 8.8: The time course of 2-Phosphoglycerate metabolite (eqn 6) where the predicted behavior by SOMA is dashed and experimentally measured is dotted

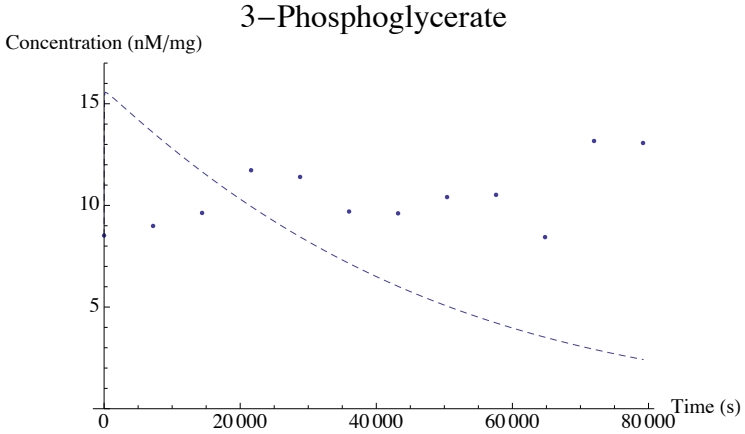

Fig. 8.9: The time course of 3-Phosphoglycerate metabolite (eqn 5) where the predicted behavior by SOMA is dashed and experimentally measured is dotted

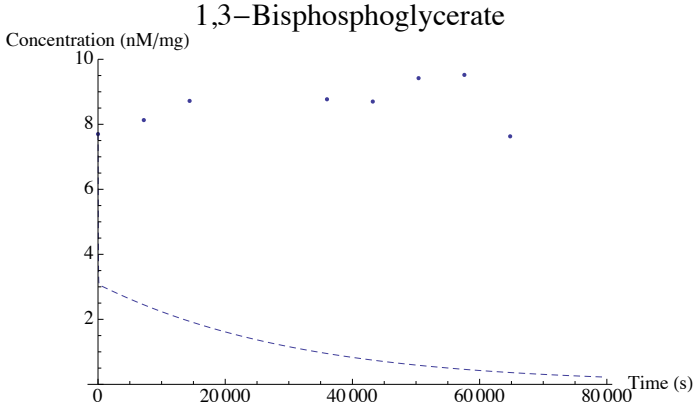

Fig. 8.10: The time course of 1, 3-Bisphosphoglycerate metabolite (eqn 4) where the predicted behavior by SOMA is dashed and experimentally measured is dotted

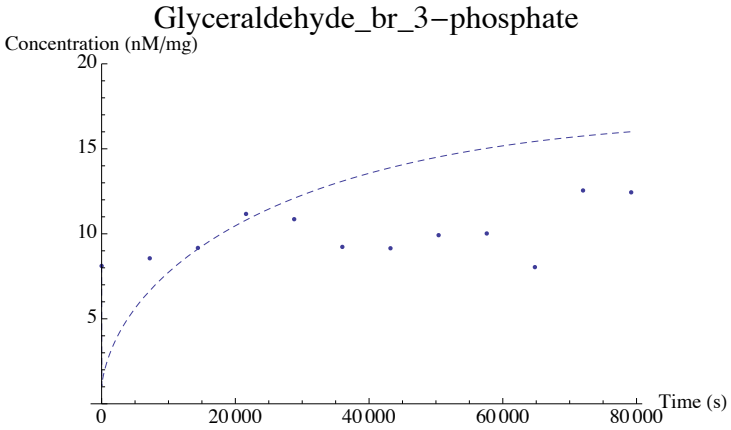

Fig. 8.11: The time course of Glyceraldehyde_br_3-phosphate (eqn 3) metabolite where the predicted behavior by SOMA is dashed and experimentally measured is dotted

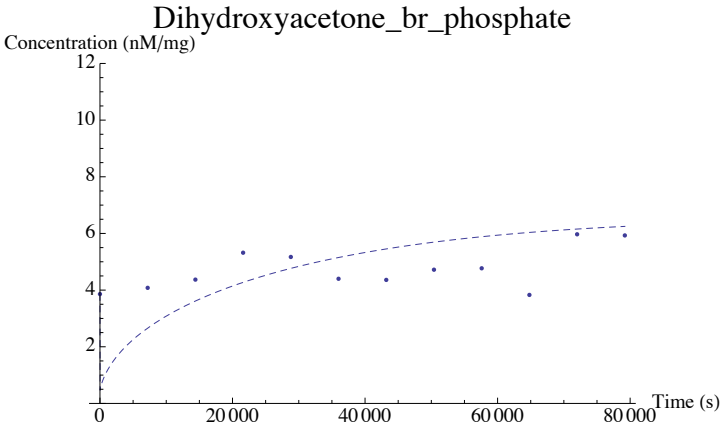

Fig. 8.12: The time course of Dihydroxyacetone_br_phosphate metabolite (eqn 2) where the predicted behavior by SOMA is dashed and experimentally measured is dotted

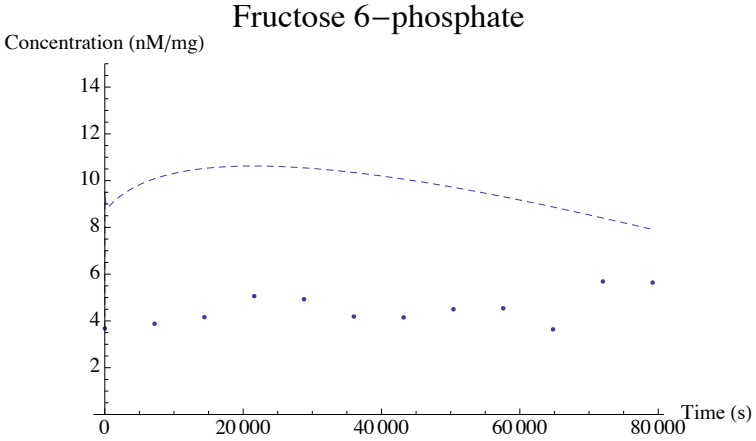

Fig. 8.13: The time course of Fructose 6-phosphate metabolite (eqn 19) where the predicted behavior by SOMA is dashed and experimentally measured is dotted

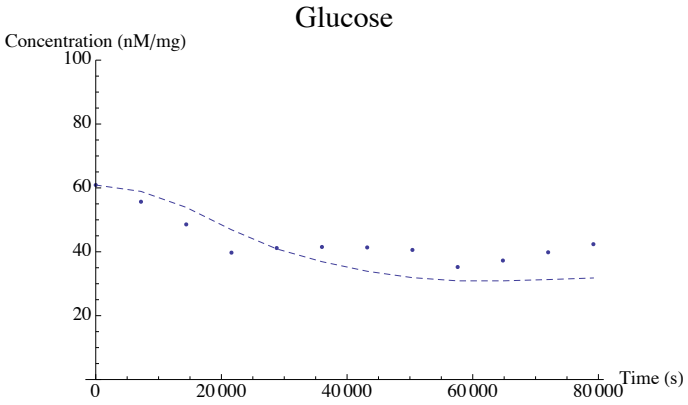

Fig. 8.14: The time course of Glucose metabolite (eqn 7) where the predicted behavior by SOMA is dashed and experimentally measured is dotted

Overall, the algorithm was able to successfully predict the dynamics of seven from twelve metabolites. To not accurate predicted dynamics could be related the following metabolites: Fructose 6-phosphate, 1, 3-Bisphosphoglycerate, 3-Phosphoglycerate, 2-Phosphoglycerate and Phosphoenolpyruvate.

8.5 Conclusions for Case study 4

In this case study, SOMA was able to correctly predict time courses of seven from twelve metabolites.

The research requires additional calculations. Possibly, number of cost function evaluations could be increased. Taking into account the fact that we have applied quite high number of cost function evaluations and it has required high computational effort, the further investigation could be carried out using more powerful computational resources.

This result could be also improved by including new experimental data. For our calculations, **we had only measured data for 12 metabolites. Overall number of the species in the system is 21.** The other way of improving results could be update of the model. As have been mentioned above, the model has been constructed using software CellDesigner based on literature and experts opinion. However, specific metabolic features of stem cells are not yet well known. Presumably, there are could be certain inaccuracies in the system of ODEs.

9 CONCLUSIONS AND DISCUSSIONS

An in-depth understanding of complex biological systems plays a key role in modern bioscience. Among many studied topics in system biology, the modeling of metabolic networks is very compelling. The complexity of interactions between components of metabolic system makes the prediction of the system behavior extremely challenging. Estimation of model parameters is required for prediction of system dynamics. One of the effective approaches in the parameter estimation problem is application of modern optimization techniques.

In present study, performance of modern evolutionary techniques in parameter estimation of well-studied metabolic systems and the metabolic system with unknown properties has been investigated. Selected evolutionary algorithms have been applied to define parameters of metabolic systems. The performance of the algorithms was different that depended on scale of a problem and also nonlinearity of the studied systems.

In all cases the optimization task was formulated as minimization problem. The purpose of an algorithm is to find the model parameters that give the best fit to experimental data.

First case study was devoted to application of three modern evolutionary techniques, DE, SOMA and GA, to parameter estimation of the well-studied metabolic system, the urea cycle of the mammalian hepatocyte. Two of applied optimization techniques yielded meaningful results. DE and SOMA algorithms provide robust and precise parameter estimation of the urea cycle model. In contrast, GA predicted correctly behavior of only three from four metabolites. Interestingly, increasing population size in GA case did not show any significant improvement in minimizing cost function value. Varying algorithms settings could improve the DE and SOMA algorithms performance. In both cases DE and SOMA produced significantly better results when the population size was increased but required huge computational effort. In terms of computational time, the most time-consuming calculations were observed in SOMA simulations. However, SOMA provided the best performance in estimating parameters.

The urea cycle experiment shows that in case where GA relatively failed, other evolutionary techniques such as DE and SOMA proved successful. It should be noted that the evolutionary techniques were firstly applied on the urea cycle model to estimate the model parameters.

In case study 2, for parameter estimation of a three-step pathway, we have considered the same three evolutionary techniques: DE, SOMA and GA.

DE with relatively high number of cost function evaluations was able to only partially predict behavior of the systems species. Decreasing of upper bound to 10^1 gave significant improvement in parameter estimation. In case of SOMA experiments with two versions AllToOne and AllToOne Rand, our results showed that the AllToOne version was able to define dynamics better than AllToOne Rand and DE results. The time courses of the systems species were predicted correctly. GA performance was significantly worse in comparison with other algorithms.

Not accurate prediction of the system dynamics in case upper bound 10^6 could be because of extremely wide range of lower and upper bounds for systems parameters. The algorithms were not able to define parameters in such enormous search space in reasonable time. The second possible reason could be high non-linearity of the system.

In case study 3, the same evolutionary algorithms were applied to parameter estimation of the glycolgenolysis model in skeletal muscle. This was first attempt to define parameters of such complex system using evolutionary computation.

DE and SOMA yielded meaningful results. The dynamics of the system was predicted correctly by these two algorithms. In contrast, GA was not capable of accurate predicting the system behavior. In estimating of most of metabolites concentration dynamics, GA failed. Varying algorithms settings in all cases gave significant improvement in minimizing cost function value.

Overall, the time courses of metabolites were predicted accurately. There are certain differences between original and predicted time courses. However, these differences are minimal with correctly predicted dynamics. Moreover, from our point of view, the result of DE and SOMA performance could be still improved by increasing cost function evaluations. On this stage of our investigation, this result is acceptable taking into account that the problem is extremely complex with high number of the system parameters.

In last case study, the best-performed algorithm – SOMA was applied to define parameters of the glycolysis model in human stem cell. SOMA was able to correctly predict time courses of seven from twelve metabolites. The research requires additional calculations. Possibly, number of cost function evaluations could be increased. Taking into account the fact that we have applied quite high number of cost function evaluations and it has required high computational effort, the further investigation could be carried out using more powerful computational resources.

This result could be also improved by including new experimental data. For our calculations, we had only measured data for 12 metabolites. Overall number

of the species in the system is 21. The other way of improving results could be update of the model. As have been mentioned above, the model has been constructed using software CellDesigner based on literature and experts opinion. However, specific metabolic features of stem cells are not yet well known. Presumably, there are could be certain inaccuracies in the system of ODEs.

The obtained results give us a reason to believe that heuristic optimization techniques are capable to accurately define parameters of such complex systems as metabolic networks. In the dissertation was shown that in cases where the most commonly used evolutionary algorithm – GA failed in predicting system dynamics, the modern evolutionary techniques such as DE and SOMA were capable of precise defining system parameters.

In the dissertation, evolutionary algorithms were firstly applied on two large-scale metabolic systems, the urea cycle model and the model of glygenolysis in skeletal muscle, which can be related to so called real-world problems.

One of **remarkable contributions** of the dissertation is that a novel, not known in bioscience evolutionary technique – SOMA was applied to define parameters of large-scale metabolic systems. The other contribution is the parameter identification of the stem cell metabolism model based on experimentally measured data. Moreover, our investigation of the system's parameters is one of the main parts in whole study of human stem cell metabolism that has been carried out in the stem cell laboratory at Department of Biology, Faculty of Medicine, Masaryk University (Brno).

Overall, the results of modeling showed that evolutionary algorithms provide an effective approach in parameter estimation of metabolic models and could be used even in large-scale problems.

The objectives of the dissertation were reached:

1. **To apply various evolutionary techniques to modeling of well-studied metabolic systems.**

   Three evolutionary techniques, GA, DE and SOMA, were applied to define parameters of three well-studied metabolic systems: the urea cycle (Case study 1), a three-step pathway (Case study 2) and the model of glycogenolysis in skeletal muscle (Case study 3). The results of the urea cycle and a three-step pathway modeling were presented on international conferences.

2. **To evaluate and compare the performance of each algorithm.**

   In each case study, performance of evolutionary algorithms was compared taking into account number of cost function evaluations. Furthermore, various algorithm settings were applied and compared.

3. **To apply selected evolutionary techniques to estimate parameters of the model of glycolysis in human stem cell based on real experimental data.**

   In case study 4, the best-performing algorithm – SOMA have been applied to define parameters of the model of glycolysis in human stem cell.

REFERENCES

[1] Alberts, Bruce et al. *Molecular Biology of the Cell*. 5th ed., revised. New York: Garland, ©2008. Chap. 1, Introduction to the cell. ISBN 978-0-8153-4105-5.

[2] Cho, Kwang-Hyun, Karl Henrik Johansson and Olaf Wolkenhauer. A hybrid systems framework for cellular processes. *BioSystems* [online]. 2005, 80, 273-282 [viewed 2010-01-13]. ISSN 0303-2647. Available at: ScienceDirect.

[3] Manca, Vincenzo and Luca Bianco. Biological networks in metabolic P systems. *BioSystems* [online]. 2008, 91, 489-498 [viewed 2011-10-01]. ISSN 0303-2647. Available at: ScienceDirect.

[4] DE JONG, HIDDE. Modeling and Simulation of Genetic Regulatory Systems: A Literature Review. *JOURNAL OF COMPUTATIONAL BIOLOGY* [online]. 2002, 9(1), 67-103 [viewed 2010-01-10]. ISSN 1557-8666.

[5] Bailey, J.E. Mathematical modeling and analysis in biochemical engineering: past accomplishments and future opportunities. *Biotechnology progress* [online]. 1998, 14(1), 8-20 [viewed 2011-10-13]. ISSN 1520-6033. Available at: DOI: 10.1021/bp9701269

[6] Chen, Luonan et al. *Modeling Biomolecular Networks in Cells: Structures and Dynamics*. London: Springer-Verlag, ©2010. ISBN 978-1-84996-213-1.

[7] Smolke, Christina D. *The metabolic pathway engineering handbook: fundamentals*. 1st ed. Boca Raton: CRC Press, ©2010. ISBN 978-1-4398-0296-0.

[8] Dräger, Andreas et al. Modeling metabolic networks in C. glutamicum: a comparison of rate laws in combination with various parameter optimization strategies. *BMC Systems Biology* [online]. 2009, 3(5) [viewed 2010-03-15]. ISSN: 1752-0509. Available at: http://www.biomedcentral.com/1752-0509/3/5.

[9] Polisetty, P.K., Voit E.O. and E.P. Gatzke. Identification of Metabolic System Parameters Using Global Optimization Methods. *Theoretical Biology and Medical Modelling* [online]. 2006, 3 (4), 1-15 [viewed 2011-09-10]. ISSN 1742-4682.

[10] Rodriguez-Fernandez, M., Egea J.A. and J.R. Banga. Novel Metaheuristic for Parameter Estimation in Nonlinear Dynamic Biological Systems. *BMC Bioinformatics* [online]. 2006, 7, 483-501[viewed 2012-09-05]. ISSN: 1471-2105.

[11] Auliac, C., Frouin V., Gidrol, X. and F. D'Alche-Buc. Evolutionary Approaches for the Reverse-Engineering of Gene Regulatory Networks: A Study on a Biologically Realistic Dataset. *BMC Bioinformatics* [online]. 2008, 9, article 91 [viewed 2010-04-09]. ISSN: 1471-2105.

[12] Noman, N., and H. Iba. Inference of Gene Regulatory Networks Using S-System and Differential Evolution. *Proc. Conf. Genetic and Evolutionary Computation* [online]. 2005, 439-446 [viewed 2010-04-09]. ISSN 9781595930101.

[13] Noman, N. and H. Iba. Inferring Gene Regulatory Networks Using Differential Evolution with Local Search Heuristics. *IEEE/ACM Trans. Computational Biology and Bioinformatics* [online]. 2007, 4 (4), 634-647 [viewed 2010-04-09]. ISSN 1545-5963.

[14] Gilman, A. and J. Ross. Genetic-Algorithm Selection of Regulatory Structure that Directs Flux in a Simple Metabolic Model. *Biophysical J* [online]. 1995, 69, 1321-1333[viewed 2010-04-09]. ISSN: 0006-3495.

[15] Patil, K.R., Rocha I., Forster J. and J. Nielsen. Evolutionary Programming as A Platform for in Silico Metabolic Engineering. BMC *Bioinformatics* [online]. 2005, 6 (1), 308 [viewed 2010-04-09]. ISSN: 1471-2105.

[16] Chaouiya, C., E. Remy, D. Thieffry. Petri net modelling of biological regulatory networks. *Journal of Discrete Algorithms* [online]. 2008, 6(2), 165-177 [viewed 2011-05-27]. ISSN 1570-8667. Available at: ScienceDirect.

[17] Balsa-Canto, E. et al. Hybrid Optimization Method with General Switching Strategy for Parameter Estimation. *BMC System Biology* [online]. 2008, 2 (26), 1-9 [viewed 2011-05-27]. ISSN: 1752-0509.

[18] Sun, J., Garibaldi J. M. and C. Hodgman. Parameter Estimation Using Metaheuristics in Systems Biology: A Comprehensive Review. *IEEE/ACM Transactions On Computational Biology and Bioinformatics* [online]. 2012, 9(1), 185-202 [viewed 2012-12-15]. ISSN 1545-5963.

[19] Modchang, C., Triampo W. and Y. Lenbury. Mathematical Modeling and Application of Genetic Algorithm to Parameter Estimation in Signal Transduction: Trafficking and Promiscuous Coupling of G-Protein Coupled Receptors. Computers in Biology and Medicine. 2008, 38, 574-582 [viewed 2012-09-23]. ISSN: 0010-4825.

[20] Morbiduccia, Umberto, Turab Andrea and Mauro Grigionia. Genetic algorithms for parameter estimation in mathematical modeling of glucose metabolism. *Computers in Biology and Medicine*. 2005, 35, 862–874 [viewed 2012-09-23]. ISSN: 0010-4825. Available at: doi:10.1016/j.compbiomed.2004.07.005.

[21] Ibrahim, B., Diekmann S., Schmitt E., and P. Dittrich. In-Silico "Modeling of the Mitotic Spindle Assembly Checkpoint". *PLoS One*. 2008, vol. 3, no. 2:e1555 [viewed 2012-11-05]. eISSN 1553-7358. Available at: doi: 10.1371/journal.pone.0001555.

[22] Morishita, R., Imade H., Ono I., Ono N. and M. Okamoto. Finding Multiple Solutions Based on an Evolutionary Algorithm for Inference of Genetic Networks by S-System. *Proc. of IEEE Congress Evolutionary Computation (CEC '03)*. 2003, 1, 615-622 [viewed 2010-03-18].

[23] Moles, C.G., P. Mendes and J.R. Banga. Parameter Estimation in Biochemical Pathways: A Comparison of Global Optimization Methods. *Genome Research*. 2003, 13, 2467-2474 [viewed 2011-11-18]. ISSN: 1549-5469. Available at: doi:10.1101/gr.1262503.

[24] Mardinoglu, A., Nielsen J. Systems medicine and metabolic modelling (Key Symposium). *Journal of INTERNAL MEDICINE* [online]. 2012, 271 (2), 142–154 [viewed 2013-01-11]. ISSN 1365-2796. Available at: doi: 10.1111/j.1365-2796.2011.02493.x.

[25] Auffray, C., Chen Z. and L. Hood. Systems medicine: the future of medical genomics and healthcare. *Genome Med* [online]. 2009, 1(2) [viewed 2011-11-18]. Available at: http://www.ncbi.nlm.nih.gov/pmc/articles/PMC2651587/.

[26] Wu, Ming and Christina Chan. Human Metabolic Network: Reconstruction, Simulation, and Applications in Systems Biology. *Metabolites* [online]. 2012, 2, 242-253 [viewed 2013-01-11]. ISSN 2218-1989. Available at: http://www.mdpi.com/2218-1989/2/1/242.

[27] Feist, Adam M. Reconstruction of Biochemical Networks in Microbial Organisms. *Nature Reviews Microbiology* [online]. 2009, 7(2), 129-143 [viewed 2011-02-10]. ISSN: 1740-1526. Available at: doi:10.1038/nrmicro1949.

[28] Kyoto Encyclopedia of Genes and Genomes (KEGG) [online database]. Japan: Kanehisa Laboratories, 1995-2012 [viewed 2012-06-20]. Available at: http://www.genome.jp/kegg/.

[29] BRaunschweig ENzyme Database (BRENDA) [online database]. Braunschweig: Technische Universität Braunschweig, release 2012.2 [viewed 2012-06-20]. Available at: http://www.brenda-enzymes.info/.

[30] Caspi, Ron et al. The MetaCyc database of metabolic pathways and enzymes and the BioCyc collection of pathway/genome databases. Nucleic Acids Research [online]. 2012, 40(D1), D742-D753 [viewed 2012-06-20]. ISSN 1362-4962. Available at: http://nar.oxfordjournals.org/content/40/D1/D742.long.

[31] Ren, Qinghu, Kaixi Chen and Ian T. Paulsen. TransportDB: a comprehensive database resource for cytoplasmic membrane transport systems and outer membrane channels. *Nucleic Acids Research* [online]. 2007, 35, D274–D279 [viewed 2012-06-20]. ISSN 1362-4962. Available at: http://nar.oxfordjournals.org/content/35/suppl_1/D274.full.pdf+html.

[32] Bairoch, A. The ENZYME database in 2000. Nucleic Acids Research [online]. 2000, 28(1), 304-305 [viewed 2012-06-20]. ISSN 1362-4962. Available at: http://nar.oxfordjournals.org/content/28/1/304.long.

[33] Ma, Hongwu et al. The Edinburgh human metabolic network reconstruction and its functional analysis. *Molecular Systems Biology* [online]. 2007, 3(135) [viewed 2012-01-10]. eISSN 1744-4292. Available at: http://www.ncbi.nlm.nih.gov/pmc/articles/PMC2013923/.

[34] Duarte, N.C. et al. Global reconstruction of the human metabolic network based on genomic and bibliomic data. *Proceedings of the National Academy of Sciences, USA* [online]. 2007, 104(6), 1777–1782 [viewed 2012-01-11]. ISSN 1091-6490. Available at: http://www.ncbi.nlm.nih.gov/pmc/articles/PMC1794290/.

[35] Domingues, Alexandre, Susana Vinga and João M Lemos. Optimization strategies for metabolic networks. *BMC Systems Biology* [online]. 2010, 4(113) [viewed 2012-05-28]. ISSN: 1752-0509. Available at: http://www.biomedcentral.com/1752-0509/4/113.

[36] Machado, Daniel et al. Exploring the gap between dynamic and constraint-based models of metabolism. *Metabolic Engineering* [online]. 2012, 14, 112–119 [viewed 2013-01-25]. ISSN 1096-7176. Available at: ScienceDirect.

[37] Bulik, S., S. Grimbs, J. Selbig and H.G. Holzhutter. Combining mechanistic and simplified enzymatic rate equations: A promising approach for speeding up the kinetic modeling of complex metabolic networks. *FEBS Journal* [online]. 2009, 276(2), 410-524 [viewed 2011-10-10]. ISSN 1742-4658. Available at: doi:10.1111/j.1742-4658.2008.06784.x.

[38] Gillespie, D.T.. The chemical Langevin equation. *Journal of Chemical Physics* [online]. 2000, 113, 297-306 [viewed 2011-10-10]. ISSN 1089-7690. Available at: http://dx.doi.org/10.1063/1.481811.

[39] Gillespie, D.T.. A General Method for Numerically Simulating the Stochastic Time Evolution of Coupled Chemical Reactions. *Journal of Computational Physics* [online]. 1976, 22(4), 403-434 [viewed 2011-10-10]. ISSN 0021-9991. Available at: ScienceDirect.

[40] Visser, D. and J. Heijnen. The Mathematics of Metabolic Control Analysis Revisited. *Metabolic Engineering* [online]. 2002, 4, 114-123 [viewed 2012-03-15]. ISSN 1096-7176. Available at: ScienceDirect.

[41] Hatzimanikatis, V., M. Emmerling, U. Sauer and J.E. Bailey. Application of mathematical tools for metabolic design of microbial ethanol production. *Biotechnology and Bioengineering* [online]. 1998, 58(2), 154-161 [viewed 2012-03-15]. ISSN 1097-0290. Available at: doi: 10.1002/(SICI)1097-0290(19980420)58:2/3<154::AID-BIT7>3.0.CO;2-K.

[42] Heinrich, R. and S. Schuster. *The Regulation of Cellular Systems*. New York: Chapman and Hall, 1996. ISBN 978-0412032615.

[43] Liebermeister, W. and E. Klipp. Bringing metabolic networks to life: convenience rate law and thermodynamic constraints. *Theoretical Biology and Medical Modelling* [online]. 2006, 3(41) [viewed 2012-03-15]. ISSN 1742-4682. Available at: http://www.ncbi.nlm.nih.gov/pmc/articles/PMC1781438/.

[44] Mulquiney, P. J. and P. W. Kuchel. *Modeling metabolism with Mathematica*. Boca Raton: CRC Press, 2003. ISBN 0-8493-1468-2.

[45] Palsson, Bernhard O. Systems Biology. *Simulation of dynamic network states*. Cambridge: Cambridge University Press, 2011. ISBN 978-1-107-00159-6.

[46] Sauro, Herbert M. *Enzyme Kinetics for Systems Biology*. First Edition. Ambrosius Publishing, 2012. ISBN-13: 978-0982477311.

[47] Turing, A.. *Intelligent machinery, unpublished report for National Physical Laboratory.* In: Michie, D. (ed.) Machine Intelligence, vol. 7, 1969; Turing, A.M. (ed.): The Collected Works, vol. 3, Ince D. North-Holland, Amsterdam, 1992.

[48] Barricelli, N.A. *Esempi Numerici di processi di evoluzione*. Methodos, 45–68, 1954.

[49] Luke, Sean. *Essentials of Metaheuristics*. USA: Lulu, 2009. ISBN 978-0-557-14859-2. Available at: http://cs.gmu.edu/~sean/book/metaheuristics/.

[50] Chong, Edwin K. P. and Stanislaw H. Żak. *An Introduction to Optimization*. 3rd ed. New York: Wiley, ©2011. ISBN 0-471-75800-0.

[51] Eiben, Agoston E. and J.E. Smith. *Introduction to Evolutionary Computing*. Berlin: Springer, 2008. ISBN 978-3540401841.

[52] Fogel, L.J., A.J. Owens and M.J. Walsh. *Artificial Intelligence through Simulated Evolution*. New York: John Wiley & Sons, ©1966.

[53] Sivanandam, S. N. and S. N. Deepa. *Introduction to Genetic Algorithms*. Berlin: Springer, 2010. ISBN 978-3642092244.

[54] Beyer, H.G. and H.P. Schwefel. Evolution strategy – a comprehensive introduction. *Natural Computing* [online]. 2002, 1(1), 3-52 [viewed 2011-02-15]. ISSN 1567-7818. Available at: doi: 10.1023/A:1015059928466.

[55] Price, K. et al. *Differential Evolution - A Practical Approach to Global Optimization*. Berlin: Springer-Verlag, 2005. ISBN 978-3540209508.

[56] Lee, K. Y. and M. A. El-Sharkawi. *Modern Heuristic Optimization Techniques: Theory and Applications to Power Systems*. New York: Wiley, ©2008. ISBN 978-0471457114.

[57] Corne, D., M. Dorigo and F. Glover. *New Ideas in Optimization*. London: McGraw-Hill, 1999. ISBN 007 7095065.

[58] Zelinka, I. SOMA - Self Organizing Migrating Algorithm. In: Onwubolu, G.C., Babu B. V., *New Optimization Techniques in Engineering*. New York: Springer-Verlag, 2004. ISBN 3-540-20167-X.

[59] Glover, F. Tabu search, part I. *ORSA Journal on Computing*. 1989,1(3), 190-206 [viewed 2010-02-15]. ISSN 0899-1499. Available at: doi: 10.1287/ijoc.1.3.190.

[60] Glover, F. Tabu search, part II. *ORSA Journal on Computing*. 1990, 2(1), 4-32 [viewed 2010-02-15]. ISSN 0899-1499. Available at: doi: 10.1287/ijoc.2.1.4.

[61] HOLLAND, J. H. *Genetic Algorithms. Scientific American*. July 1992, p. 44 – 50.

[62] STORN, RAINER and KENNETH PRICE. Differential Evolution - A Simple and Efficient Heuristic for Global Optimization over Continuous Spaces. *Journal of Global Optimization* [online]. 1997, 11, 341–359. ISSN 0925-5001. Available at: doi: 10.1023/A:1008202821328.

[63] Zelinka, I. et al. *Evoluční výpočetní techniky, principy a aplikace*. Praha: BEN, 2008. ISBN 978-80-7300-218-3.

[64] Mendes, P. Modeling large biological systems from functional genomic data: Parameter estimation. In: *Foundations of systems biology*, (ed. H. Kitano). Cambridge: MIT Press, 2001, pp. 163-186.

[65] LAMBETH, MELISSA J. and MARTIN J. KUSHMERICK. A Computational Model for Glycogenolysis in Skeletal Muscle. *Annals of Biomedical Engineering* [online]. 2002, 30 (6), 808–827 [viewed 2011-12-01]. ISSN: 1573-9686. Available at: doi: 10.1114/1.1492813.

[66] Folmes, Clifford D.L., Petras P. Dzeja, Timothy J. Nelson, and Andre Terzic. Metabolic Plasticity in Stem Cell Homeostasis and Differentiation. *ANNALS OF THE NEW YORK ACADEMY OF SCIENCES* [online]. 2012, 1254, 82-89 [viewed 2013-03-10]. Available at: doi: 10.1111/j.1749-6632.2012.06487.x.

[67] Funahashi, A., Tanimura, N., Morohashi, M., and Kitano, H., CellDesigner: a process diagram editor for gene-regulatory and biochemical

networks. *BIOSILICO* [online]. 2003, 1, 159-162 [viewed 2013-03-10]. Available at: doi:10.1016/S1478-5382(03)02370-9.

[68] Hucka, M. et al. The systems biology markup language (SBML): a medium for representation and exchange of biochemical network models. *Bioinformatics* [online]. 2003, 19 (4), 524-531 [viewed 2013-03-10]. ISSN: 1460-2059. Available at: doi: 10.1093/bioinformatics/btg015.

LIST OF AUTHORS PUBLICATIONS

1. Slustikova Lebedik A., Zelinka I. Evolutionary Algorithms for Parameter Estimation of Metabolic Systems. In Nostradamus 2013: *Prediction, Modeling and Analysis of Complex Systems Advances in Intelligent Systems and Computing*. Volume 210, 2013, pp 201-209. ISBN 978-3-319-00542-3. DOI 10.1007/978-3-319-00542-3_21.

2. Slustikova Lebedik A., Zelinka I., Jasek R. PARAMETER ESTIMATION OF A THREE-STEP PATHWAY USING EVOLUTIONARY TECHNIQUES. In MENDEL 2013: *19th International Conference on Soft Computing*. June 26-28, 2013, pp 111-116. ISSN 1803-3814.

3. Slustikova Lebedik, A., Zelinka, I. Parameter identification of urea cycle using evolutionary algorithms. In: BIOCOMP BG 2012, International Conference on Bioinformatics and Computational Biology, September 20th-21st 2012, Varna (Bulgaria). 2012, 67.

4. Ivlev, I., A. Lebedik and V. Kokh. Adenosine A2b receptor interaction investigation in silico. *Physiological Research*. 2010, 59(5), 38. ISSN 1802-9973.

5. Ivlev, I., V. Kokh and A. Lebedik. Management and assessment of lifespan of medical equipment. *Physiological Research*. 2010, 59(5), 37-38. ISSN 1802-9973.

6. Ivlev, I., A. Lebedik and V. Kokh. Simulation of adenosine receptor A2b subtype and molecules of activators and inhibitors interaction in silico. In: *YBERC 2010: The 4th Biomedical Engineering Conference of Young Biomedical Engineers and Researches, Kosice 1.-3 July 2010: conference proceedings.* ISBN: 978-80-553-0596-7.

7. Lebedik, A. S. Study of antitumor activity and neoangiogenesis stimulation by extract Uncaria Tomentosa in silico. In: *The 14th International Scientific and Practical Conference of Students, Postgraduates and Young Scientists "Modern Techniques and Technologies", Tomsk 2009: conference proceedings.* Tomsk: TPU Press, 2009.

8. Martynuk, A. V. and A. S. Lebedik. Simulation of quercetin interaction with different immunomodulatory targets in silico. In: *The 68th International Scientific and Practical Conference of Students, Tomsk 2009: conference proceedings*. Tomsk: SSMU Press, 2009.

CURRICULUM VITAE

Personal information

First name / Surname(s)	Anastasia Sluštíková Lebedik
E-mail	lebedik@fai.utb.cz
Date of birth	27 January 1986

Education

November 2009 - present - Ph.D. degree
Tomas Bata University in Zlín, Faculty of Applied Informatics
Department of Informatics and Artificial Intelligence

2003 – 2009 - Master's degree, diploma with excellence
University Siberian State Medical University, Faculty of Medical Biology
Department of Medical cybernetics

Research experience

November 2009 – present
Tomas Bata University in Zlín, Faculty of Applied Informatics
Department of Informatics and Artificial Intelligence
Doctoral thesis: Evolutionary modeling of cell processes

June 2008 – June 2009
Siberian State Medical University, Faculty of Medical Biology
Department of Biology and Genetics
Diploma thesis: Study of antitumor activity and neoangiogenesis stimulation of extract Uncaria Tomentosa in silico

November 2008 – June 2009
Siberian State Medical University, Faculty of Medical Biology
Department of Biology and Genetics
Theme: Simulation of quercetin interaction with different immunomodulatory targets in silico

Research activities

2010-2011: Project IGA/42/FAI/10/D "Evolucni synteza biomolekularnich struktur"
2012: Project IGA/FAI/2012/023 "Biological networks modeling using evolutionary algorithms"
2013: Project IGA/FAI/2013/005 "Modeling of energy metabolism in human stem cells using evolutionary algorithms"

Workshops and courses
Zuse Institute Berlin, Berlin, Germany (August 2013)
Field of study: Molecular interactions

University of Iceland, Reykjavik, Iceland (June 2013)
Field of study: Systems Biology short course

Contipro, Dolní Dobrouč (February 2013)
Field of study: Genetic methods, plasmid technology and biosensors

Conferences
MENDEL 2013: 19th International Conference on Soft Computing. June 26-28, 2013. Brno (Czech Republic)

Nostradamus 2013: Prediction, Modeling and Analysis of Complex Systems Advances in Intelligent Systems and Computing, June 3-5, 2013. Ostrava (Czech Republic)

BIOCOMP BG 2012, International Conference on Bioinformatics and Computational Biology, September 20th-21st 2012, Varna (Bulgaria).

YBERC 2010: The 4th Biomedical Engineering Conference of Young Biomedical Engineers and Researches, 1-3 July, 2010. Kosice (Sloval Republic)

Scientific awards
Diploma for the 1st place on The 4th Biomedical Engineering Conference of Young Biomedical Engineers and Researches, Kosice 1-3 July 2010

Language skills
Russian - native speaker
English - advanced
Czech - advanced

APPENDIX A

System of differential equations, which make up the urea cycle model:

$eqn_1 = c'(t) = v_{oct}(t)-v_{ass}(t);$

$eqn_2 = a'(t) = v_{as}(t)-v_{arg}(t);$

$eqn_3 = u'(t) = v_{arg}(t);$

$eqn_4 = atp'(t) = v_{atp}(t)-v_{ass}(t);$

$eqn_5 = pp'(t) = -v_{pp}(t)+v_{ass}(t);$

$eqn_6 = f'(t) = -v_{f}(t)+v_{as}(t);$

$eqn_7 = as'(t) = v_{ass}(t)-v_{as}(t);$

$eqn_8 = o'(t) = v_{arg}(t)-v_{oct}(t);$

$eqn_9 = cp'(t) = v_{cp}(t)-v_{oct}(t);$

$eqn_{10} = asp'(t) = v_{asp}(t)-v_{ass}(t);$

$eqn_{11} = amp'(t) = -v_{amp}(t)+v_{ass}(t);$

$eqn_{12} = p'(t) = -v_{p}(t)+v_{oct}(t);$

Ornithine carbamoyl transferase (OCT)

$v_{oct}(t) = e_{oct}\ (1/denom_{oct}\ )\ (cp\ (t)\ o\ (t)\ k_{1,oct}\ k_{2,oct}\ k_{3,oct}\ k_{4,oct} - c\ (t)\ p\ (t)\ k_{-4,oct}\ k_{-3,oct}\ k_{-2,oct}\ k_{-1,oct}\ );$

$denom_{oct} = c\ (t)\ k_{-3,oct}\ k_{-2,oct}\ k_{-1,oct} + p\ (t)\ (k_{-4,oct}\ k_{-2,oct}\ k_{-1,oct} + c\ (t)\ (k_{-4,oct}\ k_{-3,oct}\ k_{-2,oct} + k_{-4,oct}\ k_{-3,oct}\ k_{-1,oct}) + k_{-4,oct}\ k_{-1,oct}\ k_{3,oct} + o\ (t)\ (c\ (t)\ k_{-4,oct}\ k_{-3,oct}\ k_{2,oct} + k_{-4,oct}\ k_{2,oct}\ k_{3,oct})) + k_{-2,oct}\ k_{-1,oct}\ k_{4,oct} + k_{-1,oct}\ k_{3,oct}\ k_{4,oct} + o\ (t)\ k_{2,oct}\ k_{3,oct}\ k_{4,oct} + cp\ (t)\ (c\ (t)\ k_{-3,oct}\ k_{-2,oct}\ k_{1,oct} + k_{-2,oct}\ k_{1,oct}\ k_{4,oct} + k_{1,oct}\ k_{3,oct}\ k_{4,oct} + o\ (t)\ (c\ (t)\ k_{-3,oct}\ k_{1,oct}\ k_{2,oct} + k_{1,oct}\ k_{2,oct}\ k_{3,oct} + k_{1,oct}\ k_{2,oct}\ k_{4,oct}));$

Argininosuccinate synthetase (ASS)

$v_{ass}(t) = e_{ass}\ (1/denom_{ass}\ )\ (k_{1,ass}\ k_{2,ass}\ k_{3,ass}\ k_{4,ass}\ k_{5,ass}\ k_{6,ass}\ c\ (t)\ atp\ (t)\ asp\ (t) - k_{-1,ass}\ k_{-2,ass}\ k_{-3,ass}\ k_{-4,ass}\ k_{-5,ass}\ k_{-6,ass}\ pp\ (t)\ amp\ (t)\ as\ (t));$

$denom_{ass} = k_{-1,ass}\ k_{-2,ass}\ k_{5,ass}\ k_{6,ass}\ (k_{-3,ass} + k_{4,ass}) + k_{1,ass}\ k_{-2,ass}\ k_{-3,ass}\ k_{-4,ass}\ k_{6,ass}\ c\ (t)\ pp\ (t) + k_{1,ass}\ k_{-2,ass}\ k_{5,ass}\ k_{6,ass}\ (k_{-3,ass} + k_{4,ass})\ c\ (t) + k_{-1,ass}\ k_{3,ass}\ k_{4,ass}\ k_{5,ass}\ k_{-6,ass}\ asp\ (t)\ as\ (t) + k_{-1,ass}\ k_{3,ass}\ k_{4,ass}\ k_{5,ass}\ k_{6,ass}\ asp\ (t) + k_{1,ass}\ k_{2,ass}\ k_{-3,ass}\ k_{-4,ass}\ k_{6,ass}\ c\ (t)\ atp\ (t)\ pp\ (t) + k_{1,ass}\ k_{2,ass}\ k_{5,ass}\ k_{6,ass}\ (k_{-3,ass} + k_{4,ass})\ c\ (t)\ atp\ (t) + k_{1,ass}\ k_{-2,ass}\ k_{-3,ass}\ k_{-4,ass}\ k_{-5,ass}\ c\ (t)\ pp\ (t)\ amp\ (t) + k_{1,ass}\ k_{3,ass}\ k_{4,ass}\ k_{5,ass}\ k_{6,ass}\ c\ (t)\ asp\ (t) + k_{2,ass}\ k_{3,ass}\ k_{4,ass}\ k_{5,ass}\ k_{-6,ass}\ atp\ (t)\ asp\ (t)\ as\ (t) + k_{2,ass}\ k_{3,ass}\ k_{4,ass}\ k_{5,ass}\ k_{6,ass}\ atp\ (t)\ asp\ (t) +\ k_{-1,ass}$

$k_{3,ass}$ $k_{4,ass}$ $k_{-5,ass}$ $k_{-6,ass}$ asp (t) amp (t) as (t) + $k_{1,ass}$ $k_{2,ass}$ $k_{3,ass}$ ($k_{4,ass}$ $k_{5,ass}$ + $k_{4,ass}$ $k_{6,ass}$ + $k_{5,ass}$ $k_{6,ass}$) c (t) atp (t) asp (t) + $k_{1,ass}$ $k_{2,ass}$ $k_{3,ass}$ $k_{-4,ass}$ $k_{6,ass}$ c (t) atp (t) asp (t) pp (t) + $k_{-1,ass}$ $k_{-2,ass}$ $k_{-3,ass}$ $k_{-4,ass}$ $k_{6,ass}$ pp (t) + $k_{1,ass}$ $k_{2,ass}$ $k_{3,ass}$ $k_{4,ass}$ $k_{-5,ass}$ c (t) atp (t) asp (t) amp (t) + $k_{-1,ass}$ $k_{-2,ass}$ $k_{5,ass}$ $k_{-6,ass}$ ($k_{-3,ass}$ + $k_{4,ass}$) as (t) + $k_{1,ass}$ $k_{2,ass}$ $k_{-3,ass}$ $k_{-4,ass}$ $k_{-5,ass}$ c (t) atp (t) pp (t) amp (t) + $k_{-1,ass}$ $k_{-2,ass}$ $k_{-3,ass}$ $k_{-4,ass}$ $k_{-5,ass}$ pp (t) amp (t) + $k_{2,ass}$ $k_{3,ass}$ $k_{4,ass}$ $k_{-5,ass}$ $k_{-6,ass}$ atp (t) asp (t) amp (t) as (t) + $k_{-1,ass}$ $k_{-2,ass}$ $k_{-3,ass}$ $k_{-4,ass}$ $k_{-6,ass}$ pp (t) as (t) + $k_{2,ass}$ $k_{-3,ass}$ $k_{-4,ass}$ $k_{-5,ass}$ $k_{-6,ass}$ atp (t) pp (t) amp (t) as (t) + $k_{-1,ass}$ $k_{-2,ass}$ $k_{-5,ass}$ $k_{-6,ass}$($k_{-3,ass}$+$k_{4,ass}$) amp (t) as (t) + $k_{-1,ass}$ $k_{3,ass}$ $k_{-4,ass}$ $k_{-5,ass}$ $k_{-6,ass}$ asp (t) pp (t) amp (t) as (t) + $k_{-4,ass}$ $k_{-5,ass}$ $k_{-6,ass}$ ($k_{-1,ass}$ $k_{-2,ass}$ + $k_{-1,ass}$ $k_{-3,ass}$ + $k_{-2,ass}$ $k_{-3,ass}$) pp (t) amp (t) as (t) + $k_{1,ass}$ $k_{2,ass}$ $k_{3,ass}$ $k_{-4,ass}$ $k_{-5,ass}$ c (t) atp (t) asp (t) pp (t) amp (t) + $k_{2,ass}$ $k_{3,ass}$ $k_{-4,ass}$ $k_{-5,ass}$ $k_{-6,ass}$ atp (t) asp (t) pp (t) amp (t) as (t);

Argininosuccinate lyase (ASL)

$v_{as}(t) = e_{as}\ k_{1,as}\ k_{2,as}\ k_{3,as}$ as (t) - $k_{-3,as}\ k_{-2,as}\ k_{-1,as}$ a (t) f (t)/$denom_{as}$;

$denom_{as}$ = f (t) $k_{-2,as}\ k_{-1,as}$ + a (t) (f (t) $k_{-3,as}\ k_{-2,as}$ + $k_{-3,as}\ k_{-1,as}$ + $k_{-3,as}\ k_{2,as}$) + $k_{-1,as}\ k_{3,as}$ + $k_{2,as}\ k_{3,as}$ + as (t) (f (t) $k_{-2,as}\ k_{1,as}$ + $k_{1,as}\ k_{2,as}$ + $k_{1,as}\ k_{3,as}$);

Arginase

$v_{arg}(t) = (e_{arg}\ (k_{1,arg}\ k_{2,arg}\ k_{3,arg}$ a (t)))/$denom_{arg}$;

$denom_{arg}$ = o (t) ($k_{-3,arg}\ k_{-1,arg}$ + $k_{-3,arg}\ k_{2,arg}$) + $k_{-1,arg}\ k_{3,arg}$ + $k_{2,arg}\ k_{3,arg}$ + a (t) ($k_{1,arg}\ k_{2,arg}$ + $k_{1,arg}\ k_{3,arg}$);

Rate equations for the co-substrates and products that are peripheral to the cycle:

$v_{atp}(t) = k_{atp}$ atppool (t);
$v_{pp}(t) = k_{pp}$ pp (t);
$v_f(t) = k_f$ f (t);
$v_{cp}(t) = k_{cp}$ ampool (t);
$v_{asp}(t) = k_{asp}$ asppool (t);
$v_{amp}(t) = k_{amp}$ amp (t);
$v_p(t) = k_p$ p (t);
atppool (t) = 1.0×10^{-4};
ampool (t) = 1.0×10^{-4};
asppool (t) = 1.0×10^{-4};

Estimated parameters for the urea cycle model:

Nominal values	Values estimated by SOMA
$e_{oct} = 2.6 \times 10^{-6}$;	$e_{oct} = 1.2 \times 10^{-6}$;
$k_{1,oct} = 1.7 \times 10^{7}$;	$k_{1,oct} = 8.3 \times 10^{6}$;
$k_{-1,oct} = 63$;	$k_{-1,oct} = 44$;
$k_{2,oct} = 2.1 \times 10^{6}$;	$k_{2,oct} = 2.5 \times 10^{6}$;
$k_{-2,oct} = 1.0 \times 10^{3}$;	$k_{-2,oct} = 1.2 \times 10^{3}$;
$k_{3,oct} = 3 \times 10^{3}$;	$k_{3,oct} = 6 \times 10^{3}$;
$k_{-3,oct} = 9.0 \times 10^{4}$;	$k_{-3,oct} = 2.2 \times 10^{4}$;
$k_{4,oct} = 2.6 \times 10^{3}$;	$k_{4,oct} = 2.2 \times 10^{3}$;
$k_{-4,oct} = 5.0 \times 10^{5}$;	$k_{-4,oct} = 7.0 \times 10^{5}$;
$e_{ass} = 4.0 \times 10^{-6}$;	$e_{ass} = 6.8 \times 10^{-6}$;
$k_{1,ass} = 2.4 \times 10\text{^}5$;	$k_{1,ass} = 9.5 \times 10^{5}$;
$k_{-1,ass} = 2.3$;	$k_{-1,ass} = 1.6$;
$k_{2,ass} = 3.5 \times 10\text{^}5$;	$k_{2,ass} = 1.4 \times 10^{5}$;
$k_{-2,ass} = 10.0$;	$k_{-2,ass} = 9.6$;
$k_{3,ass} = 4.8 \times 10\text{^}5$;	$k_{3,ass} = 4.2 \times 10^{5}$;
$k_{-3,ass} = 10.0$;	$k_{-3,ass} = 9.7$;
$k_{4,ass} = 2.0 \times 10\text{^}1$;	$k_{4,ass} = 2.7 \times 10^{1}$;
$k_{-4,ass} = 8.9 \times 10\text{^}5$;	$k_{-4,ass} = 10.7 \times 10^{5}$;
$k_{5,ass} = 5.0 \times 10\text{^}1$;	$k_{5,ass} = 2.3 \times 10^{1}$;
$k_{-5,ass} = 6.4 \times 10\text{^}5$;	$k_{-5,ass} = 9.4 \times 10^{5}$;
$k_{6,ass} = 5.0 \times 10\text{^}1$;	$k_{6,ass} = 9.4 \times 10^{1}$;
$k_{-6,ass} = 1.7 \times 10\text{^}5$;	$k_{-6,ass} = 4.8 \times 10^{5}$;
$e_{as} = 2.2 \times 10^{-6}$;	$e_{as} = 1.1 \times 10^{-6}$;
$k_{1,as} = 2.7 \times 10^{6}$;	$k_{1,as} = 8.2 \times 10^{6}$;
$k_{-1,as} = 7.0 \times 10^{1}$;	$k_{-1,as} = 8.7 \times 10^{1}$;
$k_{2,as} = 7.5 \times 10^{1}$;	$k_{2,as} = 6.9 \times 10^{1}$;
$k_{-2,as} = 1.5 \times 10^{6}$;	$k_{-2,as} = 1.3 \times 10^{6}$;
$k_{3,as} = 1.1 \times 10^{3}$;	$k_{3,as} = 6.9 \times 10^{3}$;
$k_{-3,as} = 7.0 \times 10^{5}$;	$k_{-3,as} = 12.1 \times 10^{5}$;
$e_{arg} = 8.9 \times 10^{-6}$;	$e_{arg} = 7.1 \times 10^{-6}$;
$k_{1,arg} = 1.0 \times 10^{7}$;	$k_{1,arg} = 3.9 \times 10^{7}$;
$k_{-1,arg} = 5.4 \times 10^{4}$;	$k_{-1,arg} = 4.8 \times 10^{4}$;
$k_{2,arg} = 5.3 \times 10^{3}$;	$k_{2,arg} = 17.4 \times 10^{3}$;
$k_{3,arg} = 3.0 \times 10^{4}$;	$k_{3,arg} = 17.7 \times 10^{4}$;
$k_{-3,arg} = 1.0 \times 10^{7}$;	$k_{-3,arg} = 1.5 \times 10^{7}$;
$k_{atp} = 6.6 \times 10^{-2}$;	$k_{atp} = 5.1 \times 10^{-2}$;
$k_{pp} = 6.6 \times 10^{-2}$;	$k_{pp} = 8.0 \times 10^{-2}$;
$k_{f} = 6.6 \times 10^{-2}$;	$k_{f} = 4.6 \times 10^{-2}$;
$k_{cp} = 6.6 \times 10^{-2}$;	$k_{cp} = 6.9 \times 10^{-2}$;
$k_{asp} = 6.6 \times 10^{-2}$;	$k_{asp} = 10.7 \times 10^{-2}$;
$k_{amp} = 6.6 \times 10^{-2}$;	$k_{amp} = 11.6 \times 10^{-2}$;
$k_{p} = 6.6 \times 10^{-2}$;	$k_{p} = 17.9 \times 10^{-2}$;

APPENDIX B

System of differential equations, which make up a three-step pathway model:

$$\frac{dG1}{dt} = \frac{V_1}{1+\left(\frac{p}{Ki1}\right)^{ni1}+\left(\frac{Ka1}{S}\right)^{na1}} - k1 \cdot G1$$

$$\frac{dG2}{dt} = \frac{V_2}{1+\left(\frac{p}{Ki2}\right)^{ni2}+\left(\frac{Ka2}{M1}\right)^{na2}} - k2 \cdot G2$$

$$\frac{dG3}{dt} = \frac{V_3}{1+\left(\frac{p}{Ki3}\right)^{ni3}+\left(\frac{Ka3}{M2}\right)^{na3}} - k3 \cdot G3$$

$$\frac{dE1}{dt} = \frac{V_4 \cdot G1}{K_4 + G1} - k4 \cdot E1$$

$$\frac{dE2}{dt} = \frac{V_5 \cdot G2}{K_5 + G2} - k5 \cdot E2$$

$$\frac{dE3}{dt} = \frac{V_6 \cdot G3}{K_6 + G3} - k6 \cdot E3$$

$$\frac{dM1}{dt} = \frac{kcat_1 \cdot E1 \cdot \left(\frac{1}{Km1}\right) \cdot (S - M1)}{1+\frac{S}{Km1}+\frac{M1}{Km2}} - \frac{kcat_2 \cdot E2 \cdot \left(\frac{1}{Km3}\right) \cdot (M1 - M2)}{1+\frac{M1}{Km3}+\frac{M2}{Km4}}$$

$$\frac{dM2}{dt} = \frac{kcat_2 \cdot E2 \cdot \left(\frac{1}{Km3}\right) \cdot (M1 - M2)}{1+\frac{M1}{Km3}+\frac{M2}{Km4}} - \frac{kcat_3 \cdot E3 \cdot \left(\frac{1}{Km5}\right) \cdot (M2 - P)}{1+\frac{M2}{Km5}+\frac{P}{Km6}}$$

Estimated parameters for a three-step pathway model:

Nominal values	Parameter values estimated by SOMA
$V_1 = 1;$	$V_1 = 4.14;$
$Ki1 = 1;$	$Ki1 = 6.5;$
$ni1 = 2;$	$ni1 = 1.6;$
$Ka1 = 1;$	$Ka1 = 3.5;$
$na1 = 2;$	$na1 = 1.2;$
$k1 = 1;$	$k1 = 5.9;$
$V_2 = 1;$	$V_2 = 2.4;$
$Ki2 = 1;$	$Ki2 = 8.7;$
$ni2 = 2;$	$ni2 = 3.1;$
$Ka2 = 1;$	$Ka2 = 5.9;$
$na2 = 2;$	$na2 = 1.5;$
$k2 = 1;$	$k2 = 0.46;$
$V_3 = 1;$	$V_3 = 7.37;$
$Ki3 = 1;$	$Ki3 = 0.21;$
$ni3 = 2;$	$ni3 = 0.35;$
$Ka3 = 1;$	$Ka3 = 5.3;$
$na3 = 2;$	$na3 = 1.95;$
$k3 = 1;$	$k3 = 0.37;$
$V_4 = 0.1;$	$V_4 = 0.72;$
$K_4 = 1;$	$K_4 = 8.6;$
$k4 = 0.1;$	$k4 = 0.098;$
$V_5 = 0.1;$	$V_5 = 1.09;$
$K_5 = 1;$	$K_5 = 6.5;$
$k5 = 0.1;$	$k5 = 0.15;$
$V_6 = 0.1;$	$V_6 = 0.25;$
$K_6 = 1;$	$K_6 = 1.26;$
$k6 = 0.1;$	$k6 = 0.15;$
$kcat_1 = 1;$	$kcat_1 = 4.03;$
$Km1 = 1;$	$Km1 = 7.47;$
$Km2 = 1;$	$Km2 = 1.22;$
$kcat_2 = 1;$	$kcat_2 = 5.66;$
$Km3 = 1;$	$Km3 = 3.16;$
$Km4 = 1;$	$Km4 = 3.04;$
$kcat_3 = 1;$	$kcat_3 = 4.7;$
$Km5 = 1;$	$Km5 = 5.3;$
$Km6 = 1;$	$Km6 = 1.8;$

APPENDIX C

System of differential equations, which make up the model of glycogenolysis in skeletal muscle:

eqn_1= GLY'(t) = -$flux_{GP}$(t);
eqn_2= G1P'(t) = $flux_{GP}$(t)-V_{GLM}(t);
eqn_3= G6P'(t) = V_{PGLM}(t)- V_{PGI}(t);
eqn_4= F6P'(t) = V_{PGI}(t)-V_{PFK}(t);
eqn_5= FBP'(t) = V_{PFK}(t)-V_{ALD}(t);
eqn_6= DHAP'(t) = V_{ALD}(t)+V_{TPI}(t);
eqn_7= GAP'(t) = V_{ALD}(t)-V_{TPI}(t)-V_{GAPDH}(t);
eqn_8= BPG13'(t) = V_{GAPDH}(t)-V_{PGK}(t);
eqn_9= PG3'(t) = V_{PGK}(t)-V_{PGM}(t);
eqn_{10}= PG2'(t) = V_{PGM}(t)-V_{ENOL}(t);
eqn_{11}= PEP'(t) = V_{ENOL}(t)-V_{PK}(t);
eqn_{12}= PYR'(t) = V_{PK}(t)-V_{LDH}(t);
eqn_{13}= LAC'(t) = V_{LDH}(t)-output;
eqn_{14}= P_p'(t) = -$flux_{GP}$(t)-V_{GAPDH}(t)+V_{ATPase}(t);
eqn_{15}= ADP'(t) = V_{PFK}(t)-V_{PGK}(t)-V_{PK}(t)+2V_{ADK}(t)+V_{CK}(t)+V_{ATPase}(t);
eqn_{16}= ATP'(t) = -V_{PFK}(t)+V_{PGK}(t)+V_{PK}(t)-V_{ADK}(t)-V_{CK}(t)-V_{ATPase}(t);
eqn_{17}= AMP'(t) = -V_{ADK}(t);
eqn_{18}= PCr'(t) = V_{CK}(t);
eqn_{19}= CR'(t) = -V_{CK}(t);
eqn_{20}= NADH'(t) = V_{GAPDH}(t)-V_{LDH}(t);
eqn_{21}= NAD'(t) = -V_{GAPDH}(t)+V_{LDH}(t);

Glycogene Phosporylase (GPa, GPb)

$$V_{GPa}(t) = \left(V_{maxfGPa}\left(\frac{GLY(t)\,P_p(t)}{K_{iGLYfa}\,K_{P_{pa}}}\right) - V_{maxrGPa}\left(\frac{GLY(t)\,G1P(t)}{K_{GLYb}\,K_{iG1Pa}}\right)\right) \Big/ \left(1 + \frac{GLY(t)}{K_{iGLYfa}} + \frac{P_p(t)}{K_{iP_{pa}}} + \frac{GLY(t)}{K_{iGLYb}} + \frac{G1P(t)}{K_{iG1Pa}} + \frac{GLY(t)\,P_p(t)}{K_{GLYf}\,K_{iP_{pa}}} + \frac{GLY(t)\,G1P(t)}{K_{GLYb}\,K_{iG1Pa}}\right);$$

$$V_{maxrGPa} = \frac{V_{maxfGPa}\,K_{GLYb}\,K_{iG1Pa}}{K_{iGLYfa}\,K_{P_{pa}}\,K_{eqGPa}};$$

$$V_{GPb}(t) = \left(V_{maxfGPb}\left(\frac{GLY(t)\,P_p(t)}{K_{iGLYfb}\,K_{P_{pb}}}\right) - V_{maxrGPb}\left(\frac{GLY(t)\,G1P(t)}{K_{iGLYb}\,K_{G1Pb}}\right)\right)\left(\frac{AMP(t)^{nH}}{K_{AMP_{act}}}\right) \Big/ \left(1 + \frac{GLY(t)}{K_{iGLYfb}} + \frac{P_p(t)}{K_{iP_{pb}}} + \frac{GLY(t)}{K_{iGLYb}} + \frac{G1P(t)}{K_{iG1Pb}} + \frac{GLY(t)\,P_p(t)}{K_{iGLYfb}\,K_{P_{pb}}} + \frac{GLY(t)\,G1P(t)}{K_{iGLYb}\,K_{G1Pb}}\right)\left(1 + \frac{AMP(t)^{nH}}{K_{AMP_{act}}}\right);$$

$$V_{maxrGPb} = \frac{V_{maxfGPb}\,K_{iGLYb}\,K_{G1Pb}}{K_{GLYf}\,K_{iP_{pb}}\,K_{eqGPb}};$$

$$flux_{GP}(t) = frac_a V_{GPa}(t) + frac_b V_{GPb}(t);$$

Phosphoglucomutase and Phosphoglucoisomerase (PGLM and PGI)

$$V_{PGLM}(t) = \left(\left(V_{maxfPGLM}\frac{G1P(t)}{K_{G1P_{PGLM}}}\right) - \left(V_{maxrPGLM}\frac{G6P(t)}{K_{G6P_{PGLM}}}\right)\right) \Big/ \left(1 + \frac{G1P(t)}{K_{G1P_{PGLM}}} + \frac{G6P(t)}{K_{G6P_{PGLM}}}\right);$$

$$V_{maxrPGLM} = \frac{V_{maxfPGLM} K_{G6P_{PGLM}}}{K_{G1P_{PGLM}} K_{eqPGLM}};$$

$$V_{PGI}(t) = \left(\left(V_{maxfPGI}\frac{G6P(t)}{K_{G6P_{PGI}}}\right) - \left(V_{maxrPGI}\frac{F6P(t)}{K_{F6P_{PGI}}}\right)\right) \Big/ \left(1 + \frac{G6P(t)}{K_{G6P_{PGI}}} + \frac{F6P(t)}{K_{F6P_{PGI}}}\right);$$

$$V_{maxfPGI} = \frac{V_{maxrPGI} K_{G6P_{PGI}} K_{eqPGI}}{K_{F6P_{PGI}}};$$

Phosphofructokinase (PFK)

$$V_{PFK}(t) = \left(\left(V_{maxfPFK}\left(\frac{ATP(t)\,F6P(t)}{K_{ATP_{PFK}} K_{F6P_{PFK}}}\right) - V_{maxrPFK}\left(\frac{ADP(t)\,FBP(t)}{K_{ADP_{PFK}} K_{FBP_{PFK}}}\right)\right) \Big/ delta(t)\right) \Big/ \left(\left(1 + \alpha L(t)\,(delta_{act}(t)/delta(t))^3\right) / \left(1 + L(t)\,(delta_{act}(t)/delta(t))^4\right)\right);$$

$$delta(t) = \left(1 + \frac{F6P(t)}{K_{F6P_{PFK}}}\right)\left(1 + \frac{ATP(t)}{K_{ATP_{PFK}}}\right) + \frac{ADP(t)}{K_{ADP_{PFK}}} + \frac{FBP(t)}{K_{FBP_{PFK}}}\left(1 + \frac{ADP(t)}{K_{ADP_{PFK}}}\right);$$

$$delta_{act}(t) = \left(1 + \frac{F6P(t)}{K_{F6P_{act}}}\right)\left(1 + \frac{ATP(t)}{K_{ATPact}}\right) + \frac{ADP(t)}{K_{ADPact}} + \frac{FBP(t)}{K_{FBPact}}\left(1 + \frac{ADP(t)}{K_{ADPact}}\right);$$

$$\alpha = \frac{K_{F6P_{PFK}} K_{ATP_{PFK}}}{K_{F6Pact} K_{ATPact}};$$

$$L(t) = L_0\left(\left(\left(1 + \frac{ATP(t)}{K_{iATP}}\right) \Big/ \left(1 + d\frac{ATP(t)}{K_{iATP}}\right)\right)\left(\left(1 + e\frac{AMP(t)}{K_{aAMP}}\right) \Big/ \left(1 + \frac{AMP(t)}{K_{aAMP}}\right)\right)\right)^4;$$

$$V_{maxrPFK} = \frac{V_{maxfPFK} K_{ADP_{PFK}} K_{FBP_{PFK}}}{K_{ATP_{PFK}} K_{F6P_{PFK}}};$$

Aldolase and Triose Phosphate Isomerase (ALD and TPI)

$$V_{ALD}(t) = \left(\left(V_{maxfALD}\frac{FBP(t)}{K_{FBP_{ALD}}}\right) - \left(V_{maxrALD}\frac{DHAP(t)\,GAP(t)}{K_{DHAP_{ALD}} K_{GAP_{ALD}}}\right)\right) \Big/ \left(1 + \frac{FBP(t)}{K_{FBP_{ALD}}} + \frac{DHAP(t)}{K_{DHAP_{ALD}}} + \frac{GAP(t)}{K_{GAP_{ALD}}}\right);$$

$$V_{maxrALD} = \frac{V_{maxfALD} K_{DHAP_{ALD}} K_{GAP_{ALD}}}{K_{FBP_{ALD}} K_{eqALD}};$$

$$V_{TPI}(t) = \left(\left(V_{maxfTPI}\frac{GAP(t)}{K_{GAP_{TPI}}}\right) - \left(V_{maxrTPI}\frac{DHAP(t)}{K_{DHAP_{TPI}}}\right)\right) \Big/ \left(1 + \frac{DHAP(t)}{K_{DHAP_{TPI}}} + \frac{GAP(t)}{K_{GAP_{TPI}}}\right);$$

$$V_{maxrTPI} = \frac{V_{maxfTPI}\, K_{DHAP_{TPI}}}{K_{GAP_{TPI}}\, K_{eqTPI}};$$

Glyceraldehyde-3-Phosphate Dehydrogenase (GAPDH)

$$V_{GAPDH}(t) = \left(\left(V_{maxfGAPDH}\frac{GAP(t)\, NAD(t)\, P_p(t)}{K_{GAP_{GAPDH}}\, K_{NAD_{GAPDH}}\, K_{P_{pGAPDH}}}\right) - \left(V_{maxrGAPDH}\frac{BPG13(t)\, NADH(t)}{K_{BPG13_{GAPDH}}\, K_{NADH_{GAPDH}}}\right)\right) \Big/ D_{GAPDH}(t);$$

$$D_{GAPDH}(t) = 1 + \frac{GAP(t)}{K_{GAP_{GAPDH}}} + \frac{NAD(t)}{K_{NAD_{GAPDH}}} + \frac{P_p(t)}{K_{P_{pGAPDH}}} + \frac{GAP(t)\, NAD(t)}{K_{GAP_{GAPDH}}\, K_{NAD_{GAPDH}}} +$$
$$\frac{GAP(t)\, NAD(t)\, P_p(t)}{K_{GAP_{GAPDH}}\, K_{NAD_{GAPDH}}\, K_{P_{pGAPDH}}} + \frac{BPG13(t)}{K_{BPG13_{GAPDH}}} + \frac{NADH(t)}{K_{NADH_{GAPDH}}} + \frac{BPG13(t)\, NADH(t)}{K_{BPG13_{GAPDH}}\, K_{NADH_{GAPDH}}};$$

$$V_{maxrGAPDH} = \frac{V_{maxfGAPDH}\, K_{BPG13_{GAPDH}}\, K_{NADH_{GAPDH}}}{K_{GAP_{GAPDH}}\, K_{NAD_{GAPDH}}\, K_{P_{pGAPDH}}\, K_{eqGAPDH}};$$

Phosphoglycerate Kinase (PGK)

$$V_{PGK}(t) = \left(\left(V_{maxfPGK}\frac{BPG13(t)\, ADP(t)}{K_{BPG13_{PGK}}\, K_{ADP_{PGK}}}\right) - \left(V_{maxrPGK}\frac{PG3(t)\, ATP(t)}{K_{PG3_{PGK}}\, K_{ATP_{PGK}}}\right)\right) \Big/$$
$$\left(1 + \frac{BPG13(t)}{K_{BPG13_{PGK}}} + \frac{ADP(t)}{K_{ADP_{PGK}}} + \frac{BPG13(t)\, ADP(t)}{K_{BPG13_{PGK}}\, K_{ADP_{PGK}}} + \frac{PG3(t)}{K_{PG3_{PGK}}} + \frac{ATP(t)}{K_{ATP_{PGK}}} + \frac{PG3(t)\, ATP(t)}{K_{PG3_{PGK}}\, K_{ATP_{PGK}}}\right);$$

$$V_{maxfPGK} = \frac{V_{maxrPGK}\, K_{BPG13_{PGK}}\, K_{ADP_{PGK}}\, K_{eqPGK}}{K_{PG3_{PGK}}\, K_{ATP_{PGK}}};$$

Phosphoglyceromutase and Enolase (PGM and ENOL)

$$V_{PGM}(t) = \left(\left(V_{maxfPGM}\frac{PG3(t)}{K_{PG3_{PGM}}}\right) - \left(V_{maxrPGM}\frac{PG2(t)}{K_{PG2_{PGM}}}\right)\right) \Big/ \left(1 + \frac{PG3(t)}{K_{PG3_{PGM}}} + \frac{PG2(t)}{K_{PG2_{PGM}}}\right);$$

$$V_{maxrPGM} = \frac{V_{maxfPGM}\, K_{PG2_{PGM}}}{K_{PG3_{PGM}}\, K_{eqPGM}};$$

$$V_{ENOL}(t) = \left(\left(V_{maxfENOL}\frac{PG2(t)}{K_{PG2_{ENOL}}}\right) - \left(V_{maxrENOL}\frac{PEP(t)}{K_{PEP_{ENOL}}}\right)\right) \Big/ \left(1 + \frac{PG2(t)}{K_{PG2_{ENOL}}} + \frac{PEP(t)}{K_{PEP_{ENOL}}}\right);$$

$$V_{maxrENOL} = \frac{V_{maxfENOL}\, K_{PEP_{ENOL}}}{K_{PG2_{ENOL}}\, K_{eqENOL}};$$

Pyruvate Kinase (PK)

$$V_{PK}(t) = \left(\left(V_{maxfPK}\frac{PEP(t)\,ADP(t)}{K_{PEP_{PK}}\,K_{ADP_{PK}}}\right) - \left(V_{maxrPK}\frac{PYR(t)\,ATP(t)}{K_{PYR_{PK}}\,K_{ATP_{PK}}}\right)\right) \Big/ \left(1 + \frac{PEP(t)}{K_{PEP_{PK}}} + \frac{ADP(t)}{K_{ADP_{PK}}} + \frac{PEP(t)\,ADP(t)}{K_{PEP_{PK}}\,K_{ADP_{PK}}} + \frac{PYR(t)}{K_{PYR_{PK}}} + \frac{ATP(t)}{K_{ATP_{PK}}} + \frac{PYR(t)\,ATP(t)}{K_{PYR_{PK}}\,K_{ATP_{PK}}}\right);$$

$$V_{maxrPK} = \frac{V_{maxfPK}\,K_{ATP_{PK}}\,K_{PYR_{PK}}}{K_{PEP_{PK}}\,K_{ADP_{PK}}\,K_{eqPK}};$$

Lactate Dehydrogenase (LDH)

$$V_{LDH}(t) = \left(\left(V_{maxfLDH}\frac{PYR(t)\,NADH(t)}{K_{PYR_{LDH}}\,K_{NADH_{LDH}}}\right) - \left(V_{maxrLDH}\frac{LAC(t)\,NAD(t)}{K_{LAC}\,K_{NAD_{LDH}}}\right)\right) \Big/ \left(1 + \frac{PYR(t)}{K_{PYR_{LDH}}} + \frac{NADH(t)}{K_{NADH_{LDH}}} + \frac{PYR(t)\,NADH(t)}{K_{PYR_{LDH}}\,K_{NADH_{LDH}}} + \frac{LAC(t)}{K_{LAC}} + \frac{NAD(t)}{K_{NAD_{LDH}}} + \frac{LAC(t)\,NAD(t)}{K_{LAC}\,K_{NAD_{LDH}}}\right);$$

$$V_{maxrLDH} = \frac{V_{maxfLDH}\,K_{LAC}\,K_{NAD_{LDH}}}{K_{PYR_{LDH}}\,K_{NADH_{LDH}}\,K_{eqLDH}};$$

Creatine Kinase (CK)

$$V_{CK}(t) = \left(\left(V_{maxrCK}\frac{ATP(t)\,CR(t)}{K_{iATP_{CK}}\,K_{CR}}\right) - \left(V_{maxfCK}\frac{ADP(t)\,PCr(t)}{K_{iADP_{CK}}\,K_{PCr}}\right)\right) \Big/ \left(1 + \frac{ADP(t)}{K_{iADP_{CK}}} + \frac{PCr(t)}{K_{iPCr}} + \frac{ADP(t)\,PCr(t)}{K_{iADP_{CK}}\,K_{PCr}} + \frac{ATP(t)}{K_{iATP_{CK}}} + \frac{ATP(t)\,CR(t)}{K_{iATP_{CK}}\,K_{CR}}\right);$$

$$V_{maxfCK} = \frac{V_{maxrCK}\,K_{iATP_{CK}}\,K_{CR}\,K_{eqCK}}{K_{iADP_{CK}}\,K_{PCr}};$$

Adenylate Kinase (ADK)

$$V_{ADK}(t) = \left(\left(V_{maxfADK}\frac{ATP(t)\,AMP(t)}{K_{ATP_{ADK}}\,K_{AMP_{ADK}}}\right) - \left(V_{maxrADK}\frac{ADP(t)\,ADP(t)}{K_{ADP_{ADK}}\,K_{ADP_{ADK}}}\right)\right) \Big/ \left(1 + \frac{ATP(t)}{K_{ATP_{ADK}}} + \frac{AMP(t)}{K_{AMP_{ADK}}} + \frac{ATP(t)\,AMP(t)}{K_{ATP_{ADK}}\,K_{AMP_{ADK}}} + \frac{2\,ADP(t)}{K_{ADP_{ADK}}} + \frac{ADP(t)\,ADP(t)}{K_{ADP_{ADK}}\,K_{ADP_{ADK}}}\right);$$

$$V_{maxrADK} = \frac{V_{maxfADK}\,K_{ADP_{ADK}}\,K_{ADP_{ADK}}}{K_{ATP_{ADK}}\,K_{AMP_{ADK}}\,K_{eqADK}};$$

ATPase

$$V_{ATPase}(t) = k\,ATP(t);$$

$$k = 0.075;$$

Estimated parameters for the model of glycogenolysis in skeletal muscle:

Nominal values of parameters	The estimated parameters by SOMA
$frac_a = 0.5;$	
$frac_b = 0.5;$	
$V_{maxfGPa} = 0.02;$	$V_{maxfGPa} = 0.08;$
$K_{iGLYfa} = 2;$	$K_{iGLYfa} = 3.8;$
$K_{P_{pa}} = 4;$	$K_{P_{pa}} = 10.4;$
$K_{GLYb} = 0.15;$	$K_{GLYb} = 0.96;$
$K_{iG1Pa} = 10.1;$	$K_{iG1Pa} = 12.8;$
$K_{iP_{pa}} = 4.7;$	$K_{iP_{pa}} = 16.7;$
$K_{GLYf} = 1.7;$	$K_{GLYf} = 6.05;$
$K_{eqGPa} = 0.42;$	$K_{eqGPa} = 0.12;$
$V_{maxfGPb} = 0.03;$	$V_{maxfGPb} = 0.11;$
$K_{iGLYfb} = 15;$	$K_{iGLYfb} = 28.6;$
$K_{P_{pb}} = 0.2;$	$K_{P_{pb}} = 0.79;$
$K_{iGLYb} = 4.4;$	$K_{iGLYb} = 4.9;$
$K_{G1Pb} = 1.5;$	$K_{G1Pb} = 3.7;$
$nH = 1.75;$	
$K_{AMP_{act}} = 1.9 \times 10^{-6};$	$K_{AMP_{act}} = 3.7 \times 10^{-6};$
$K_{iP_{pb}} = 4.6;$	$K_{iP_{pb}} = 9.9;$
$K_{iG1Pb} = 7.4;$	$K_{iG1Pb} = 3.9;$
$K_{eqGPb} = 0.42;$	$K_{eqGPb} = 0.25;$
$V_{maxfPGLM} = 0.48;$	$V_{maxfPGLM} = 0.50;$
$K_{G1P_{PGLM}} = 0.063;$	$K_{G1P_{PGLM}} = 0.22;$
$K_{G6P_{PGLM}} = 0.03;$	$K_{G6P_{PGLM}} = 0.63;$
$K_{eqPGLM} = 16.62;$	$K_{eqPGLM} = 6.04;$
$V_{maxrPGI} = 0.88;$	$V_{maxrPGI} = 3.07;$
$K_{G6P_{PGI}} = 0.48;$	$K_{G6P_{PGI}} = 0.33;$
$K_{F6P_{PGI}} = 0.119;$	$K_{F6P_{PGI}} = 0.38;$
$K_{eqPGI} = 0.45;$	$K_{eqPGI} = 0.06;$
$V_{maxfPFK} = 0.056;$	$V_{maxfPFK} = 0.07;$
$K_{ATP_{PFK}} = 0.08;$	$K_{ATP_{PFK}} = 0.79;$
$K_{F6P_{PFK}} = 0.18;$	$K_{F6P_{PFK}} = 0.51;$
$K_{ADP_{PFK}} = 2.7;$	$K_{ADP_{PFK}} = 10.7;$
$K_{FBP_{PFK}} = 4.02;$	$K_{FBP_{PFK}} = 4.02;$
$K_{ATPact} = 0.25;$	$K_{ATPact} = 0.04;$
$K_{F6Pact} = 20;$	$K_{F6Pact} = 48;$
$K_{FBPact} = 4.02;$	$K_{FBPact} = 11.2;$
$K_{ADPact} = 2.7;$	$K_{ADPact} = 26.3;$
$K_{iATP} = 0.87;$	$K_{iATP} = 0.91;$
$K_{aAMP} = 0.06;$	$K_{aAMP} = 0.08;$
$L_0 = 13;$	
$d = 0.01;$	
$e = 0.01;$	

$V_{maxfALD} = 0.104;$
$K_{DHAP_{ALD}} = 2;$
$K_{GAP_{ALD}} = 1;$
$K_{FBP_{ALD}} = 0.05;$
$K_{eqALD} = 9.5 \times 10^{-5};$
$V_{maxfTPI} = 12;$
$K_{DHAP_{TPI}} = 0.61;$
$K_{GAP_{TPI}} = 0.32;$
$K_{eqTPI} = 0.052;$
$V_{maxfGAPDH} = 1.265;$
$K_{BPG13_{GAPDH}} = 0.0008;$
$K_{NADH_{GAPDH}} = 0.0033;$
$K_{GAP_{GAPDH}} = 0.0025;$
$K_{NAD_{GAPDH}} = 0.09;$
$K_{P_{pGAPDH}} = 0.29;$
$K_{eqGAPDH} = 0.089;$
$V_{maxrPGK} = 1.12;$
$K_{BPG13_{PGK}} = 0.002;$
$K_{ADP_{PGK}} = 0.008;$
$K_{PG3_{PGK}} = 1.2;$
$K_{ATP_{PGK}} = 0.35;$
$K_{eqPGK} = 57\,109;$
$V_{maxfPGM} = 1.12;$
$K_{PG2_{PGM}} = 0.014;$
$K_{PG3_{PGM}} = 0.2;$
$K_{eqPGM} = 0.18;$
$V_{maxfENOL} = 0.192;$
$K_{PEP_{ENOL}} = 0.37;$
$K_{PG2_{ENOL}} = 0.1;$
$K_{eqENOL} = 0.49;$
$V_{maxfPK} = 1.44;$
$K_{ATP_{PK}} = 1.13;$
$K_{PYR_{PK}} = 7.05;$
$K_{PEP_{PK}} = 0.08;$
$K_{ADP_{PK}} = 0.3;$
$K_{eqPK} = 10\,304;$
$V_{maxfLDH} = 1.92;$
$K_{LAC} = 17;$
$K_{NAD_{LDH}} = 0.849;$
$K_{PYR_{LDH}} = 0.335;$
$K_{NADH_{LDH}} = 0.002;$
$K_{eqLDH} = 16\,198;$

$V_{maxfALD} = 0.96;$
$K_{DHAP_{ALD}} = 8.8;$
$K_{GAP_{ALD}} = 3.6;$
$K_{FBP_{ALD}} = 0.33;$
$K_{eqALD} = 16.8 \times 10^{-5};$
$V_{maxfTPI} = 16;$
$K_{DHAP_{TPI}} = 0.34;$
$K_{GAP_{TPI}} = 0.50;$
$K_{eqTPI} = 0.39;$
$V_{maxfGAPDH} = 7.2;$
$K_{BPG13_{GAPDH}} = 0.002;$
$K_{NADH_{GAPDH}} = 0.005;$
$K_{GAP_{GAPDH}} = 0.007;$
$K_{NAD_{GAPDH}} = 0.12;$
$K_{P_{pGAPDH}} = 0.37;$
$K_{eqGAPDH} = 0.17;$
$V_{maxrPGK} = 7.6;$
$K_{BPG13_{PGK}} = 0.013;$
$K_{ADP_{PGK}} = 0.05;$
$K_{PG3_{PGK}} = 3.02;$
$K_{ATP_{PGK}} = 0.23;$
$K_{eqPGK} = 6013;$
$V_{maxfPGM} = 3.59;$
$K_{PG2_{PGM}} = 0.010;$
$K_{PG3_{PGM}} = 1.36;$
$K_{eqPGM} = 0.37;$
$V_{maxfENOL} = 0.89;$
$K_{PEP_{ENOL}} = 2.92;$
$K_{PG2_{ENOL}} = 0.96;$
$K_{eqENOL} = 0.42;$
$V_{maxfPK} = 4.9;$
$K_{ATP_{PK}} = 2.05;$
$K_{PYR_{PK}} = 10.2;$
$K_{PEP_{PK}} = 0.06;$
$K_{ADP_{PK}} = 0.46;$
$K_{eqPK} = 43\,104;$
$V_{maxfLDH} = 4.78;$
$K_{LAC} = 39;$
$K_{NAD_{LDH}} = 0.56;$
$K_{PYR_{LDH}} = 0.35;$
$K_{NADH_{LDH}} = 0.006;$
$K_{eqLDH} = 12\,892;$

$V_{maxrCK} = 0.5;$
$K_{iATP_{CK}} = 3.5;$
$K_{CR} = 3.8;$
$K_{iADP_{CK}} = 0.135;$
$K_{iPCr} = 3.9;$
$K_{PCr} = 1.11;$
$K_{eqCK} = 233;$
$V_{maxfADK} = 0.88;$
$K_{ADP_{ADK}} = 0.35;$
$K_{ATP_{ADK}} = 0.27;$
$K_{AMP_{ADK}} = 0.32;$
$K_{eqADK} = 2.21;$

$V_{maxrCK} = 0.609;$
$K_{iATP_{CK}} = 27.4;$
$K_{CR} = 4.6;$
$K_{iADP_{CK}} = 1.29;$
$K_{iPCr} = 17.3;$
$K_{PCr} = 2.02;$
$K_{eqCK} = 368;$
$V_{maxfADK} = 0.95;$
$K_{ADP_{ADK}} = 0.74;$
$K_{ATP_{ADK}} = 0.03;$
$K_{AMP_{ADK}} = 0.24;$
$K_{eqADK} = 2.49;$

APPENDIX D

System of differential equations, which make up the model of glycolysis in human stem cell:

$$\text{eqn1} = \text{ADP}'(t) == -(K\_r19\ \text{ADP}(t)\ \text{PEP}(t)) / (Km\_ADP\_r19\ Km\_PEP\_r19 + Km\_PEP\_r19\ \text{ADP}(t) + Km\_ADP\_r19\ \text{PEP}(t) + \text{ADP}(t)\ \text{PEP}(t)) - \left(\frac{K\_Fr16\ \text{ADP}(t)\ \text{BPG13}(t)}{Km\_13BPG\_r16\ Km\_ADP\_r16} - \frac{K\_Rr16\ \text{PG3}(t)\ \text{ATP}(t)}{Km\_3PG\_r16\ Km\_ATP\_r16}\right) \Big/ \left(1 + \frac{\text{ADP}(t)}{Km\_ADP\_r16} + \frac{\text{BPG13}(t)}{Km\_13BPG\_r16} + \frac{\text{ADP}(t)\ \text{BPG13}(t)}{Km\_13BPG\_r16\ Km\_ADP\_r16} + \frac{\text{PG3}(t)}{Km\_3PG\_r16} + \frac{\text{ATP}(t)}{Km\_ATP\_r16} + \frac{\text{PG3}(t)\ \text{ATP}(t)}{Km\_3PG\_r16\ Km\_ATP\_r16}\right) + (K\_r5\ \text{GLY}(t)\ \text{ATP}(t)) / (Km\_ATP\_r5\ Km\_Glu\_r5 + Km\_ATP\_r5\ \text{GLY}(t) + Km\_Glu\_r5\ \text{ATP}(t) + \text{GLY}(t)\ \text{ATP}(t)) + (K\_r9\ \text{F6P}(t)\ \text{ATP}(t)) / (Km\_ATP\_r9\ Km\_F6P\_r9 + Km\_ATP\_r9\ \text{F6P}(t) + Km\_F6P\_r9\ \text{ATP}(t) + \text{F6P}(t)\ \text{ATP}(t));$$

$$\text{eqn2} = \text{DHAP}'(t) == -\frac{\frac{K\_Fr12\ \text{DHAP}(t)}{Km\_DHAP\_r12} - \frac{K\_Rr12\ \text{GAP}(t)}{Km\_G3P\_r12}}{1 + \frac{\text{DHAP}(t)}{Km\_DHAP\_r12} + \frac{\text{GAP}(t)}{Km\_G3P\_r12}} + \left(-(Km\_G3P\_re14\ K\_Rre14\ \text{DHAP}(t)\ \text{GAP}(t)) / Km\_DHAP\_re14 + \frac{K\_Fre14\ \text{FBP}(t)}{Km\_F16BP\_re14}\right) \Big/ \left(1 + \frac{\text{DHAP}(t)}{Km\_DHAP\_re14} + \frac{\text{GAP}(t)}{Km\_G3P\_re14} + \frac{Km\_G3P\_re14\ \text{DHAP}(t)\ \text{GAP}(t)}{Km\_DHAP\_re14} + \frac{\text{FBP}(t)}{Km\_F16BP\_re14}\right);$$

$$\text{eqn3} = \text{GAP}'(t) == \frac{\frac{K\_Fr12\ \text{DHAP}(t)}{Km\_DHAP\_r12} - \frac{K\_Rr12\ \text{GAP}(t)}{Km\_G3P\_r12}}{1 + \frac{\text{DHAP}(t)}{Km\_DHAP\_r12} + \frac{\text{GAP}(t)}{Km\_G3P\_r12}} - \left(-\frac{K\_Rr14\ \text{BPG13}(t)\ \text{NADH}(t)}{Km\_13BPG\_r14\ Km\_NADH\_r14} + \frac{K\_Fr14\ \text{GAP}(t)\ \text{NADp}(t)}{Km\_G3P\_r14\ Km\_NADp\_r14}\right) \Big/ \left(1 + \frac{\text{GAP}(t)}{Km\_G3P\_r14} + \frac{\text{BPG13}(t)}{Km\_13BPG\_r14} + \frac{\text{NADH}(t)}{Km\_NADH\_r14} + \frac{\text{BPG13}(t)\ \text{NADH}(t)}{Km\_13BPG\_r14\ Km\_NADH\_r14} + \frac{\text{NADp}(t)}{Km\_NADp\_r14} + \frac{\text{GAP}(t)\ \text{NADp}(t)}{Km\_G3P\_r14\ Km\_NADp\_r14}\right) + \left(-(Km\_G3P\_re14\ K\_Rre14\ \text{DHAP}(t)\ \text{GAP}(t)) / Km\_DHAP\_re14 + \frac{K\_Fre14\ \text{FBP}(t)}{Km\_F16BP\_re14}\right) \Big/ \left(1 + \frac{\text{DHAP}(t)}{Km\_DHAP\_re14} + \frac{\text{GAP}(t)}{Km\_G3P\_re14} + \frac{Km\_G3P\_re14\ \text{DHAP}(t)\ \text{GAP}(t)}{Km\_DHAP\_re14} + \frac{\text{FBP}(t)}{Km\_F16BP\_re14}\right);$$

$$\text{eqn4} = \text{BPG13}'(t) == \left(-\frac{K\_Rr14\ \text{BPG13}(t)\ \text{NADH}(t)}{Km\_13BPG\_r14\ Km\_NADH\_r14} + \frac{K\_Fr14\ \text{GAP}(t)\ \text{NADp}(t)}{Km\_G3P\_r14\ Km\_NADp\_r14}\right) \Big/ \left(1 + \frac{\text{GAP}(t)}{Km\_G3P\_r14} + \frac{\text{BPG13}(t)}{Km\_13BPG\_r14} + \frac{\text{NADH}(t)}{Km\_NADH\_r14} + \frac{\text{BPG13}(t)\ \text{NADH}(t)}{Km\_13BPG\_r14\ Km\_NADH\_r14} + \frac{\text{NADp}(t)}{Km\_NADp\_r14} + \frac{\text{GAP}(t)\ \text{NADp}(t)}{Km\_G3P\_r14\ Km\_NADp\_r14}\right) - \left(\frac{K\_Fr16\ \text{ADP}(t)\ \text{BPG13}(t)}{Km\_13BPG\_r16\ Km\_ADP\_r16} - \frac{K\_Rr16\ \text{PG3}(t)\ \text{ATP}(t)}{Km\_3PG\_r16\ Km\_ATP\_r16}\right) \Big/ \left(1 + \frac{\text{ADP}(t)}{Km\_ADP\_r16} + \frac{\text{BPG13}(t)}{Km\_13BPG\_r16} + \frac{\text{ADP}(t)\ \text{BPG13}(t)}{Km\_13BPG\_r16\ Km\_ADP\_r16} + \frac{\text{PG3}(t)}{Km\_3PG\_r16} + \frac{\text{ATP}(t)}{Km\_ATP\_r16} + \frac{\text{PG3}(t)\ \text{ATP}(t)}{Km\_3PG\_r16\ Km\_ATP\_r16}\right);$$

$$\text{eqn5} = \text{PG3}'(t) == -\frac{\frac{\text{r17`K\_Fr17}\,\text{PG3}(t)}{\text{r17`Km\_3PG\_r17}} - \frac{\text{r17`K\_Rr17}\,\text{PG2}(t)}{\text{r17`Km\_2PG\_r17}}}{1 + \frac{\text{PG3}(t)}{\text{r17`Km\_3PG\_r17}} + \frac{\text{PG2}(t)}{\text{r17`Km\_2PG\_r17}}} + \left(\frac{\text{K\_Fr16 ADP}(t)\,\text{BPG13}(t)}{\text{Km\_13BPG\_r16 Km\_ADP\_r16}} - \frac{\text{K\_Rr16 PG3}(t)\,\text{ATP}(t)}{\text{Km\_3PG\_r16 Km\_ATP\_r16}}\right) \Big/ \left(1 + \frac{\text{ADP}(t)}{\text{Km\_ADP\_r16}} + \frac{\text{BPG13}(t)}{\text{Km\_13BPG\_r16}} + \frac{\text{ADP}(t)\,\text{BPG13}(t)}{\text{Km\_13BPG\_r16 Km\_ADP\_r16}} + \frac{\text{PG3}(t)}{\text{Km\_3PG\_r16}} + \frac{\text{ATP}(t)}{\text{Km\_ATP\_r16}} + \frac{\text{PG3}(t)\,\text{ATP}(t)}{\text{Km\_3PG\_r16 Km\_ATP\_r16}}\right);$$

$$\text{eqn6} = \text{PG2}'(t) == \frac{\frac{\text{r17`K\_Fr17}\,\text{PG3}(t)}{\text{r17`Km\_3PG\_r17}} - \frac{\text{r17`K\_Rr17}\,\text{PG2}(t)}{\text{r17`Km\_2PG\_r17}}}{1 + \frac{\text{PG3}(t)}{\text{r17`Km\_3PG\_r17}} + \frac{\text{PG2}(t)}{\text{r17`Km\_2PG\_r17}}} - \frac{\frac{\text{K\_Fr18}\,\text{PG2}(t)}{\text{Km\_2PG\_r18}} - \frac{\text{K\_Rr18}\,\text{PEP}(t)}{\text{Km\_PEP\_r18}}}{1 + \frac{\text{PG2}(t)}{\text{Km\_2PG\_r18}} + \frac{\text{PEP}(t)}{\text{Km\_PEP\_r18}}};$$

$$\text{eqn7} = \text{GLY}'(t) == \text{K\_re19 GLUout}(t) - (\text{K\_r5 GLY}(t)\,\text{ATP}(t)) / (\text{Km\_ATP\_r5 Km\_Glu\_r5} + \text{Km\_ATP\_r5 GLY}(t) + \text{Km\_Glu\_r5 ATP}(t) + \text{GLY}(t)\,\text{ATP}(t));$$

$$\text{eqn8} = \text{PYR}'(t) == -\text{K\_re20 PYR}(t) + (\text{K\_r19 ADP}(t)\,\text{PEP}(t)) / (\text{Km\_ADP\_r19 Km\_PEP\_r19} + \text{Km\_PEP\_r19 ADP}(t) + \text{Km\_ADP\_r19 PEP}(t) + \text{ADP}(t)\,\text{PEP}(t)) - \left(\frac{\text{K\_Fre17 PYR}(t)\,\text{NADH}(t)}{\text{Km\_NADH\_re17 Km\_Pyr\_re17}} - \frac{\text{K\_Rre17 LAC}(t)\,\text{NADp}(t)}{\text{Km\_Lac\_re17 Km\_NADp\_re17}}\right) \Big/ \left(1 + \frac{\text{PYR}(t)}{\text{Km\_Pyr\_re17}} + \frac{\text{LAC}(t)}{\text{Km\_Lac\_re17}} + \frac{\text{NADH}(t)}{\text{Km\_NADH\_re17}} + \frac{\text{PYR}(t)\,\text{NADH}(t)}{\text{Km\_NADH\_re17 Km\_Pyr\_re17}} + \frac{\text{NADp}(t)}{\text{Km\_NADp\_re17}} + \frac{\text{LAC}(t)\,\text{NADp}(t)}{\text{Km\_Lac\_re17 Km\_NADp\_re17}}\right);$$

$$\text{eqn9} = \text{PEP}'(t) == \frac{\frac{\text{K\_Fr18}\,\text{PG2}(t)}{\text{Km\_2PG\_r18}} - \frac{\text{K\_Rr18}\,\text{PEP}(t)}{\text{Km\_PEP\_r18}}}{1 + \frac{\text{PG2}(t)}{\text{Km\_2PG\_r18}} + \frac{\text{PEP}(t)}{\text{Km\_PEP\_r18}}} - (\text{K\_r19 ADP}(t)\,\text{PEP}(t)) / (\text{Km\_ADP\_r19 Km\_PEP\_r19} + \text{Km\_PEP\_r19 ADP}(t) + \text{Km\_ADP\_r19 PEP}(t) + \text{ADP}(t)\,\text{PEP}(t));$$

$$\text{eqn10} = \text{LAC}'(t) == -\text{K\_re22 LAC}(t) + \left(\frac{\text{K\_Fre17 PYR}(t)\,\text{NADH}(t)}{\text{Km\_NADH\_re17 Km\_Pyr\_re17}} - \frac{\text{K\_Rre17 LAC}(t)\,\text{NADp}(t)}{\text{Km\_Lac\_re17 Km\_NADp\_re17}}\right) \Big/ \left(1 + \frac{\text{PYR}(t)}{\text{Km\_Pyr\_re17}} + \frac{\text{LAC}(t)}{\text{Km\_Lac\_re17}} + \frac{\text{NADH}(t)}{\text{Km\_NADH\_re17}} + \frac{\text{PYR}(t)\,\text{NADH}(t)}{\text{Km\_NADH\_re17 Km\_Pyr\_re17}} + \frac{\text{NADp}(t)}{\text{Km\_NADp\_re17}} + \frac{\text{LAC}(t)\,\text{NADp}(t)}{\text{Km\_Lac\_re17 Km\_NADp\_re17}}\right);$$

$$\text{eqn11} = \text{NADH}'(t) == \left(-\frac{\text{K\_Rr14 BPG13}(t)\ \text{NADH}(t)}{\text{Km\_13BPG\_r14 Km\_NADH\_r14}} + \frac{\text{K\_Fr14 GAP}(t)\ \text{NADp}(t)}{\text{Km\_G3P\_r14 Km\_NADp\_r14}}\right) \Big/ \left(1 + \frac{\text{GAP}(t)}{\text{Km\_G3P\_r14}} + \frac{\text{BPG13}(t)}{\text{Km\_13BPG\_r14}} + \frac{\text{NADH}(t)}{\text{Km\_NADH\_r14}} + \frac{\text{BPG13}(t)\ \text{NADH}(t)}{\text{Km\_13BPG\_r14 Km\_NADH\_r14}} + \frac{\text{NADp}(t)}{\text{Km\_NADp\_r14}} + \frac{\text{GAP}(t)\ \text{NADp}(t)}{\text{Km\_G3P\_r14 Km\_NADp\_r14}}\right) - \left(\frac{\text{K\_Fre17 PYR}(t)\ \text{NADH}(t)}{\text{Km\_NADH\_re17 Km\_Pyr\_re17}} - \frac{\text{K\_Rre17 LAC}(t)\ \text{NADp}(t)}{\text{Km\_Lac\_re17 Km\_NADp\_re17}}\right) \Big/ \left(1 + \frac{\text{PYR}(t)}{\text{Km\_Pyr\_re17}} + \frac{\text{LAC}(t)}{\text{Km\_Lac\_re17}} + \frac{\text{NADH}(t)}{\text{Km\_NADH\_re17}} + \frac{\text{PYR}(t)\ \text{NADH}(t)}{\text{Km\_NADH\_re17 Km\_Pyr\_re17}} + \frac{\text{NADp}(t)}{\text{Km\_NADp\_re17}} + \frac{\text{LAC}(t)\ \text{NADp}(t)}{\text{Km\_Lac\_re17 Km\_NADp\_re17}}\right);$$

$$\text{eqn12} = (\text{NADp})'(t) == -\left(-\frac{\text{K\_Rr14 BPG13}(t)\ \text{NADH}(t)}{\text{Km\_13BPG\_r14 Km\_NADH\_r14}} + \frac{\text{K\_Fr14 GAP}(t)\ \text{NADp}(t)}{\text{Km\_G3P\_r14 Km\_NADp\_r14}}\right) \Big/ \left(1 + \frac{\text{GAP}(t)}{\text{Km\_G3P\_r14}} + \frac{\text{BPG13}(t)}{\text{Km\_13BPG\_r14}} + \frac{\text{NADH}(t)}{\text{Km\_NADH\_r14}} + \frac{\text{BPG13}(t)\ \text{NADH}(t)}{\text{Km\_13BPG\_r14 Km\_NADH\_r14}} + \frac{\text{NADp}(t)}{\text{Km\_NADp\_r14}} + \frac{\text{GAP}(t)\ \text{NADp}(t)}{\text{Km\_G3P\_r14 Km\_NADp\_r14}}\right) + \left(\frac{\text{K\_Fre17 PYR}(t)\ \text{NADH}(t)}{\text{Km\_NADH\_re17 Km\_Pyr\_re17}} - \frac{\text{K\_Rre17 LAC}(t)\ \text{NADp}(t)}{\text{Km\_Lac\_re17 Km\_NADp\_re17}}\right) \Big/ \left(1 + \frac{\text{PYR}(t)}{\text{Km\_Pyr\_re17}} + \frac{\text{LAC}(t)}{\text{Km\_Lac\_re17}} + \frac{\text{NADH}(t)}{\text{Km\_NADH\_re17}} + \frac{\text{PYR}(t)\ \text{NADH}(t)}{\text{Km\_NADH\_re17 Km\_Pyr\_re17}} + \frac{\text{NADp}(t)}{\text{Km\_NADp\_re17}} + \frac{\text{LAC}(t)\ \text{NADp}(t)}{\text{Km\_Lac\_re17 Km\_NADp\_re17}}\right);$$

$$\text{eqn13} = \text{G6P}'(t) == -\frac{\text{K\_re18 G6P}(t)}{\text{Km\_G6P\_re18} + \text{G6P}(t)} - \frac{\frac{\text{K\_Fr6 G6P}(t)}{\text{Km\_G6P\_r6}} - \frac{\text{K\_Rr6 F6P}(t)}{\text{Km\_F6P\_r6}}}{1 + \frac{\text{G6P}(t)}{\text{Km\_G6P\_r6}} + \frac{\text{F6P}(t)}{\text{Km\_F6P\_r6}}} + (\text{K\_r5 GLY}(t)\ \text{ATP}(t)) \Big/ (\text{Km\_ATP\_r5 Km\_Glu\_r5} + \text{Km\_ATP\_r5 GLY}(t) + \text{Km\_Glu\_r5 ATP}(t) + \text{GLY}(t)\ \text{ATP}(t));$$

$$\text{eqn14} = \text{R5P}'(t) == \frac{\text{K\_re18 G6P}(t)}{\text{Km\_G6P\_re18} + \text{G6P}(t)};$$

$$\text{eqn15} = \text{GLUout}'(t) == -\text{K\_re19 GLUout}(t);$$

$$\text{eqn16} = \text{PYRmit}'(t) == \text{K\_re20 PYR}(t) - \frac{\text{K\_re21 PYRmit}(t)}{\text{Km\_Pyr\_mit\_re21} + \text{PYRmit}(t)};$$

$$\text{eqn17} = \text{ACo}'(t) == \frac{\text{K\_re21 PYRmit}(t)}{\text{Km\_Pyr\_mit\_re21} + \text{PYRmit}(t)};$$

$$eqn18 = LACout'(t) == K\_re22\ LAC(t);$$

$$eqn19 = F6P'(t) == \frac{\frac{K\_Fr6\ G6P(t)}{Km\_G6P\_r6} - \frac{K\_Rr6\ F6P(t)}{Km\_F6P\_r6}}{1 + \frac{G6P(t)}{Km\_G6P\_r6} + \frac{F6P(t)}{Km\_F6P\_r6}} - (K\_r9\ F6P(t)\ ATP(t)) /$$
$$(Km\_ATP\_r9\ Km\_F6P\_r9 + Km\_ATP\_r9\ F6P(t) + Km\_F6P\_r9\ ATP(t) + F6P(t)\ ATP(t));$$

$$eqn20 = FBP'(t) == -\left(-(Km\_G3P\_re14\ K\_Rre14\ DHAP(t)\ GAP(t)) / Km\_DHAP\_re14 + \frac{K\_Fre14\ FBP(t)}{Km\_F16BP\_re14}\right) /$$
$$\left(1 + \frac{DHAP(t)}{Km\_DHAP\_re14} + \frac{GAP(t)}{Km\_G3P\_re14} + \frac{Km\_G3P\_re14\ DHAP(t)\ GAP(t)}{Km\_DHAP\_re14} + \frac{FBP(t)}{Km\_F16BP\_re14}\right) +$$
$$(K\_r9\ F6P(t)\ ATP(t)) /$$
$$(Km\_ATP\_r9\ Km\_F6P\_r9 + Km\_ATP\_r9\ F6P(t) + Km\_F6P\_r9\ ATP(t) + F6P(t)\ ATP(t));$$

$$eqn21 = ATP'(t) == (K\_r19\ ADP(t)\ PEP(t)) / (Km\_ADP\_r19\ Km\_PEP\_r19 +$$
$$Km\_PEP\_r19\ ADP(t) + Km\_ADP\_r19\ PEP(t) + ADP(t)\ PEP(t)) +$$
$$\left(\frac{K\_Fr16\ ADP(t)\ BPG13(t)}{Km\_13BPG\_r16\ Km\_ADP\_r16} - \frac{K\_Rr16\ PG3(t)\ ATP(t)}{Km\_3PG\_r16\ Km\_ATP\_r16}\right) /$$
$$\left(1 + \frac{ADP(t)}{Km\_ADP\_r16} + \frac{BPG13(t)}{Km\_13BPG\_r16} + \frac{ADP(t)\ BPG13(t)}{Km\_13BPG\_r16\ Km\_ADP\_r16} + \right.$$
$$\left. \frac{PG3(t)}{Km\_3PG\_r16} + \frac{ATP(t)}{Km\_ATP\_r16} + \frac{PG3(t)\ ATP(t)}{Km\_3PG\_r16\ Km\_ATP\_r16}\right) -$$
$$(K\_r5\ GLY(t)\ ATP(t)) / (Km\_ATP\_r5\ Km\_Glu\_r5 + Km\_ATP\_r5\ GLY(t) +$$
$$Km\_Glu\_r5\ ATP(t) + GLY(t)\ ATP(t)) - (K\_r9\ F6P(t)\ ATP(t)) /$$
$$(Km\_ATP\_r9\ Km\_F6P\_r9 + Km\_ATP\_r9\ F6P(t) + Km\_F6P\_r9\ ATP(t) + F6P(t)\ ATP(t));$$

Estimated parameters for the model of glycolysis in human stem cell:

K_Glu = 0.92;
K_r5 = 7.44;
Km_Glu_r5 = 2.65;
Km_ATP_r5 = 2.68;
K_Fr6 = 9.14;
K_Rr6 = 6.67;
Km_G6P_r6 = 2.61;
Km_F6P_r6 = 8.23;
K_r9 = 7.81;
Km_F6P_r9 = 8.06;
Km_ATP_r9 = 4.81;
K_Fr12 = 6.14;
K_Rr12 = 3.78;
Km_DHAP_r12 = 1.27;
Km_G3P_r12 = 3.64;
K_Fr14 = 8.54;
Km_G3P_r14 = 8.11;
Km_NADp_r14 = 4.62;
K_Rr14 = 5.29;
Km_13BPG_r14 = 3.12;
Km_NADH_r14 = 2.24;
K_Fr16 = 2.41;
Km_13BPG_r16 = 4.62;
Km_ADP_r16 = 8.79;
K_Rr16 = 0.58;
Km_3PG_r16 = 0.76;
Km_ATP_r16 = 3.31;

K_Fr17 = 0.16;
Km_3PG_r17 = 0.46;
K_Rr17 = 1.79;
Km_2PG_r17 = 1.06;
K_Fr18 = 4.25;
K_Rr18 = 7.36;
Km_2PG_r18 = 6.70;
Km_PEP_r18 = 7.77;
K_r19 = 3.62;
Km_PEP_r19 = 2.55;
Km_ADP_r19 = 4.01;
K_Fre14 = 4.41;
K_Rre14 = 2.31;
Km_F16BP_re14 = 8.09;
Km_DHAP_re14 = 5.30;
Km_G3P_re14 = 2.64;
K_Fre17 = 7.62;
Km_Pyr_re17 = 0.08;
Km_NADH_re17 = 0.17;
Km_Lac_re17 = 0.83;
Km_NADp_re17 = 5.68;
K_Rre17 = 0.92;
K_re18 = 0.02;
Km_G6P_re18 = 0.89;
$K\_re19 = 1.46 \times 10^{5}$;
K_re20 = 0.49;
K_re21 = 5.63;
Km_Pyr_mit_re21 = 6.11;
K_re22 = 2.09;